FACULTY OF PURE AND APPLIED SCIENCES
DEPARTMENT OF BIOLOGICAL SCIENCES

INVESTIGATING THE FUNCTION OF LONG INTERGENIC NON-CODING RNAS IN *SACCHAROMYCES CEREVISIAE*

DIMITRIS KYRIAKOU

A dissertation submitted to the University of Cyprus in partial fulfilment of the requirements for the Degree of Doctor of Philosophy Dissertation

MARCH 2017

Validation Page

PhD Candidate: Dimitris Kyriakou

Doctoral Thesis Title: Investigating the function of long intergenic non-coding RNAs in *Saccharomyces cerevisiae*.

The present Doctoral Dissertation was submitted in partial fulfillment of the requirements for the degree of Doctor of Philosophy at the Department of Biological Sciences and was approved on the 08.03.2017 by the members of the Examination Committee.

Examination Committee:

- **Research Supervisor:** Dr. Antonis Kirmizis
- **Committee Member:** Dr. Vasilis Promponas
- **Committee Member:** Dr. Katerina Strati
- **Committee Member:** Dr. Igor Ulitsky
- **Committee Member:** Dr. Pantelis Hatzis

Declaration of Doctoral Candidate

The present doctoral dissertation was submitted in partial fulfillment of the requirements for the degree of Doctor of Philosophy of the University of Cyprus. It is a product of original work of my own, unless otherwise mentioned through references, notes, or any other statements.

……..….**DIMITRIS**…**KYRIAKOU**……[Full name of Doctoral Candidate]

……..……..[Signature]

Περίληψη

Το γονιδίωμα διαφόρων ευκαρυωτικών οργανισμών μεταφράζεται σχεδόν σε όλο το μήκος τους και αυτό το φαινόμενο ονομάζεται διάτρητη μεταγραφή. Μέσω της διάτρητης μεταγραφής παράγεται ένα τεράστιος αριθμός μακριών μη-κωδικών ριβονουκλεοτιδίων (long non-coding RNAs – lncRNAs). Επειδή γνωρίζουμε τον βιολογικό ρόλο μόνο μερικών lncRNAs, είναι αβέβαιο αν όλα έχουν βιολογική σημασία. Επομένως σε αυτή την μελέτη αναλύσαμε τον ρόλο των lncRNAs βασιζόμενοι στις γενετικές τους αλληλεπιδράσεις με γονίδια που εκφράζουν πρωτεΐνες. Χρησιμοποιήσαμε την τεχνική SGA (Synthetic Genetic Array) για να αναγνωρίσουμε όλες τις γενετικές αντιδράσεις στον ευκαρυοτικό μικροοργανισμό *Saccharomyces cerevisiae* (*S.cerevisiae*). Για να βελτιστοποιήσουμε την τεχνική SGA, χρησιμοποιήσαμε το lncRNA *TLC1* το οποίο λειτουργεί ως εκμαγείο για την σύνθεση τελομερών από το ένζυμο τελομεράση. Μετά χρησιμοποιήσαμε την τεχνική SGA για να αναγνωρίσουμε τις γενετικές αλληλεπιδράσεις μεταξύ γονιδίων και έξι ενδογονιδιακών lncRNAs (long intergenic non-coding RNAs - lincRNAs) για τα οποία δεν γνωρίζαμε τον βιολογικό τους ρόλο. Βασιζόμενοι στις γενετικές τους αντιδράσεις με γονίδια καταφέραμε να προσδιορίσουμε τις βιολογικές διαδικασίες στις οποίες αυτά τα έξι lincRNAs ενδεχομένως να εμπλέκονται. Μέτα επικεντρώσαμε την έρευνα στην εκτενέστερη ανάλυση του βιολογικού ρόλου ενός από τα έξι lincRNAs, το οποίο ονομάζεται *SUT457*. Ανακαλύψαμε ότι το lincRNA *SUT457* εμπλέκεται στην οργάνωση των τελομερών. Συνδυασμός της διαγραφής του *SUT457* και του *TLC1* οδηγεί σε γρηγορότερη γήρανση των κυττάρων που είναι ενδεικτικό του ότι η διαδικασία της ρύθμισης του μονόκλωνου DNA των τελομερών δεν λειτουργεί φυσιολογικά. Ακολούθως, αποδείξαμε ότι η απουσία του *SUT457* οδηγεί σε μακρύτερο μονόκλωνο DNA στα τελομερή μέσω μιας διαδικασίας που εξαρτάται από την εξωνουκλεάση Exo1. Επίσης αποδείξαμε ότι το *SUT457* ρυθμίσει το μονόκλωνο DNA των τελομερών δουλεύοντας μακριά από το σημείο έκφρασης του (*trans-acting*). Συλλογικά αποδείξαμε ότι μπορούμε να βρούμε τον βιολογικό ρόλο των lincRNAs βασιζόμενοι στις γενετικές τους αλληλεπιδράσεις και προτείνουμε ότι αυτή η προσέγγιση μπορεί να χρησιμοποιηθεί και για τον χαρακτηρισμό lincRNAs στον άνθρωπο.

Abstract

Eukaryotic genomes are pervasively transcribed, producing a vast number of long non-coding RNAs (lncRNAs). Only a few of them have been functionally characterized so far, thus their biological significance is yet under debate. Even less lncRNAs have been annotated as essential hence implying that the majority of them may be functionally redundant. Therefore, we hypothesized that the function of lncRNAs could be revealed by systematic construction of double mutant yeast strains, each one bearing a lncRNA deletion in combination with protein-coding gene deletions. To address this hypothesis, we utilized Synthetic Genetic Array (SGA) for long intergenic non-coding RNAs (lincRNAs) in *Saccharomyces cerevisiae* in order to identify their genetic interactions (GIs) with protein-coding genes. We validated this approach by demonstrating that the known biological role of a well described lincRNA called *TLC1* (TeLomerase Component 1) can be inferred through its GI network. We subsequently performed SGA screens on a set of uncharacterized lincRNAs and uncovered their connection to diverse cellular processes. We focused on one of the tested lincRNAs, *SUT457*, which showed genetic interactions with genes involved in telomere organization. Deeper investigation showed that loss of *SUT457* induces premature senescence in telomerase-deficient cells and resulted in telomeric overhang accumulation compared to wild type (WT) yeast cells. We discovered that the telomeric overhang accumulation intensified after subculturing of *sut457Δ* cells in an Exo1-dependent manner. Furthermore, the GI profile of *SUT457* was distinct from that of its neighboring genes suggesting that *SUT457* may function independently to its genomic location. This was supported by the fact that ectopic expression of *SUT457* exhibited WT telomeric overhang phenotype, revealing that SUT457 is working in *trans*. Overall, this study demonstrated that; a) Genetic interaction profiling can be used for functional characterization of a plethora, if not for all lncRNAs in yeast and possibly can be implemented in other complex organisms, b) SGA screens implicate lincRNAs in various cellular procedures, in addition to their well-described role in gene transcription and c) SUT457 is a novel *trans*-acting telomere organization lincRNA involved in telomeric overhang homeostasis by an Exo1-dependent manner. In conclusion, by characterizing the biological role of lincRNAs in the eukaryotic model organism *Saccharomyses cerevisiae* we added evidence on the growing perception that long ncRNAs are functionally significant molecules which add complexity to the biological systems by affecting a variety of cellular processes.

Acknowledgments

I would like to thank my supervisor Dr. Antonis Kirmizis for the opportunity to work in his lab and for supporting me all the way during my PhD study. I would also like to express my gratitude to all the members of Kirmizis lab, to my family and friends for all their support.

Dedication

This Ph.D Thesis is dedicated to my wife Katerina Marinou for all the support all these years!

Table of Contents

List of figures

List of tables

List of abbreviations

bps - base pairs
cDNA - complementary DNA
CUTs - Cryptic unstable transcripts
CRISPR - Clustered Regularly Interspaced Short Palindromic Repeats
FET - Fisher's exact test
FOA -Fluoroorotic Acid
CD-CUTs - Cytoplasmically degraded-CUTs
GI – genetic interaction
GO - Gene Ontology
IP- Immunoprecipitation
lincRNA – long intergenic non-coding RNA
miRNA - micro-RNA
MUTs - Meiotic unannotated transcripts
ncRNA – non-coding RNA
NGI - negative genetic interaction
NGE - neighbouring gene effect
nt - Nucleotide
OD - optical density
ORF - open reading frame
PCR - Polymerase Chain Reaction
PGI - positive genetic interaction
qPCR - Quantitative PCR
RNA - ribonucleic acid
rRNA - ribosomic RNA
SGA - Synthetic genetic array
siRNA – small interfering RNA
snoRNA – small nucleolar RNA
snRNA – small nuclear RNA
ssDNA – single strand DNA
SUT – stable unannotated transcript
TERC - TelomErase RNA Component
TERRA - Telomeric repeat-containing RNA
TLC1 - TeLomerase Component 1
TMLs -Telomerase Mutant LncRNAs
WT - wild type
XUTs - Xrn1-sensitive unstable transcripts

Chapter 1 – Introduction

1.1 Pervasive transcription

The completion of the human genome sequencing in 2003 revealed that ~25000 protein-coding genes occupy a very small fraction of the genomic DNA (1%). Thus, it was inferred that 99% of the human genome is 'junk' DNA without any functional potential. However, genome-wide transcriptional studies revealed that eukaryotic genomes are transcribed across their full length and this procedure was called pervasive transcription [1]. Today we know that up to 98% of human genome is transcribed, however only 1-2% is translated into proteins (exonic DNA) [2–4]. Pervasive transcription produces protein-coding transcripts (mRNAs) and the well described housekeeping non-coding RNAs (tRNAs, rRNAs, snRNA and snoRNAs) but also generates a plethora of non-coding RNAs (ncRNAs) with distinct regulatory cellular roles. The regulatory ncRNAs can be divided into two categories according to their size; short (<=200 nucleotides) and long (>200 nucleotides) ncRNAs [1,4–8] (**Figure 1.1**). Short ncRNAs (sncRNAs) such as short interfering RNAs (siRNAs) and microRNAs (miRNAs) have been extensively studied and are known to regulate the expression of individual or groups of genes and mRNA editing and stability and are involved in antiviral response control [9]. Long non-coding RNAs (lncRNAs) are less studied and so far appear to have biological roles that are mainly associated with gene regulation. Hence, the large majority of lncRNAs remain functionally uncharacterized.

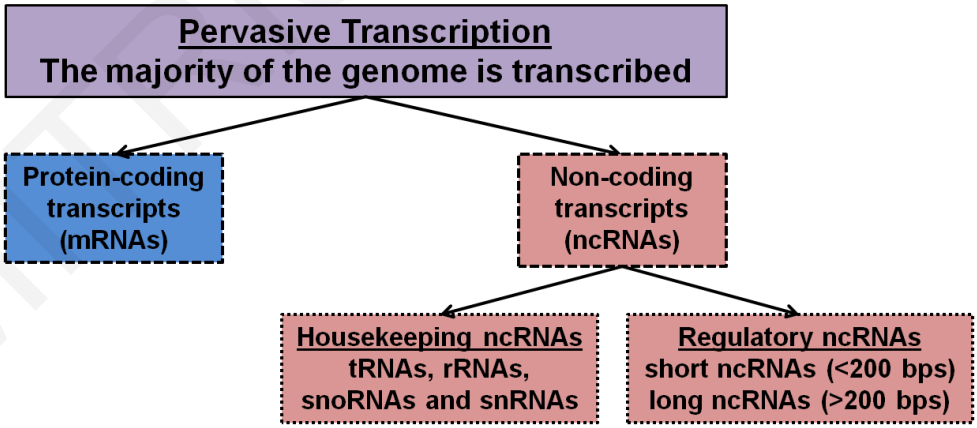

Figure 1.1: Holistic view of pervasively transcribed RNAs. Pervasive transcription generates protein-coding RNAs, housekeeping non-coding RNAs which support the maintenance of basic cellular needs and non-coding RNAs with presumed regulatory functions that assure adaptation to changing cell needs and offer phenotypic variability [9].

1.2 lncRNA synthesis and transcriptional regulation

The majority of lncRNAs are transcribed by RNA polymerase II (Pol II) in the same manner as protein-coding gene transcription and the lncRNA transcripts have similar features as mRNAs [10]. The promoters of lncRNAs loci are enriched with active histone marks and the RNA transcript can be 5'-capped, spliced and polyadenylated. However, lncRNAs tend to be shorter than mRNAs, they have lower expression levels and significantly lower sequence conservation between different species compared to mRNAs (see chapter 1.6). In some cases, lncRNAs are transcribed by the RNA Polymerase III complex [11] or they can be generated as byproducts of snoRNA splicing [12]. lncRNAs can be transcribed from intergenic and intragenic loci. The genomic locus of an intragenic ncRNA partially or fully overlaps with other gene(s). Contrary, long intergenic or intervening non coding RNAs (lincRNAs) are transcribed from areas located between genes (**Figure 1.2**). Some lncRNAs are also expressed at telomeres (TERRA) [13].

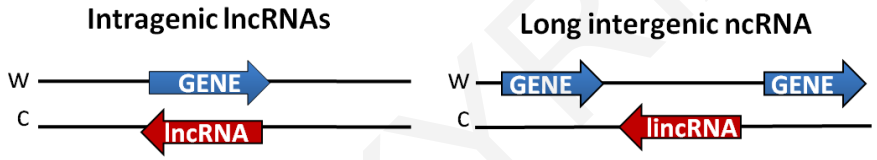

Figure 1.2: Schematic representation of intragenic and intergenic lncRNAs. Intragenic lncRNA could be located within an intron, exon or across the entire coding-gene, in a sense or anti-sense orientation. Long intergenic ncRNAs (lincRNAs) do not overlap any gene.

Many previous studies have focused on intragenic lncRNAs and revealed that they are involved in the regulation of their overlapping gene expression. Also, some intergenic lncRNAs control the expression of neighboring genes. The transcriptional orientation of a lncRNA compared to its adjacent gene can be a decisive factor for its effect on gene expression. Specifically, antisense lncRNAs that are transcribed from the opposite DNA strand compared to their neighboring gene can be categorized as convergent or divergent. Convergent (natural antisense transcripts or NATs) are lncRNAs expressed from a locus that is positioned antisense and downstream from sense neighboring gene. NATs transcription can lead to down-regulation of their overlapping gene. Divergent are antisense lncRNAs expressed from a locus that is positioned upstream from the neighboring gene and they are generally referred as uaRNAs (upstream antisense RNAs). Divergent transcription can initiate at both the protein-coding locus and at the uaRNA locus, however transcriptional elongation of the lncRNA usually is not completed. Lastly, lncRNA transcription is classified as tandem to the neighboring mRNA transcription when the two are on the same strand (**Figure 1.3**) [14].

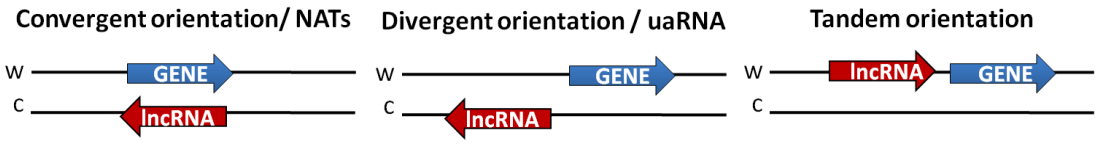

Figure 1.3: Types of lncRNA orientation compared to the expression of a neighboring gene. All NATs are intragenic. Even though only intergenic examples of uaRNAs and tandemly orientated lncRNAs are shown in this figure, lncRNAs from these two groups can overlap other genes (intragenic).

The expression of lncRNAs is more tightly regulated than that of mRNAs. In fact, the transcriptional levels of lncRNAs can be differentially regulated according to cell-type, tissue-type, developmental stage or pathological condition [15]. Several mechanisms take place to regulate lncRNA expression. Studies in yeast have shown that divergent lncRNAs are enriched by unique epigenetic marks (H3K56ac), specific chromatin remodelers (SWI/SNF, CAF1) and specific modifications of RNA polymerase II (Tyr1P) that repress their expression, while allowing the protein-coding gene to be expressed [16,17]. Also, polyadenylation signals (PARs) terminate divergent lncRNA transcription and at the same time U1 snRNP splicing signals found on the protein-coding gene ensure productive splicing and elongation of the sense transcript [18]. Studies in human cells have shown that the expression of lncRNAs is orchestrated by Dicer I / microRNAs and the transcription factor MYC in a manner that is decoupled from mRNA regulation [19].

1.3 Post-transcriptional modification of lncRNAs

lncRNAs, just like mRNAs, undergo a series of post-transcriptional modifications that can regulate their transcriptional elongation (e.g. polyadenylation), molecular stability (e.g. 5' terminal methylguanosine cap) and function (e.g. splicing) [10]. Also, lncRNA maturation involves procedures unique only to them. For example, two well described human lncRNAs, *MALAT1* and *NEAT1*, have tRNA like structures which are cleaved by RNase P cleavage in order to become mature and functional [20]. Also, back-splicing or canonical intron splicing can post-transcriptionally alter linear lncRNAs and lead to circularly structured RNAs acquiring new functional properties [21]. Non-polyadenylated lncRNAs are processed by other protein complexes, such as the Integrator and the Microprocessor complexes, which cleave the nascent transcript and terminate its transcription or generate smaller unstable lncRNAs [22,23].

1.4 lncRNA localization

lncRNAs are found both in the nucleus, in the cytosol and in mono- and polyribosomal complexes [14,24]. Nascent nuclear lncRNAs can accumulate around their locus (accumulate *in-cis*) or they can be moved to a different location away from their transcriptional site (in *trans* localization). Nuclear lncRNAs that accumulate *in cis* can be *cis*-acting, meaning that they exert their role only in the vicinity of their transcriptional site (**Figure 1.4A**). It is also possible that in-*cis* accumulated lncRNAs can also function in a nuclear location away from their locus and therefore, defined as *trans*-acting (**Figure 1.4B**). Nuclear lncRNAs which are *trans*-localized are bound by one or more proteins that dictate their transport to different locations on the genomic DNA and in special ribonucleoprotein structures inside the nucleus called nuclear bodies (**Figure 1.4C**). lncRNAs are also able to export from the nucleus and enter the cytoplasm where they stay bound on proteins or on ribosomes (**Figure 1.4D**). The lncRNAs found in the cytoplasm and the ones that are *trans*-localized in the nucleus are categorized as t*rans-acting* [14].

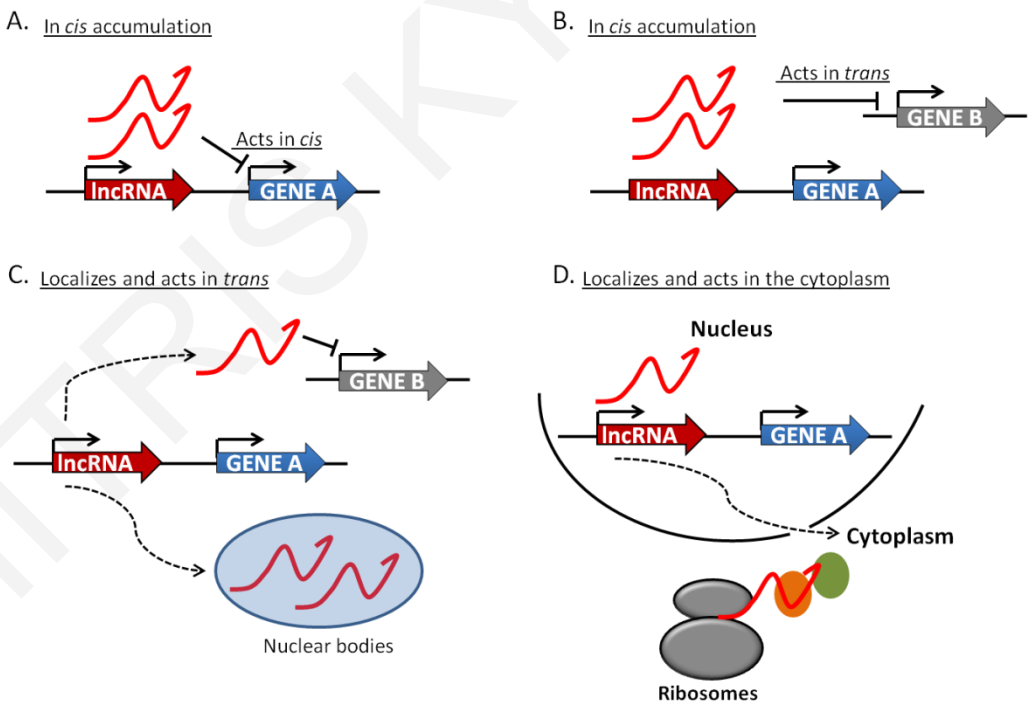

Figure 1.4: Localization and function of lncRNAs. A. and B. In *cis* accumulated nuclear lncRNAs (red curvy lines) stay in the area where they are transcribed and control gene expression of neighboring genes (act in *cis*) **(A)** or of distant genes (act in *trans*) **(B)**. **C.** The nuclear lncRNA transcripts localize in *trans* since they are transferred away from their locus after their transcription and they act in *trans* by controlling the expression of distant genes or by taking part in ribonucleoprotein bodies in the nucleus. **D.** lncRNAs can be exported to the cytoplasm where they

can physically bind to ribosomes and regulate the posttranslational modifications of other proteins (orange and green circles).

The nuclear localization of each lncRNA is regulated by several mechanisms including the 3D structure of chromosomes, protein-lncRNA interactions and ribonucleic nuclear retention elements (RNREs) found on the lncRNA transcript. Specifically, lncRNA nucleo-cytoplasmic shuttling is blocked by alternative splicing, lack of poly(A) tail and RNREs. Also, binding to nuclear matrix proteins (e.g. hnRNP U keeps lncRNA *FIRRE* in the nucleus) and chromosome looping retain lncRNAs on the genomic DNA. Nuclear lncRNAs are able to accumulate in *cis* by binding of transcription factors and chromatin organizers or by forming bonds with the local genomic DNA. An example, is the *cis*-acting *CCAT1-L* lncRNA, which is expressed upstream of the *MYC* gene. *CCAT1-L* physically interacts with the chromatin remodeler *CTCF* in order to regulate *MYC* expression [25]. In *cis* localized lncRNAs are also able to act in *trans* due to the 3D organization of the chromosomes, as in the case of lncRNA *FIRRE* which is transcribed at the X chromosome but contacts five other chromosomal regions that are distant from its transcriptional site [26].

Trans-acting lncRNAs can be translocated away from their transcriptional site with the help of proteins that physically interact with them. A well-described example of a lncRNA that is translocated and functions in *trans* is the human lncRNA *HOTAIR,* which it is shuttled from its transcriptional site at chromosome 12 to chromosome 2 by the Suz12 protein [27]. *HOTAIR* also binds numerous other genomic sites across the genome and interacts with polycomb complex proteins and histone deacetylaces in order to control gene expression in *trans* [28]. In addition, some other *trans*-acting lncRNAs are relocated to specific membrane-less lncRNA-protein structures generally referred as nuclear bodies (**Figure 1.4**) which can control particular nuclear processes [29].

Cytoplasmic lncRNAs can influence mRNA translation, protein posttranslational modification and thus, indirectly affect gene expression [14]. A representative example of a cytoplasmic lncRNA is *CCAT1-short* which is generated after 3'end processing of the full length *CCAT1* transcript in the nucleus and then transferred into the cytoplasm [25].

1.5 lncRNA degradation

lncRNA degradation is an effective way to limit the number of transcripts pervasively produced from the genome. Studies on rapidly degraded nuclear lncRNAs in yeast, called CUTs (cryptic unstable transcripts), have revealed that they are the target of several decay pathways, some of which work in humans as well. CUTs are targeted and degraded by the exosome due to poly(A) degradation tags that are added to them

immediately after their synthesis [30–33]. Human lncRNAs with similar properties to yeast CUTs, such as the uaRNAs, transcriptional start site-associated RNAs (TSSa-RNAs), promoter-associated ncRNAs and promoter upstream transcripts (PROMPTs) are also degraded by the exosome [34]. In yeast, CUTs are targeted also by the 5' – 3' exonuclease Xrn1 exonuclease and the nonsense-mediated decay (NMD) pathway in the cytoplasm [35,36]. The NMD pathway is also active in the cytoplasm of many other organisms such as *Arabidopsis thaliana*, zebrafish and humans and it is more sensitive towards lncRNAs than mRNAs [37]. In contrast to rapidly degrading lncRNAs, a group of yeast lncRNAs evades degradation in the nucleus, and are appropriately called SUTs (Stable Unannotated Transcripts). SUTs are decapped and could be degraded in the cytoplasm by the 5'-3' RNA exonuclease Xrn1 [7,8,38].

1.6 Conservation of lncRNAs

lncRNAs are more conserved than neutrally evolving genetic elements (e.g. introns or other gene sites which can have mutations without altering the function of the protein produced). Nevertheless, identification of orthologous lncRNAs is challenging because their primary nucleotide sequence differs even among closely related species [39]. A small number of homologous lncRNAs were identified through their similarity in short sequence motifs and secondary structures [10,40,41]**.** The sequence of the genomic area flanking the lncRNA can also be conserved between two species (referred to as synteny), which could reveal in certain cases homology between lncRNAs that do not share similarity in their own primary sequence. Syntenic lncRNAs satisfy certain criteria such as being at the same distance from the conserved neighboring genes and should have the same relative orientation to their adjacent genes in both species [39,42]. lncRNA conservation among different species can provide key information for speculating which lncRNAs are functional and which are important for studying in model organisms. For example, the discovery of a mouse lncRNA that is homologous to a human pathogenic lncRNA could be useful for drug testing. The conservation of lncRNAs remains a great challenge in the field and it might not even be dependent on sequence similarities but on other properties yet to be discovered.

1.7 Coding potential of lncRNAs

Most of the lncRNAs have features similar to mRNAs, thus it is possible that some of them encode for peptides. This argument is supported also by the fact that the average size of lncRNAs in vertebrates is ~1000 bps consequently it is possible to contain multiple open reading frames (ORFs) just by chance [43]. Specifically, ORFs less than 10% of the

full RNA could occur by chance [44]. .Indeed, studies that mapped start and stop codons on the nucleotide sequence of various lncRNAs have revealed several hidden ORFs. Computational studies are used to determine the coding potential of lncRNA ORFs according to mRNA-associated features. ORFs that generate functional proteins should contain specific nucleotide frequencies, termed as ‘‘non-random codon usage’’, which lack from truly non-coding RNAs. Lastly, the ORFs should consist of codon sequence which can be mapped on already existing peptides, in order to be considered as coding [43].

Ribosome-protected fragments revealed by ribosome-affinity studies have nucleotide-alignment with lncRNAs, however, it is still unclear whether these lncRNAs can produce functional proteins [44]. In fact, such ribosome protected fragments are found on the non-translated RNAs of telomerase and RNase P complex and also on 5’UTRs of mRNAs [44–46]. Furthermore, ribosome profiling of lncRNAs shows different characteristics to that observed on mRNAs. For example, ribosome occupancy on mRNAs significantly decreases after a stop codon. In contrary, ribosomes do not detach after stop codons on lncRNAs, thus showing that they can accurately distinguish between canonical ncRNAs and protein-coding RNAs [45]. Additionally, sensitive mass spectrometry failed to detect any products that could originate from ORFs hidden in lncRNAs sequences in two tested human cell lines [10]. Conclusively, it has been suggested that binding of lncRNAs to ribosomes might represent a translation-dependent degradation process that controls the levels of lncRNAs within the cell [44].

Despite the current belief that most lncRNAs do not possess coding potential, a few studies have shown that peptides are encoded by a transcript previously annotated as lncRNA. For example, a 46 and a 34 aminoacid long peptides called myoregulin (MLN) and dwarf open reading frame (DWORF) respectively were expressed by skeletal muscle-specific RNAs, previously annotated as lncRNAs [47,48]. The distinction between coding and non-coding RNAs became even more challenging with the discovery of bifunctional RNAs. Bifunctional RNAs not only work as lncRNAs but they can also be transcribed into functional proteins [49]. Studies on lncRNAs that reach translation, suggest that the peptides produced might serve as a platform for protein evolution [44].

Experimental evidence is required to assign lncRNAs as coding. Specifically, the coding potential of an RNA transcript can be initially tested by in *vitro* translation experiments followed by the detection of the relative peptides. Follow up experiments include the development of antibodies that can be used in immunoblotting or immunohistochemistry to detect the target peptides in *vivo*. Finally, the coding potential of a non-coding transcript can be validated through complementation assays, where the expression of the lncRNA with mutated ORFs will be tested for rescuing a lncRNA-associated phenotype [44]. Such complementation assays can also be performed for

bifunctional RNAs since the few characterized examples of this group suggest different functions for the lncRNA and the peptide expressed.

1.8 Molecular functions of lncRNAs

To date, the function of most identified lncRNAs remains unknown. In this section of Chapter 1, we focus on those few lncRNAs that have been functionally defined in order to provide the current knowledge on the molecular activity of these versatile molecules.

1.8.1 lncRNAs regulate gene expression

Early studies on lncRNA functionality revealed that the lncRNA transcripts or even the transcriptional process itself can affect the expression of adjacent or distant genes by a variety of molecular mechanisms. lncRNAs can physically bind to more than one histone modification factors and chromatin remodelers and coordinate their actions to target loci (**Figure 1.5A**). An extensively studied example is the human lincRNA *HOTAIR* (*HOX* transcript antisense RNA 1) which physically associates with two histone modifiers, *PRC2* and *LSD1,* which are responsible for enforcing repressive epigenetic modifications to their target genes [50]. lncRNAs are also involved in gene imprinting, meaning that they affect the epigenetic silencing of one of the two gene alleles based on their parental origin (**Figure 1.5B**). A well-studied example is lncRNA *Airn* which is expressed only in the paternally inherited allele. *Airn* transcript blocks the expression of both the overlapping and a neighboring gene. In contrary, *Airn* expression is blocked by DNA methylation in the maternal allele, therefore allowing the expression of proximal genes [51,52]. Chromatin manipulation by lncRNAs also occurs during dosage compensation of X chromosomes. Specifically, one of the two X chromosomes are deactivated in each cell of a female body in order to match the genetic information of the single X chromosome in males. *XIST* lncRNA is responsible for chromosome-wide transcriptional silencing of one of the two X chromosomes. *XIST* is randomly expressed from one of the two X chromosomes (from the one that will be silenced and regardless of parental origin) and then spreads across the X chromosome to mediate the deposition of suppressive histone modifications and DNA methylation (**Figure 1.5C**) [53].

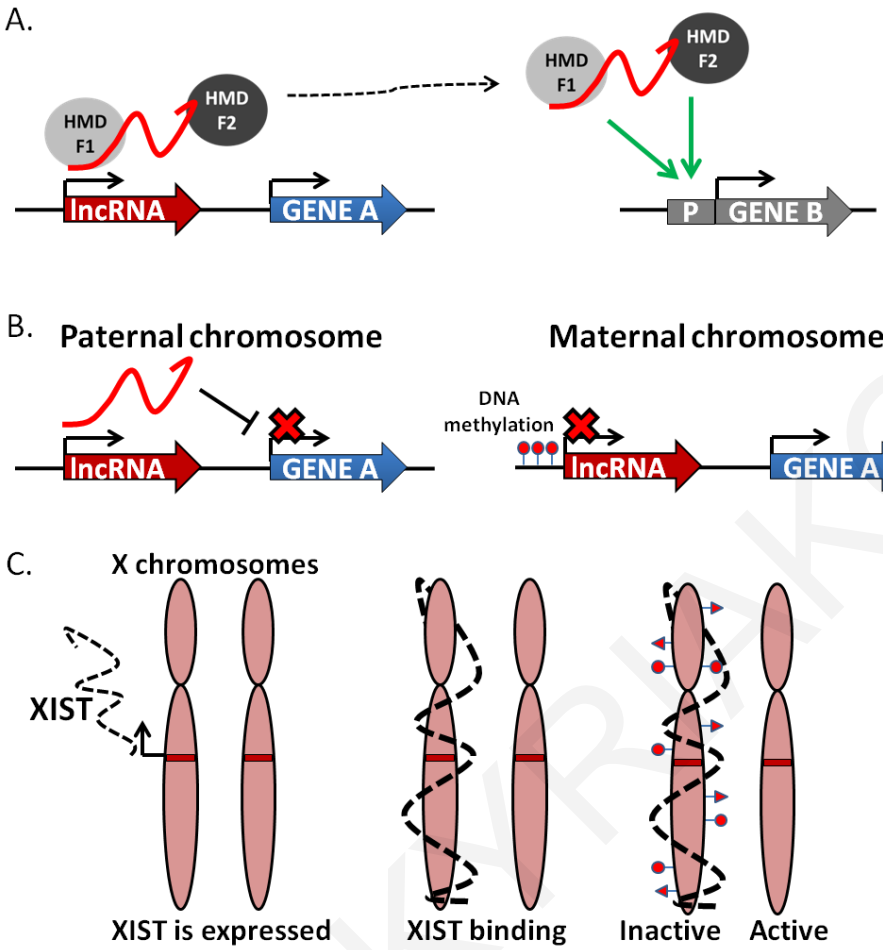

Figure 1.5: lncRNA transcripts control gene expression through chromatin modifications. A. Two histone modification factors (HMDF) are using a *trans*-acting lncRNA (red curvy line) as a scaffold in order to regulate the expression of target genes (e.g. Gene B) in a coordinated manner. The same procedure can be used for regulating the expression of neighboring genes (e.g. Gene A). **B.** Schematic illustration of a lncRNA at an imprinted locus. The paternally expressed lncRNA (red curvy line) can block the expression of Gene A. The maternal copy of the lncRNA locus is silenced by DNA methylation (red circles), thus allowing the expression of Gene A. **C.** Dosage compensation by *XIST*. The lncRNA *XIST* is expressed randomly from one of the two X chromosomes in a cell and then works in cis by physically binding to the same chromosome in order to mediate the deposition of histone modifications (red triangles) and DNA methylation (red circles) which result in silencing of the entire X chromosome.

Chromatin modifications are not the only way through which lncRNAs affect gene expression. lncRNAs can also bind to RNA polymerase II (e.g. *Alu* repeat-containing RNA) and to transcription factors (e.g. *HSR1* lncRNA binds on the transcription factor *HSF1*) and regulate their functions (**Figure 1.6A and B**) [54,55]. Additionally, lncRNAs can bind to genomic DNA forming RNA-DNA structures. Such an example is the non-coding *DHFR* that blocks the formation of the transcription pre-initiation complex, therefore blocking gene expression (**Figure 1.6C**) [56]. lncRNAs can also affect gene

expression by inhibiting the nucleocytoplasmic shuttling of transcriptional regulators (e.g. lncRNA *NRON* blocks *NFAT* shuttling) or the nuclear sub-compartment localization of a histone modifier (**Figure 1.6D**) (e.g. *MALAT1* affects Polycomb 2 nuclear localization). Last but not least, a distinct class of lncRNAs which are expressed from enhancers (eRNAs), can activate the Mediator complex which then mediates DNA looping between the enhancer and a target gene in order to enhance its expression (**Figure 1.6E**).

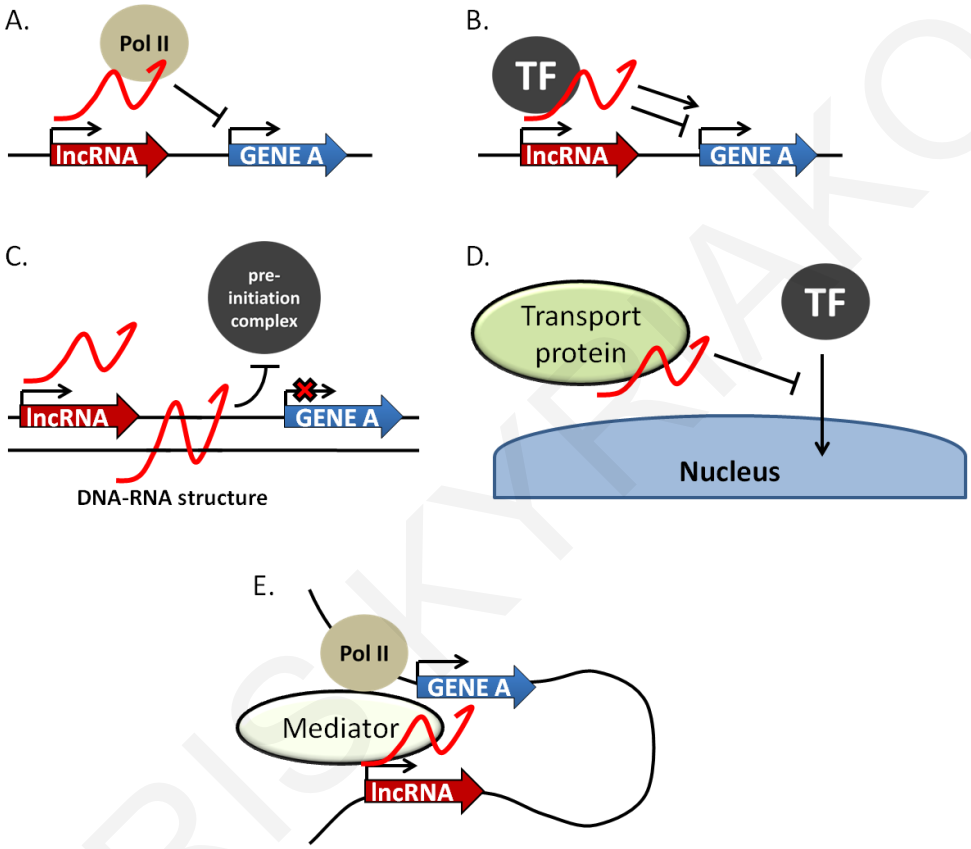

Figure 1.6: lncRNA transcripts regulate gene expression by several mechanisms aside chromatin modulation. A. and B. The expressed lncRNA (red curvy line) physically binds to RNA polymerase II (PolI) (**A**) or to transcription factors (TF) (**B**) and regulates their transcriptional activity towards other genes (e.g., Gene A). **C.** The lncRNA forms a DNA-RNA structure that blocks the binding of the pre-initiation complex on Gene A therefore inhibiting its expression. **D.** The nucleocytoplasmic shuttling of a transcription factor is blocked by the physical interaction between its transporter protein and the lncRNA (red curvy line). **E.** lncRNAs expressed from enhancers bind to the Mediator complex and cause chromosome looping which leads to activation of Gene A expression.

In addition, the act of lncRNA transcription (not the lncRNA transcript), can itself control the expression of adjacent genes in a process generally known as transcriptional interference. For example, transcriptional interference occurs when uaRNAs transcription blocks binding of the Pol II machinery to the promoter of a neighboring gene (**Figure 1.7A**). Moreover, transcriptional interference also occurs when the RNA Pol II complexes,

which actively transcribe both a sense gene and an antisense lncRNA (e.g. NATs), collide with one another and stop both transcriptions (**Figure 1.7B**) [57]. Well described example of a lncRNA that control the expression of a neighboring gene through transcriptional interference is the yeast antisense *IME4* lncRNA which control the transcription of the overlapping gene *IME4* [52,58,59]. In addition to transcriptional interference the transcriptional process of some lncRNAs (e.g. *IME1*, *GAL10-1* and *PHO84* lncRNAs in yeast) can lead to chromatin changes at nearby promoters and thus influencing their expression. For example, lncRNA transcription could facilitate changes in histone modifications, nucleosome occupancy and even the composition of transcription factors to the proximal genomic regions (**Figure 1.7C**) [60–62].

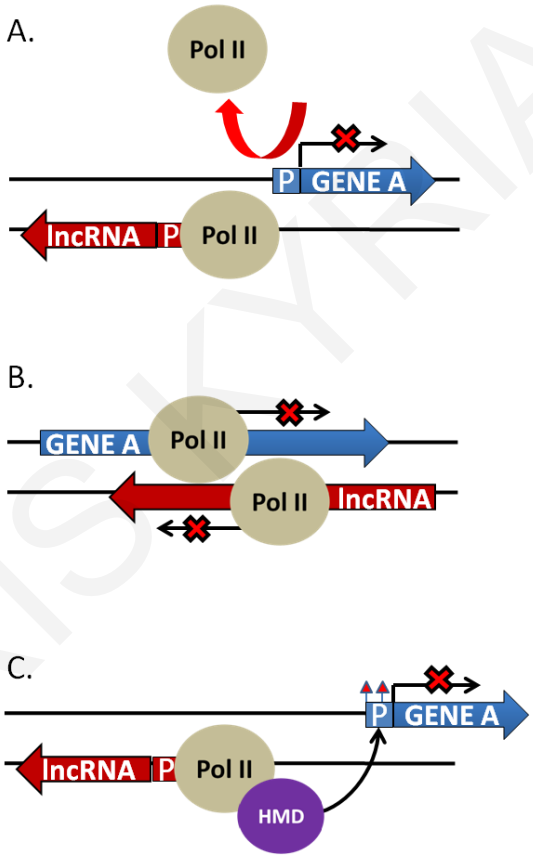

Figure 1.7: lncRNA transcription regulates gene expression of neighboring genes. A. and B. Transcriptional interference mechanisms. The transcription of the lncRNA locus (red arrow) blocks the expression of Gene A by stopping RNA Polymerase II binding to its promoter (**A**) or by Pol II collision (**B**). **C.** lncRNA transcription promotes histone modification changes (HMD: histone modifier) on the promoter (P) of the neighboring Gene A causing gene silencing.

1.8.2 Post-transcriptional regulation of mRNAs by lncRNAs

Several examples of functionally characterized lncRNAs show that they can have roles beyond transcriptional regulation. Specifically, lncRNAs can impact on most of the

stages involved in post-transcriptional mRNA processing. For instance, some antisense lncRNAs, which belong to the NAT family (e.g. antisense lncRNA loci of *cErbAalpha* and *MYC* genes), bind on the mRNA expressed from the sense overlapping gene and the resulting RNA-RNA duplex molecule can inhibit mRNA splicing (**Figure 1.8A**) [63,64]. Also, physical interaction between lncRNAs and splicing factors can affect the splicing pattern of their target pre-mRNAs (**Figure 1.8B**). One such example is the lncRNA *MALAT1* which binds on Ser/Arg splicing factors and influences their nuclear distribution and activity [65]. Some lncRNAs affect enzymatic mRNA editing procedures, such as adenosine to inosine conversion which is important for RNA structure, splicing, translation and microRNA (miRNA) binding (**Figure 1.8A**) [66]. mRNA-lncRNA interaction can increase translation of the mRNA target as in the case of the antisense mouse lncRNA called *Uchl1AS* which anneals to *Uchl1* mRNA [67]. RNA-RNA duplex formation between lncRNA and mRNA targets can also influence the stability of the latter group. Specifically, mRNAs are targeted more easily by RNA decay mechanisms, thus leading to their destruction [68]. In contrary, mRNA stability can be increased since lncRNAs can compete with miRNAs for binding on their mRNA targets [69]. lncRNAs can also act as microRNA decoys, reducing the number of free microRNAs that can block the expression of specific mRNAs. For example, the lncRNA *IPS1* in Arabidopsis thaliana binds on miR-399 and keeps it away from its target mRNAs (**Figure 1.8C**) [70].

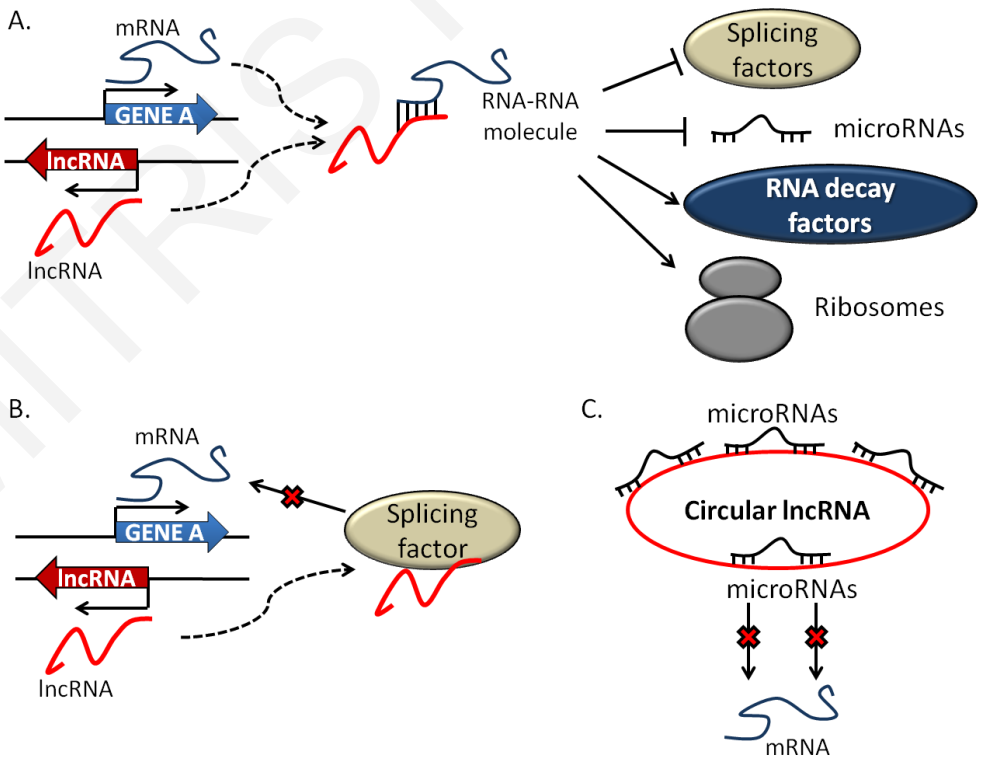

Figure 1.8: lncRNAs regulate mRNA processing by a variety of mechanisms. A. mRNA produced by Gene A (blue curvy line) and lncRNA produced from an antisense overlapping lncRNA

locus (red curvy line) bind together to form an RNA-RNA duplex. The lncRNA-mRNA interaction can protect the mRNA from splicing and microRNA-directed degradation or increase mRNA affinity by decay factors and by ribosomes. **B.** The lncRNA (red curvy line) binds on a splicing factor and blocks the splicing of a target pre-mRNA produced by Gene A. **C.** Circular lncRNA acts as a miRNA sponge since it binds and retains multiple miRNAs away from mRNA targets.

1.8.3 lncRNAs regulate protein activity

lncRNAs can regulate the function of proteins involved in gene expression such as chromatin remodelers and transcription factors as described above, however lncRNAs are also able to affect proteins involved in other biological processes. LncRNAs can be harbored onto splicing factors such as the *C.elegans* lncRNA *rncs-1* which binds and regulates the function of Dicer and other proteins towards small ncRNA processing (**Figure 1.9A**) [71]. Also, exoribonucleases involved in antiviral infections are targeted and regulated by viral lncRNAs (**Figure 1.9B**) [72]. One of the most described roles of lncRNAs is to act as scaffolds to organize higher-order complexes called ribonucleoprotein particles (RNPs). The structure of an RNP and subsequently its role as a multitasking group of proteins is supported by the scaffold lncRNA [73]. Well described examples of RNPs which are not involved in gene transcription are Telomerase complex and SRP (signal recognition particle). Telomerase complex carries an RNA component called TERC (TLC1 in yeast) which is used as a template for the synthesis of telomeres after each cell-cycle but also works as a scaffold for the formation of the complex (**Figure 1.9C**) [74]. SRP complex is responsible for moving nascent peptides from the ribosome to the endoplasmic reticulum and *SRP* lncRNA is used as a scaffold for organizing parts of this process [75]. Collectively, these data support the notion that lncRNAs are more than just a transcriptional noise, and raise challenges for further studies to be conducted.

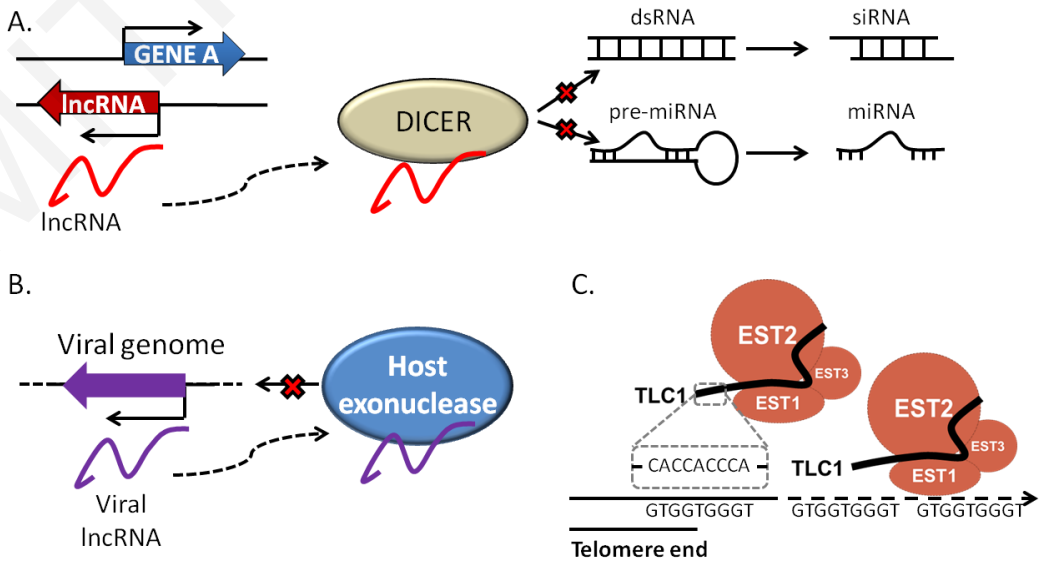

Figure 1.9: lncRNAs regulate protein activity in various cellular processes. A. The lncRNA transcript (red curvy line) physically associates with Dicer and affects the processing of small ncRNAs (double stranded RNAs (dsRNA) to small interfering RNA (siRNA) and pre-miRNA to miRNA). **B.** A viral lncRNA (purple curvy line) deactivates a host exonuclease. **C.** The yeast telomerase RNA called TLC1 (black curvy line) is used as a scaffold for the formation of telomerase on telomere ends and as a template for telomere synthesis.

1.9 lncRNAs in cell differentiation, tissue development and diseases

Transcriptome studies revealed groups of lncRNAs expressed in cell-type specific manner and during certain developmental stages, suggesting that these molecules are important regulators of cell fate. Accordingly, several lncRNAs have been implicated in embryonic development, cell differentiation, induced pluripotency and associated diseases [76–78].

1.9.1 lncRNAs regulate cell differentiation

Mutation or deletion of lncRNAs involved in X chromosome inactivation (e.g. loss of *Tsix* function) can dysregulate this process and lead to embryonic lethality in mice [79,80] or lead to maturation defects and tumorigenesis (deletion of *Xist*) [81]. lncRNAs expressed from *HOX* gene clusters are involved in cell differentiation and embryo body development. For example, knockdowns of the lncRNAs: *HOTTIP* altered the limb morphogenesis of chick embryos [82] and *HOTAIR* led to developmental defects [83]. However, upregulation of *HOTAIR* was observed in different cancers where it suppresses the expression of tumor suppressor genes [50].

Large groups of lncRNAs are expressed specifically from induced pluripotent stem cells (iPSCs) or embryonic stem cells (ESCs) and their expression pattern correlates with the expression pattern of key growth factors such as *OCT4*, *NANOG* and *SOX2* which control pluripotency. Also, lncRNAs are controlled by cell-differentiation pathways, for example the WiNTRLINC1 lncRNA which is regulated by the Wnt-pathway in intestinal stem cells and is responsible for colon cancer development [84]. Loss-of-function of the pluripotency-associated lncRNAs resulted in exit of cells from the pluripotent state and to cancer development [84–88].

1.9.2 lncRNAs 'fine-tune' organ development

The central nervous system (CNS) shows extensive lncRNA transcription and several lncRNAs have defined roles in neurogenesis. A prime example is *MALAT1* which regulates synapse formation. Knockdown of *MALAT1* in mouse neural cells decreases synapse density and dendrite growth [89]. Additionally the expression patterns of some lncRNAs expressed in the brain, such as *HAR1A* and *Evf2*, correlate with the expression of proteins involved in brain development [90,91]. lncRNAs are also involved in retina, heart, skeletal muscle, skin and hematopoietic developments and their deregulation leads to associated diseases [92].

1.9.3 lncRNAs in cancer

Genome-wide studies have revealed that one third of all genetic variants that are related to tumorigenesis are located inside non-coding genomic regions [93]. Accordingly, some lncRNAs work as oncogenes and tumor suppressors and are involved in proliferation, survival, invasion and metastasis of cancer cells and in tumor angiogenesis [94]. lncRNAs that affect cancer growth are upregulated or downregulated during cancer, they affect the expression of other genes and regulate the progress of tumorigenic pathways in cancer cells [95].

Because some lncRNAs are expressed in a tissue specific manner they can be used as diagnostic tools and as therapeutic targets for specific types of cancers [96]. Examples of tumor suppressor lncRNAs are *lincRNA-p21*, *lncRNA-LET*, *NKILA* and *NBAT-1* which are involved in prostate cancer, lung adenocarcinoma, skin cancer and renal carcinoma respectively [97–100]. Some oncogenic lncRNAs are *ANRIL*, *PCA3*, *HOTTIP* and *HOTAIR* implicated in cervical cancer, prostate cancer, hepatocellular carcinoma, pancreatic cancer, gastric cancer and colorectal cancer [101–104]. Notably, some lncRNAs, such as *H19*, *BANCR*, *MALAT1* and *XIST* work both as oncogenes and as tumor suppressors in several cancer types [105].

1.10 lncRNAs in *Saccharomyces cerevisiae*

1.10.1 Budding yeast - an excellent model organism

Saccharomyces cerevisiae (budding yeast) is a unicellular eukaryotic organism which is viable at both diploid and haploid states (16 chromosomes). *S.cerevisiae* has approximately 6000 protein-coding genes, where only ~1200 are essential (their deletion is lethal for the mutant haploid cell) and ~30% of the yeast proteins have human

orthologues. Budding yeast has a relatively simple genome (very few intronic sequences, small gaps between protein-coding genes) and is amenable to extensive genomic manipulation by simple experimental tools. Based on the above characteristics, *S.cerevisiae* is a favourite system to interrogate the function of new genetic elements such as lncRNAs.

1.10.2 Pervasive transcripts in *S.cerevisiae*

Genome-wide transcriptional studies have revealed that up to 85% of *S.cerevisiae* genome is pervasively transcribed, producing approximately 75% protein-coding and 25% long non-coding transcripts (**Figure 1.10**) [106–108]. To note, budding yeast transcriptome is deprived from short ncRNAs. Yeast lncRNAs can be divided into 2 broad groups: stable and unstable transcripts. Specifically, lncRNAs sensitive to RNA decay factors (Rrp6, Xrn1 and Rat1 respectively) are grouped to CUTs (cryptic unstable transcripts), XUTs (Xrn1-sensitive unstable transcripts) and TERRAs (telomeric repeat-containing RNAs) [7,8,33,107,109–112]. Some lncRNAs are expressed only under specific conditions such as MUTs (Meiotic unannotated transcripts) [113], CD-CUTs (Cytoplasmically degraded-CUTS) [114], stress-inducible lncRNAs [115] and TMLs (Telomerase Mutant LncRNAs) [116]. In addition, the stable lncRNAs in wild-type yeast, defined as SUTs (Stable Unannotated Transcripts), represent approximately 12% of the yeast transcriptome [7]. SUTs evade degradation in the nucleus and they are processed in the cytoplasm by Xrn1 exonuclease in a similar manner to mRNAs [38]. Thus, it was suggested that SUTs may be functionally important [10,117].

Very few SUTs have been functionally characterized and the majority of them have been associated with regulation of gene expression. For example, transcription of the lncRNA designated as *IRT1* (*IME1* Regulatory Transcript 1, also known as *SUT643*) represses the expression of its adjacent *IME1* protein-coding gene by establishing repressive chromatin modifications at the *IME1* promoter [62]. Additionally, transcription of the *GAL10* lncRNA (aka *SUT013*) recruits similar chromatin modifying activities to alter nucleosome occupancy and to repress the expression of *GAL1* and *GAL10* [61,118]. Other steady-state yeast lncRNAs control gene expression through transcriptional interference, such as *IME4*-antisense lncRNA and *SRG1* lncRNA which block the transcription of *IME4* [58] and *SER3* genes [119].

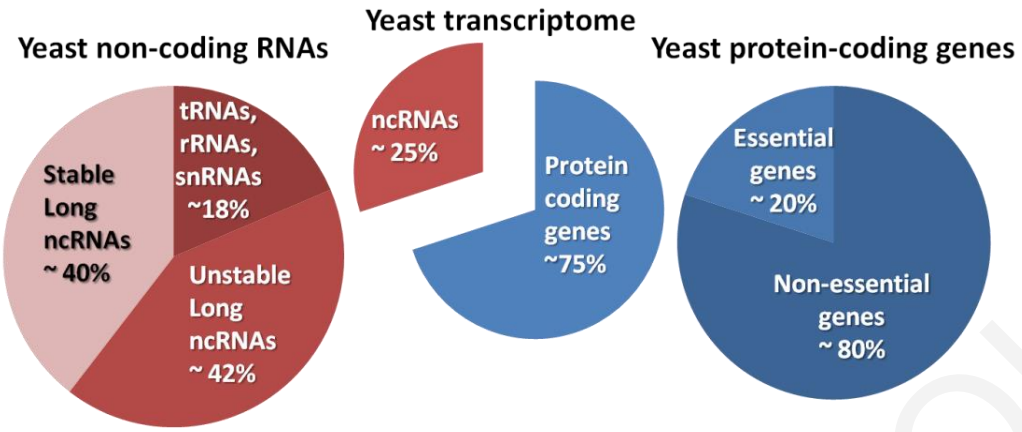

Figure 1.10: Protein-coding and non-coding transcripts in *Saccharomyces cerevisiae*. Yeast transcriptome is composed of 75% protein-coding transcripts versus 25% non-coding transcripts (middle pie chart). Yeast non-coding RNAs are divided to housekeeping (18%), stable (40%) and unstable (42%) ncRNA transcripts (red coloured pie chart) [7]. One fifth of the protein-coding genes in yeast lead to lethality upon their deletions (essential genes). The rest 80% of yeast protein-coding genes are considered non-essential (blue coloured pie chart).

1.10.3 TLC1: a model lncRNA in a model organism

TLC1 (TeLomerase Component 1) is the single most characterised yeast lincRNA that works in-*trans.* After its transcription from a non-telomeric locus on chromosome II (**Figure 1.11**), TLC1 is trafficked to all the telomeres through a chain of physical interactions of telomere organization factors [120–124]. TLC1 is one of the few lncRNAs found in a model organism with an identified functional orthologue in human cells (TERC). TLC1 and its human orthologue TERC differ in size and nucleotide sequence, nevertheless they both support the formation of telomerase complex and work as templates for telomere synthesis [125–127]. Henceforth, *TLC1* represents an example which illustrates that the function of a lncRNA can be conserved in higher eukaryotes despite changes in its sequence.

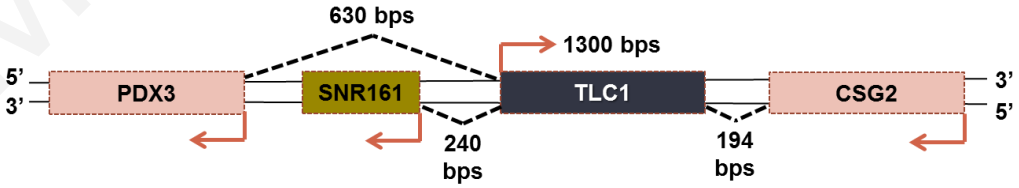

Figure 1.11: Schematic of the *TLC1* locus indicating the distance from neighbouring genes. The orientation of transcription is shown by orange arrows.

Telomerase complex is formed by using TLC1 as a lncRNA-scaffold. The protein components of telomerase complex (Est1, Est2 and Est3) bind onto TLC1 to form a

functional complex [128,129]. The role of the telomerase complex is to solve the end replication problem. Specifically, during each cycle of DNA replication a small fragment on the end of each newly synthesized chromosome is lost due to the removal of the last okasaki fragment. Then, telomerase synthesizes telomeric DNA using TLC1 as a template, thus preventing telomere shortening during each cell division (**Figure 1.12A**) [130,131]. Deletion of *TLC1* locus results to impaired function of telomerase complex therefore telomeres get shorter with each cell-cycle. In the absence of functional telomerase, telomeres are significantly shortened and cells stop dividing and senesce [132]**.** Within a population of senescing cells some survivors arise by fixing their telomere length through a 'back-up' DNA recombination-based mechanism [133]. This alternative telomere maintenance mechanism is mediated by two Rad52-dependent DNA recombination pathways; the frequently occurring Rad51, Rad54, Rad55 and Rad57 pathway and the less frequent Mre11, Rad50, Xrs2 and Rad59 pathway (**Figure 1.12B**) [133–136]. Several other individual proteins or complexes, such as the INO80 complex (Ino80, Ies1, Ies2, Ies3, Ies4, Ies5, Ies6, Taf14, Arp8 and Nhp10) also support telomeric length maintenance via homologous recombination [137–140].

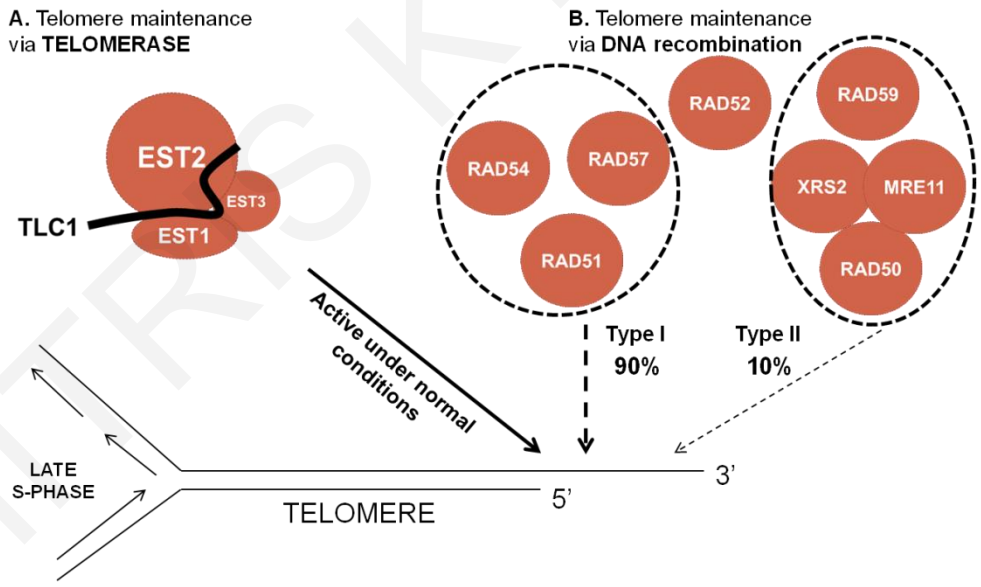

Figure 1.12: Schematic representation of telomere maintenance mechanisms in *S.cerevisiae*. A. Telomere maintenance via telomerase complex elongates telomeres during late S-phase. **B.** In the absence of active telomerase two telomere recombination pathways are activated in order to maintain telomere length. Rad51-dependent pathway (Type I survivors) (left) which is activated 90% of the time versus 10% activation frequency of Rad50-dependent pathway (Type II survivors) (right). Both pathways are controlled by Rad52 protein.

Telomerase is recruited on telomeres at a single-stranded DNA fragment (12-14 nucleotides) located at the 3'-end of telomeres, called telomeric overhang (**Figure 1.13**).

Telomeric overhangs are used as a substrate for the RNA moiety of the telomerase complex [124,138,141–147].

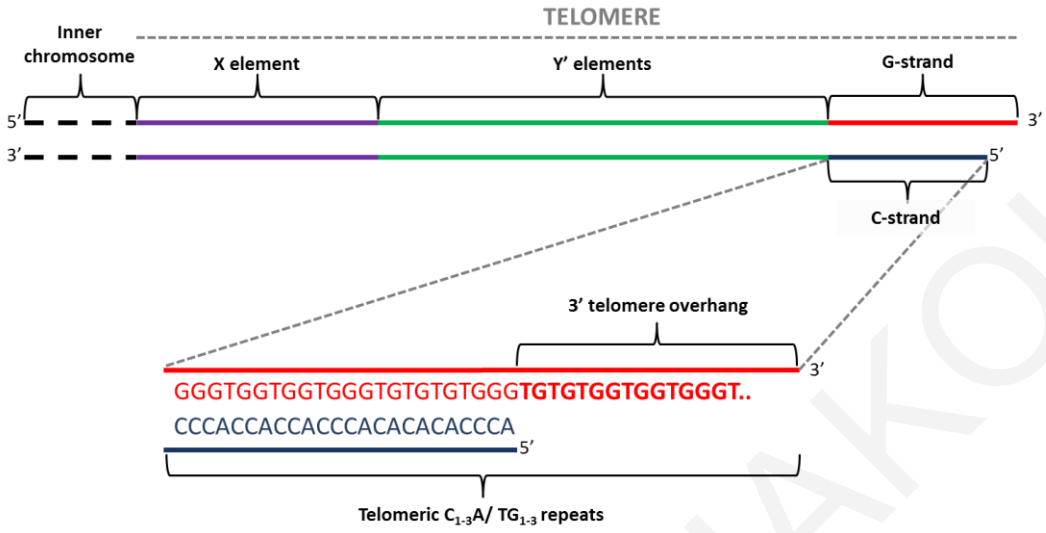

Figure 1.13: Schematic representation of a yeast telomere. Telomeres are divided into three distinct parts: X-element located in the inner site, 0 to 4 Y' elements found within the middle of the telomere and telomeric repeat strands (275-375 bps) at the end. The telomeric non-canonical repeats form the 5' C-strand ($C_{1-3}A$) and the 3' G-strand (TG_{1-3}). The G-strand is longer than the C-strand, thus forming the telomeric overhang (12-15 nucleotides).

Recruitment of telomerase on the telomeric end is facilitated by telomere-capping factors which bind both on *TLC1* and on telomerase proteins. The telomere-capping factors are tethered on the single and double strand of telomeres and play a critical role in preserving the wild-type size of telomeric overhangs during each cell division. Telomere-capping is an evolutionary conserved mechanism and formation of telomeric overhangs occurs independently of telomerase action [148]. Specifically, the capping factors block the degradation of the 5' telomeric C-rich strand (**Figure 1.13**) which is targeted and degraded by the exonucleases Exo1 and the MRX complex (Mre11-Xrs2-Rad50) [145]. The nuclease activity of these enzymes towards chromosome ends is inhibited by telomeric capping factors such as Rap1, Rif1 and Rif2 that block MRX access, and the CST (Cdc13-Stn1-Ten1) and Ku (yKU70/80) complexes which protect telomeres from Exo1-mediated degradation (**Figure 1.14**) [149,150]. Defects in telomere capping that can impact on the activity of exonucleases towards telomere ends lead to various problems including premature senescence, cell-cycle arrest and accumulation of telomeric ssDNA [149,151–153].

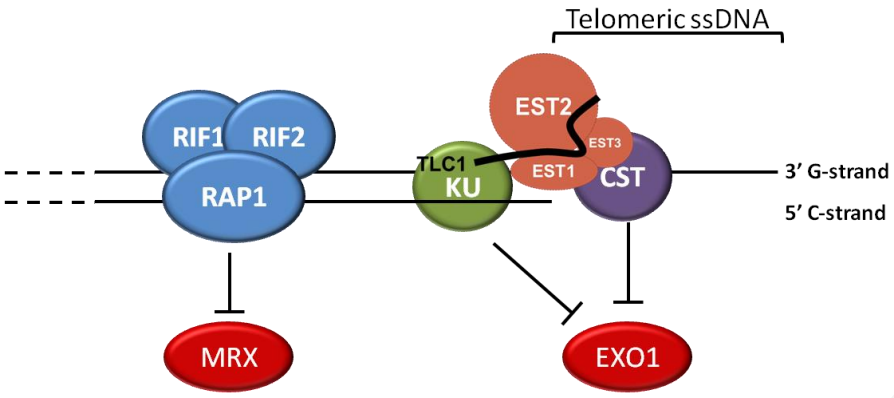

Figure 1.14: Telomere capping in yeast. The CST complex (Cdc13, Stn1, and Ten1) binds on telomeric ssDNA and the KU complex (Yku70/80) binds on both strands of telomeric DNA. CST and KU complexes block Exo1 (5'-3' exonuclease) from degrading the telomeric C-strand. Several Rif1-Rif2-Rap1 complexes are also localized across the telomere end and block the 3'-5' double-strand DNA exonuclease activity of MRX complex (Mre11, Xrs2, Rad50) towards the C-strand. MRX and Exo1 telomere accessibility is allowed only during late S-phase. The CST and KU complexes support telomerase harbouring on telomeres during late S-phase/G2.

1.11 Significance, Hypothesis and Aims

1.11.1 Significance

Genome-wide transcriptional analysis of several higher and lower eukaryotes showed that the ratio of non-coding to protein-coding DNA significantly increases as we move up on the evolutionary ladder [2]. For example, the majority of yeast genome (~85%) is pervasively transcribed; however most of the transcripts produced are mRNAs. In contrary, higher and more complex eukaryotes have much more ncRNA transcripts than protein-coding transcripts (**Figure 15).** These data raise the possibility that ncRNAs might either represent leftovers of evolution or they could possess unexpected functions that contribute to the developmental complexity of higher organisms [86,154–156]. Functional characterization of ncRNAs is therefore critical in order to answer the fundamental riddle of their biological significance.

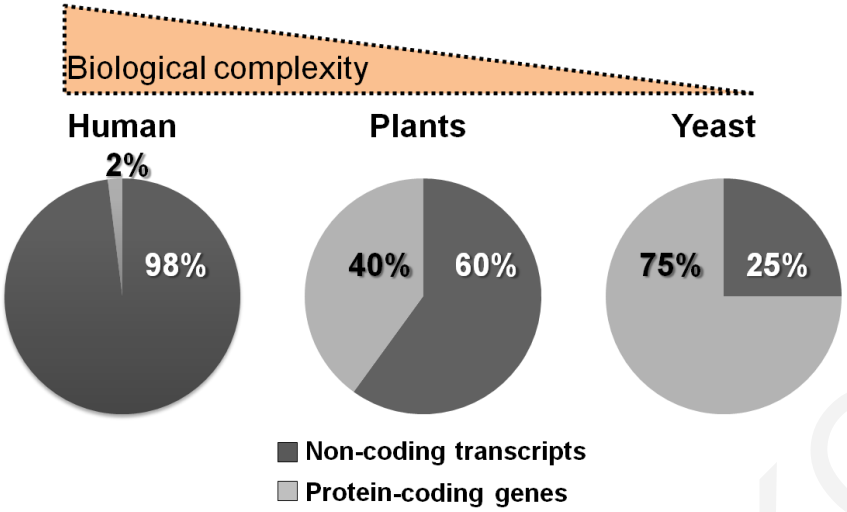

Figure 1.15: The ratio of non-coding to protein-coding transcripts increases with organism's complexity. The non-coding transcripts represent 98% of human transcriptome, 60% of plant (*Arabidopsis thaliana*) transcriptome and only 25% of yeast transcripts.

Even though long intergenic ncRNAs (lincRNAs) represent the most abundant category of lncRNAs in human cells (>10000 lincRNAs) [14], still they are the least studied. Importantly, the functional characterization of just a few lincRNAs has revealed the great importance of these molecules [157]. Illustrative examples of human lincRNAs include *HOTAIR* which works as a scaffold for multiple histone modifiers and is involved in cancer metastasis [50,158] and *HOTTIP* which is a transcriptional activator and is implicated in hepatocellular carcinoma [82]. Other functionally significant human lincRNAs include *lincRNA-p21* (transcriptional repressor of >1000 genes, trigger p53-depent apoptosis) [159] and *TUG1* (p53-induced transcriptional repressor, cell-cycle regulation) [160]. Representative examples of functionally characterized lincRNAs in *S.cerevisiae* are yTLC1/hTERC (template RNA for telomere DNA synthesis) [125,126], *SRG1* (repression of *SER3* gene transcription by nucleosome rearrangement) [161] and *IRT1* (repression of lncRNA *IME1* expression, regulate yeast gametogenesis) [162]. Collectively, the few examples of functionally characterized lincRNAs demonstrate that these molecules can have both in *cis* and in *trans* functions with diverse modes of action, since they can work as scaffolds, protein transporters and mediators of chromatin changes. Accumulating evidence suggests that lncRNAs are multipurpose since they support significant biological processes including cell-cycle regulation, apoptosis, meiosis, control of gene transcription, telomere maintenance and response to external stimuli [87,127,163,164]. Notably, increasing examples of lincRNAs are implicated in cell differentiation and development [165] and are associated to diseases such as cancer and neural disorders [166,167]. Based on the above findings, lincRNAs most likely have a significant biological impact and therefore, their functional characterization has attracted much attention in recent years.

In an attempt to elucidate the functions of lincRNAs in eukaryotic cells we are focusing on the intergenic SUTs of the model organism *S.cerevisiae*. The stability of SUTs within the nucleus of wild-type yeast cells under physiological growth conditions [7] implies that some, if not all, are functional and can support physiological cellular processes. In contrast to most studies, we are focusing on the role of lncRNAs that are not rapidly degraded and do not overlap other genes, thus we are anticipating to unveil functions for lncRNAs beyond transcriptional regulation of neighboring genes. Additionally, even though most of the known lncRNAs work in-*cis* to exhibit their activity, this study provides the possibility to discover lincRNAs that function in-*trans.* Most importantly, since it is widely accepted that only few essential lncRNAs exist, we investigated the function of SUTs in synthetic double knockout conditions in order to circumvent functional redundancy which can, in many cases, conceal the function of these molecules [168]. Collectively, we provide insights into the mode of action of lincRNAs and contribute towards the accumulation of valuable knowledge regarding the cellular roles of yeast lncRNAs, which could be conserved in human cells.

1.11.2 Hypothesis

Several studies claim that depletion of individual lncRNAs does not reveal any phenotypic effect that could suggest a putative function for the tested lncRNAs, therefore raising the possibility that these molecules might not be functional. However, it has been proposed that the biological impact of a lncRNA deletion might be masked by molecules which support the same cellular process as the lncRNA, therefore complementing its loss [168–171]. In simple terms, lncRNAs might be redundant with other genes. Consequently, we hypothesised that we can overcome the functional redundancy of lncRNAs by creating double knockout strains in a high-throughput scale. Each constructed double knockdown strain will carry deletion of the targeted lncRNA combined with a protein-coding gene deletion. A library of double knockout strains will reveal phenotypes unseen in a single lincRNA deletion strain, therefore identifying genetic interactions between the lncRNA and its functionally complementary genes. A genetic interaction between two loci indicates that they are involved in the same biological process [172]. Thus, we hypothesised that the biological function of a lincRNA can be inferred by its genetic interaction with protein-coding genes. Precisely, identifying genetic interactions for lincRNAs will allow us to link the tested transcript with cellular processes described for functionally complementary genes. For example, the deletion of an unannotated lincRNA combined with the deletion of a protein-coding gene which is involved in DNA replication will stop this procedure and subsequently block cell growth if the tested lincRNA is also involved in this process. Thus, in this example the growth change of the double deletion strain compared to the growth of

the individual single deletion strains indicates a genetic interaction between the tested lincRNA and the protein-coding gene and infers that the lincRNA is involved in DNA replication.

1.11.3 Aims of current work

Aim 1: Unveil the function of lincRNAs by identification and systematic profiling of their genetic interactions with protein-coding genes

A genetic interaction (GI) occurs when the combination of two mutations leads to a phenotype which differs from that of each single deletion strain. Each genetic interaction indicates that the two tested genes function in the same biological process. Therefore, the biological role of an unannotated locus can be revealed by its genetic interaction with annotated genes. Genetic interaction profiling has been extensively used for characterizing protein-coding genes, however this is the first time that is used for functional characterization of lncRNAs. We chose to study intergenic lncRNAs (do not overlap any other genes) in order to retain all the remaining transcripts intact after we delete the lincRNA locus.

To address this aim we will utilize an automated high-throughput assay called SGA (Synthetic genetic array) in order to combine the deletion of each protein-coding gene in the non-essential yeast deletion collection (~4500 genes / ~80% of yeast proteome) with the deletion of each lincRNA under study. Thus, each SGA will generate a library of ~4500 double mutant strains, each one carrying a protein-coding gene deletion and a deletion of the lincRNA of interest. The genetic interactions will be revealed by growth changes of each double deletion strain compared to the corresponding single deletion strains. The genetic interaction between a lincRNA and a protein coding gene indicates that the two are working in the same cellular process. Therefore, all the protein-coding genes which show GI with a lincRNA can be then listed according to their Gene Ontology annotations, thus unveiling the putative functions of the tested lincRNA.

Due to its well-described function, the lincRNA *TLC1* serves as a great proof of principle for this approach in yeast. After validating that SGA can reveal the known functions of *TLC1*, we can target unannotated lincRNAs that are stable in the nucleus, called SUTs (Stable Unannotated Transcripts). SUTs are interesting to study since they represent ~12% of all transcripts in budding yeast and only few of them have been characterized so far. Most of the characterized SUTs work in-*cis* to control gene expression of neighboring genes. However, SUTs stability might also imply functionality beyond their transcriptional site. Specifically, this project aims to unveil *trans*-acting lincRNAs by comparing the genetic interaction network of each SUT with those of its

neighboring genes. Collectively, we aim to obtain insights about the biological role and the mode of action of the tested lincRNAs based on their GI profiles.

Aim 2: Validation and in depth analysis of lincRNA functions derived by their GI profiles

The genetic studies described above will provide clues about the function of each lincRNA, however they will not describe in detail how each lincRNA implements its roles. During this aim we will validate the SGA-derived cellular role of lincRNAs and gain insights about their underlying molecular pathways(s). Specifically, positive GIs will lead us to the identification of molecular pathways which contain the tested lincRNA and its negative GIs can show pathways which work in parallel to the lincRNA pathway. Therefore, based on literature describing the molecular properties of genes in enriched GI groups, we can postulate the putative pathways and physical interactors or other co-factors of the lincRNA and design experiment for exploring lincRNA's involvement in these procedures. Collectively, the utility of genetic interaction maps in deciphering and in depth analysis of the function of long non-coding RNAs in yeast can be demonstrated by this study.

Chapter 2 - Methodology

2.1 Yeast strains, plasmids, primers and probes

Yeast strains used in this study are described in **Table 2.1**. SGA query strains were constructed by substituting the *TLC1*, *EST1* or a candidate SUT locus with the NatMX4 cassette, which confers cloNAT (Nourseothricin) antibiotic resistance, in Y7092 background strain (*MATalpha can1Δ::STE2pr-Sp_his5 lyp1Δ his3Δ1 leu2Δ0 ura3Δ0 met15Δ0*). The PCR fragment used for the above deletions was generated by primers listed in **Table 2.2**. The SGA library consists of 4289 BY4741 (MATa his3Δ1 leu2Δ0 ura3Δ0 met15Δ0) single knockout strains with each one carrying deletion of a non-essential gene. The genes were replaced with the antibiotic marker KanMX4, which confers resistance to G418 (Geneticin). The *exo1Δ* strain was constructed from scratch by transforming BY4741 cells with a PCR fragment that replaced the *EXO1* ORF with the KanMX4 cassette. The Y8835 strain in which the *HIS3* gene is substituted by NatMX4 cassette is used as the query strain in control SGA screens [173].

All isogenic strains used for follow-up experiments were generated by crossing the *sut457Δ* single mutant with single knockout strains of interest. Diploid cells were sporulated on 2% potassium acetate for 7 days at room temperature. Tetrads were isolated and subsequently manipulated using a dissection microscope (SporePlay, Singer Instruments) to generate isogenic wild-type, single and double mutant strains. All genotypes were verified by PCR analysis. For constructing the strains expressing SUT457 ectopically, isogenic WT and *sut457Δ* cells were subcultured to passage 5 and then transformed with a PCR fragment containing the *SUT457* sequence. The PCR fragment was integrated on chromosome V by homologous recombination in front of the *URA3* promoter. The ectopic expression of SUT457 was verified by quantitative real-time PCR (qRT-PCR).

Table 2.1: Yeast strains used in this study.

	Reference Number	Name	Genotype	Source
1	AK104	BY4741 (WT)	*MAT*a *ura3Δ0 leu2Δ0 his3Δ0 met15Δ0*	Euroscarf
2	AK547	Y8835 (WT)	*MATα can1Δ::STE2pr-his5 lyp1Δ ura3Δ::NatMX leu2Δ0 his3Δ1 met15Δ0 cyh2*	C. Boone
3	AK204	Y7092 (WT)	*MATα can1Δ::STE2pr-his5 lyp1Δ ura3Δ0 leu2Δ0 his3Δ1 met15Δ0*	C. Boone
4	AK586	*yku70Δ*	BY4741/Y7092 hybrid, *yku70Δ::KanMX4*	This study
5	AK587	*yku70Δsut457Δ*	BY4741/Y7092 hybrid, *yku70Δ::KanMX4,*	This study

			sut457Δ::NatMX4	
6	AK588	*mre11Δ*	BY4741/Y7092 hybrid, *mre11Δ::KanMX4*	This study
7	AK589	*mre11Δsut457Δ*	BY4741/Y7092 hybrid, *mre11Δ::KanMX4, sut457Δ::NatMX4*	This study
8	AK590	*rad51Δ*	BY4741/Y7092 hybrid, *rad51Δ::KanMX4*	This study
9	AK591	*rad51Δsut457Δ*	BY4741/Y7092 hybrid, *rad51Δ::KanMX4, sut457Δ::NatMX4*	This study
10	AK592	*rad52Δ*	BY4741/Y7092 hybrid, *rad52Δ::KanMX4*	This study
11	AK593	*rad52Δsut457Δ*	BY4741/Y7092 hybrid, *rad52Δ::KanMX4, sut457Δ::NatMX4*	This study
12	AK594	*rad57Δ*	BY4741/Y7092 hybrid, *rad57Δ::KanMX4*	This study
13	AK595	*rad57Δsut457Δ*	BY4741/Y7092 hybrid, *rad57Δ::KanMX4, sut457Δ::NatMX4*	This study
14	AK596	*rad59Δ*	BY4741/Y7092 hybrid, *rad59Δ::KanMX4*	This study
15	AK597	*rad59Δsut457Δ*	BY4741/Y7092 hybrid, *rad59Δ::KanMX4, sut457Δ::NatMX4*	This study
16	AK598	*tgs1Δ*	BY4741/Y7092 hybrid, *tgs1Δ::KanMX4*	This study
17	AK599	*tgs1Δsut457Δ*	BY4741/Y7092 hybrid, *tgs1Δ::KanMX4, sut457Δ::NatMX4*	This study
18	AK600	*pbp2Δ*	BY4741/Y7092 hybrid, *pbp2Δ::KanMX4*	This study
19	AK601	*pbp2Δsut457Δ*	BY4741/Y7092 hybrid, *pbp2Δ::KanMX4, sut457Δ::NatMX4*	This study
20	AK602	*hek2Δ*	BY4741/Y7092 hybrid, *hek2Δ::KanMX4*	This study
21	AK603	*hek2Δsut457Δ*	BY4741/Y7092 hybrid, *hek2Δ::KanMX4, sut457Δ::NatMX4*	This study
22	AK604	*gbp2Δ*	BY4741/Y7092 hybrid, *gbp2Δ::KanMX4*	This study
23	AK605	*gbp2Δsut457Δ*	BY4741/Y7092 hybrid, *gbp2Δ::KanMX4, sut457Δ::NatMX4*	This study
24	AK606	*hsc82Δ*	BY4741/Y7092 hybrid, *hsc82Δ::KanMX4*	This study
25	AK607	*hsc82Δsut457Δ*	BY4741/Y7092 hybrid, *hsc82Δ::KanMX4, sut457Δ::NatMX4*	This study
26	AK608	*cgi121Δ*	BY4741/Y7092 hybrid, *cgi121Δ::KanMX4*	This study
27	AK609	*cgi121Δsut457Δ*	BY4741/Y7092 hybrid, *cgi121Δ::KanMX4, sut457Δ::NatMX4*	This study
28	AK610	*exo1Δ*	BY4741/Y7092 hybrid, *exo1Δ::KanMX4*	This study
29	AK611	*exo1Δsut457Δ*	BY4741/Y7092 hybrid, *exo1Δ::KanMX4, sut457Δ::NatMX4*	This study
30	AK612	WT [Ura3pr::NTR]	BY4741/Y7092 hybrid, Ura3pr::NTR	This study
31	AK613	*sut457Δ* [Ura3pr::NTR]	BY4741/Y7092 hybrid, Ura3pr::NTR, sut457Δ::NatMX4	This study
32	AK614	WT [Ura3pr::SUT457]	BY4741/Y7092 hybrid, Ura3pr::SUT457	This study
33	AK615	*sut457Δ* [Ura3pr::SUT457]	BY4741/Y7092 hybrid, Ura3pr::SUT457, sut457Δ::NatMX4	This study

34	AK414	*tlc1Δ*	Y7092, *tlc1Δ::NatMX4*	This study
35	AK423	*est1Δ*	Y7092, *est1Δ::NatMX4*	This study
36	AK616	*sut457Δ*	Y7092, *sut457Δ::NatMX4*	This study
37	AK262	*sut014Δ*	Y7092, *sut014Δ::NatMX4*	This study
38	AK418	*sut451Δ*	Y7092, *sut451Δ::NatMX4*	This study
39	AK422	*sut469Δ*	Y7092, *sut469Δ::NatMX4*	This study
40	AK416	*sut042Δ*	Y7092, *sut042Δ::NatMX4*	This study
41	AK411	*sut123Δ*	Y7092, *sut123Δ::NatMX4*	This study
42	SGA-v2 library	SGA library	BY4741, non-essential *orfΔ::KanMX4 library*	C. Boone

Table 2.2: Primers and probes used in this study.

		Gene expression analysis	
	Primers	**Forward (5'-3')**	**Reverse (5'-3')**
1	SYP1	GATTCAACTCGCTGGGAGAG	GTTCTCCACGGATTCCTTCA
2	RPS14A	GAACCAAGACTCCAGGTCCA	ATCTGGCCAAAGCTCTCAAA
3	SUT457	TAGCGACAGTGGAGGTGCTA	ACAGGCGGCTATCATGTTTC
4	SNR65	GCTAGATAGTATCTGAAAGCATTCAAAC	GTTCAGAGATTTAAAACTGTCGAAAACA
		Gene deletion	
	Primers	**Forward (5'-3')**	**Reverse (5'-3')**
1	Delete *SUT042*	CTGCATTCTTCTTCCATCGTCCAGTGATATCGGTAAACCGGTAGCTTTTTCTTAAACATGGAGGCCCAGAATACCCT	AACATAAGCATGATAAATAAAAAATGCAAGATCCGCTCTCAAATTCTTTACAACGCAGTATAGCGACCAGCATTCAC
2	Delete *SUT123*	CCGCATACATTCGAACCATTACCAGAAAAACATGGAGGCCCAGAATACCCT	TAATTTTAATACTTCCCACAAGTTTGCCCAGTATAGCGACCAGCATTCAC
3	Delete *SUT014*	CGCGAATAAGTCGATATTTATGCATGGATATTTGGCCTTTTACGACACTTATTCACATGGAGGCCCAGAATACCCT	TAGAATATCCATTGTATAATATAAAAGAAAATGAAACAGTAATTATATTATATTCAGTATAGCGACCAGCATTCAC
4	Delete *SUT451*	TCACATTGTGTTGAGCACTGATAGATTAATACTATATTTCTGCTAGGTGCGGACATGGAGGCCCAGAATACCCT	ACTGTAGTCGACAGAAGGAATTTCAGTCTCTTCAATACTGCCATAGTTCAGTATAGCGACCAGCATTCAC
5	Delete *SUT457*	TTCTTTGTATTTCGTGAAAACTTGAATGCAATATAGAGTTTTTCAATCTGCAAACATGGAGGCCCAGAATACCCT	TTTTTTTTGAAGGAGGCGCGCATAAAATAATCTCACACTATTTTGAACATTGCCAGTATAGCGACCAGCATTCAC
6	Delete *SUT469*	GCAATAGCTTTTCGTGACTTGTTTTAAATACAAGGCATATAGGCGCAGCTTCACCACATGGAGGCCCAGAATACCCT	AGATCCGGTTGTTCTCAACCTTCTACATTAAGACATACTTCTACGATTTTCGAAT CAGTATAGCGACCAGCATTCAC
7	Delete *TLC1*	GTTCTCAATTAAAAGACCTTCTTTGTAGCTTTTAGTGTGATTTTTCTGGTTTGAGACATGGAGGCCCAGAATACCCT	TTATTTGTATATTGTATATTCTAAAAAGAAGAAGCCATTTGGTGGGCTTTATTACAGTATAGCGACCAGCATTCAC
8	Delete *EST1*	AAACTTATCAGGGGAAAAAGTATATTCCATTAAATGACACATGCCACCATAGATAACATGGAGGCCCAGAATACCCT	GTCGTCATAATATATTTCATATTATGATTTTTTCCCTCACCATTACTTGTTCTC CAGTATAGCGACCAGCATTCAC

9	Delete *EXO1*	GACCACATTAAAATAAAAGGAGCTCGAAA AAACTGAAAGGCGTAGAAAGGAACATGG AGGCCCAGAATACCCT	ATTTTCATTTGAAAAATATACCTCCG ATATGAAACGTGCAGTACTTAACTTC AGTATAGCGACCAGCATTCAC
		Biotinylated probes	
1	C1-3A probe (against telomeric repeats)	CACCACACCCACACACCACACCCACA - BIOTIN	
2	SUT457probe1	GCACCAACCTGACTGTGAATGCGTAAGC TGAAACA – BIOTIN	
3	SUT457probe2	BIOTIN – ATTAGCGACAGTGGAGGTGCTAGTAC	
4	ACT1	GGGCAACTCTCAATTCGTTGTAGAAGGT ATGATGCCAGATCTTTTCCATATCGTCCC AGTTGGTGACAATACCGTGTTCAATTGG GTAAC- BIOTIN	

2.2 Selection of intergenic SUTs

To select intergenic SUTs, we developed an in-house perl script (filter-SUTs-2.pl) which identified among all SUTs listed in supplementary material of Xu and colleagues [7] the ones that did not overlap any of the genomic features (file SGD_features.tab, date stamp 20070811, listed in **Table 2.3**) annotated in the SGD database (http://www.yeastgenome.org; accessed: Jan 2013). For any given SUT, genomic elements in both strands were taken into account.

Table 2.3: Genomic features considered for selecting intergenic SUTs.

	Genomic features
1	ARS
2	ARS consensus sequence
3	CDEI
4	CDEII
5	CDEIII
6	CDS
7	ORF
8	X_element_combinatorial_repeats
9	X_element_core_sequence
10	Y'_element
11	binding_site
12	centromere
13	external_transcribed_spacer_region

14	five_prime_UTR_intron
15	insertion
16	internal_transcribed_spacer_region
17	intron
18	long_terminal_repeat
19	ncRNA
20	non_transcribed_region
21	noncoding_exon
22	not in systematic sequence of S288C
23	not physically mapped
24	plus_1_translational_frameshift
25	pseudogene
26	rRNA
27	repeat_region
28	retrotransposon
29	snRNA
30	snoRNA
31	tRNA
32	telomere
33	telomeric_repeat
34	transposable_element_gene

2.3 Synthetic Genetic Array (SGA)

The knockout query strain harbouring the deletion of interest (Y7092), in this case of a lincRNA or *EST1* gene, was crossed against the SGA single deletion library described above. The diploid cells were sporulated, germinated and passaged as previously described [173] using a BM3-BC colony processing robot (S&P Robotis Inc). Haploid mutants containing the deletion of interest (lincRNA or *EST1*) and/or the corresponding protein-coding gene deletion were isolated as described previously [173] apart from the following modifications in the protocol in order to improve population purity: 1) strains were pinned 2 times instead of 1 on media selecting for *can1Δ*, *lyp1Δ* and STE2pr-Sp_his5, and 2) strains were pinned 2 times instead of one on media selecting for double deletions (**Figure 2.1**). The same procedure was followed in parallel SGA screens using the control query strain (Y8835).

Quantification of yeast colony size on the final selection plates of the SGA screen was accomplished using spImager (S&P robotics Inc). For each plate we carried out normalization procedure (using a custom built perl script) based on the average colony growth detected on the specific plate, in order to correct for uneven plate growth. We excluded from further analysis: (i) colonies on the periphery of the plate (YOR202W), (ii) genes for which the single deletion strain harbouring the relative library gene deletion

grew less than 60% of the average growth, and (iii) linkage group loci (composed of 30 genes upstream and downstream from the query gene of interest) to avoid artefacts related to potential linkage disequilibrium [173]. Finally, we report as potential GIs those genes for which the double deletion strain has at least a ±30% change in growth fitness compared to the single deletion strain. This threshold was defined based on growth changes observed for known *TLC1* genetic interactions.

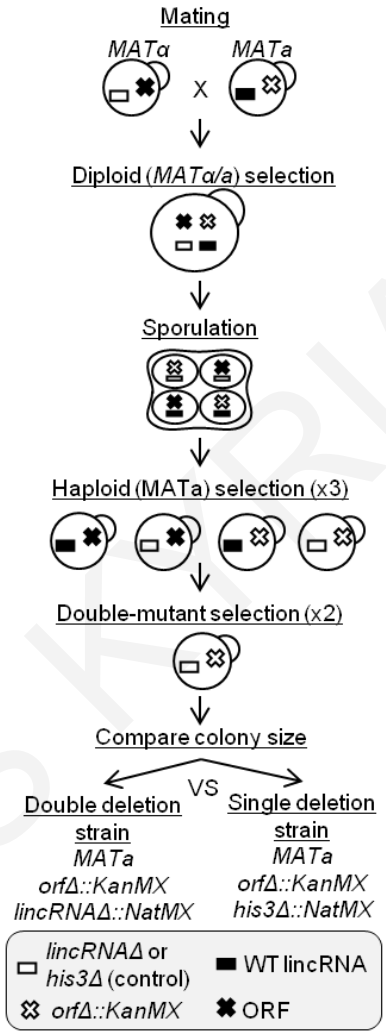

Figure 2.1: Schematic illustration of the SGA screening procedure used for studying lincRNAs. A query strain (MATα) carrying deletion of a lincRNA (white box) is mated to an array of 4289 single knockout strains (MATa), each lacking a non-essential protein-coding gene (white X mark). Following several selection steps, double mutant strains are isolated and their growth fitness is compared to the corresponding single deletion strains derived from a parallel control SGA screen.

2.4 Gene ontology (GO) analysis

The genes corresponding to the negative genetic interactions identified in each SGA screen were grouped into their annotated GO biological processes according to the

Saccharomyces Genome Database (SGD) GO Slim Mapper (http://www.yeastgenome.org/cgi-bin/GO/goSlimMapper.pl). A comprehensive list of all 102 GO biological processes used during this analysis is provided in **Table 2.4**. The Fisher's exact test (significance level α=0.05) was used to identify statistical significant enriched GO terms. The same GO analysis was performed on NGI datasets generated in this work and NGIs obtained from previous studies.

Table 2.4: List of all analysed Gene Ontology Slim terms. Gene Ontology Slim Biological Processes can be found by http://www.yeastgenome.org/cgi-bin/GO/goSlimMapper.pl

	Gene Ontology Slim Biological Processes (March/2016)
1	amino acid transport
2	biological process unknown
3	carbohydrate metabolic process
4	carbohydrate transport
5	cell budding
6	cell morphogenesis
7	cell wall organization or biogenesis
8	cellular amino acid metabolic process
9	cellular ion homeostasis
10	cellular respiration
11	cellular response to DNA damage stimulus
12	chromatin organization
13	chromosome segregation
14	cofactor metabolic process
15	conjugation
16	cytokinesis
17	cytoplasmic translation
18	cytoskeleton organization
19	DNA recombination
20	DNA repair
21	DNA replication
22	DNA-templated transcription, elongation
23	DNA-templated transcription, initiation
24	DNA-templated transcription, termination
25	endocytosis
26	endosomal transport
27	exocytosis
28	generation of precursor metabolites and energy
29	Golgi vesicle transport
30	histone modification
31	invasive growth in response to glucose limitation
32	ion transport
33	lipid metabolic process

34	lipid transport
35	meiotic cell cycle
36	membrane fusion
37	membrane invagination
38	mitochondrial translation
39	mitochondrion organization
40	mitotic cell cycle
41	mRNA processing
42	not_yet_annotated
43	nuclear transport
44	nucleobase-containing compound transport
45	nucleobase-containing small molecule metabolic process
46	nucleus organization
47	oligosaccharide metabolic process
48	organelle assembly
49	organelle fission
50	organelle fusion
51	organelle inheritance
52	other
53	peptidyl-amino acid modification
54	peroxisome organization
55	protein acylation
56	protein alkylation
57	protein complex biogenesis
58	protein dephosphorylation
59	protein folding
60	protein glycosylation
61	protein lipidation
62	protein maturation
63	protein modification by small protein conjugation or removal
64	protein phosphorylation
65	protein targeting
66	proteolysis involved in cellular protein catabolic process
67	pseudohyphal growth
68	regulation of cell cycle
69	regulation of DNA metabolic process
70	regulation of organelle organization
71	regulation of protein modification process
72	regulation of translation
73	regulation of transport
74	response to chemical stimulus
75	response to heat
76	response to osmotic stress
77	response to oxidative stress
78	response to starvation

79	ribosomal large subunit biogenesis
80	ribosomal small subunit biogenesis
81	ribosomal subunit export from nucleus
82	ribosome assembly
83	RNA catabolic process
84	RNA modification
85	RNA splicing
86	rRNA processing
87	signaling
88	snoRNA processing
89	sporulation
90	telomere organization
91	transcription from RNA polymerase I promoter
92	transcription from RNA polymerase II promoter
93	transcription from RNA polymerase III promoter
94	translational elongation
95	translational initiation
96	transmembrane transport
97	transposition
98	tRNA aminoacylation for protein translation
99	tRNA processing
100	vacuole organization
101	vesicle organization
102	vitamin metabolic process

2.5 Venn diagrams

Venn diagrams for GI datasets were generated using the on-line tool Venny *2.0* (http://bioinfogp.cnb.csic.es/tools/venny/). Significance of the overlap between gene sets was evaluated using the hypergeometric test, as implemented in the R function 'phyper' (http://www.R-project.org/), setting the significance level to α=0.05.

2.6 RNA isolation and gene expression analysis

Total RNA from logarithmically grown (OD 0.8) yeast cells was isolated using the hot phenol extraction method [174] and treated with the TURBO DNA-free DNase kit (Ambion, AM1907). For cDNA preparation, 0.5 μg RNA (DNase treated) was treated with PrimeScript Reverse Transcriptase (Takara, 2680A). The quantity of cDNA was determined by qRT-PCR analysis performed on a Bio-Rad CFX96 Real-Time PCR system using SYBR Green (Kapa SYBR Fast Master Mix # KK4602) and the primers listed in **Table 2.2.**

2.7 Northern blot analysis

Isolated total RNA was first treated with DNAse and then mixed with 10μl deionized Formamide, 3.5μl 37% Formaldehyde and 2μl loading buffer (0.1M MOPS pH7, 40mM Sodium acetate, 5mM EDTA pH8.0) to a final volume of 20 μl. The sample was then heated at 70 ^{0}C for 10 min and electrophoresed on agarose-formaldehyde gel (1% agarose, 200mM MOPS pH7, 10mM EDTA, 50mM NaOAC, 6.7% formaldehyde) at 100 volts for 30 minutes. The gel was stained with ethidium bromide (0.75 ug/ml) to ensure RNA integrity and then equilibrated with 10x SSC buffer for 30 min (150 mM NaCl and 15 mM sodium citrate, pH7) prior to transferring onto Hybond-N+membrane (GE Healthcare, RPN303B) using overnight capillary transfer with 20X SSC. The RNA was UV cross-linked (700 Joules/cm2) onto the membrane and hybridized with 50ng/ml biotinylated probes (**Table 2.2**) in 25 ml Church buffer (0.5M $NaPO_4$ pH 7.2, 1mM EDTA pH 8, 7% SDS, 1% BSA) at 50 ^{0}C overnight. The membrane was treated with Chemiluminescent Nucleic Acid Detection Module (ThermoFisher Scientific, 89880) and then exposed using the UVP Bioimaging system (Syngene).

2.8 Native and denatured southern blotting

Genomic DNA from non-synchronized saturated cell cultures was digested overnight with *XhoI* (Takara, 1094A) and then separated on 1% agarose gel (15 cm in length) for 18 hours at 25 volts. E.coli exonuclease I digestion (New England biolabs, M0293S) was performed prior to *XhoI* digestion of the genomic DNA. Analysis of the telomeric single-stranded overhangs was performed under native conditions by treating the agarose gel with 10X SSC buffer (0.17 M Trisodium citrate, 1.5M NaCl) for 30 minutes at room temperature (RT). The DNA bands were then transferred onto Hybond-N+membrane (GE Healthcare, RPN303B) using a Trans-Blot Semi-Dry electrophoretic transfer cell (Bio-Rad Laboratories) as previously described [175]. The DNA was UV cross-linked (700 Joules/cm2) on the membrane and hybridized with 50ng/ml biotinylated $C_{1\text{-}3}A$ probe (**Table 2.2**) in 25ml Church buffer (0.5M $NaPO_4$ pH 7.2, 1mM EDTA pH 8, 7% SDS, 1% BSA) at 50^{0}C overnight. Probe-bound DNA fragments corresponding to telomeric single-stranded overhangs were treated with the Chemiluminescent Nucleic Acid Detection Module Kit (ThermoFisher Scientific, 89880) and detected using the UVP Bioimaging system (Syngene). Following detection of the single-stranded telomeric overhang, the blot was incubated under denaturing conditions (0.4 M NaOH, 0.1% SDS) at 45^{0}C for 30 minutes. The blot was then probed and processed as above to detect denatured telomeric fragments. The intensity of the signals corresponding to native and

denatured Y' telomeric bands were quantified by histogram analysis (Adobe Photoshop CC 2015).

2.9 Single-colony re-streaking assay

Isogenic haploid strains derived from tetrad dissection are streaked on solid YPAD (Yeast extract, Peptone, Adenine hemisulphate, Dextrose) medium and incubated at 30^{o}C for 2 days until the appearance of single colonies (~25 cell divisions) corresponding to passage 1. Then, individual colonies from each wild-type and mutant strain were sequentially re-streaked on new solid YPAD plates until the appearance of colonies corresponding to passage 5 [140]**.**

2.10 Senescence assay

A single colony from each indicated isogenic haploid strain was used to inoculate YPAD liquid medium and the culture was grown overnight at 30^{0}C until saturation. The following day each culture was diluted to OD_{600} of 0.01 in fresh YPAD medium, incubated for 24 hours at 30^{0}C and the OD_{600} was then determined corresponding to the value of passage 1. The culture was then re-diluted to OD_{600} of 0.01 and the same procedure was repeated for passages 2-10 [140]**.**

2.11 Growth assays by serial spotting

Haploid cells from a selected tetrad were incubated separately in 5ml YPAD o/n at 30^{o}C. The next day they were diluted to OD ~ 0.1 in 5ml YPAD and allowed to grow to OD 0.6 - 0.8. Then 100μl of each culture was serially diluted, placed on SC complete plates and incubated in 30^{o}C for 2 days.

2.12 Growth assay in liquid cultures

Cells were grown overnight in liquid rich (YPAD) medium at 30°C until saturation. Cultures were then diluted to O.D. 0.1 in liquid medium with 2% glucose and grown at 30°C. The OD_{600} of each strain was measured every 1 hour for a total of 24hours using Infinite M200 (Tecan Trading AG).

Chapter 3 – Results

(Text and figures of this Chapter were adapted from Kyriakou et al., 2016 [176])

3.1 SGA reveals diverse functions for yeast lincRNAs

Although genome-wide transcriptional studies have revealed that an enormous amount of non-coding RNAs are being synthesized by the *S. cerevisiae* genome, a relatively small number of these lincRNAs have been functionally characterised [10,177]. We reasoned that we could obtain insights about the function of yeast lincRNAs by mapping comprehensively their genetic interactions through an approach that has been previously applied for protein-coding genes [178]. Therefore, we employed the SGA methodology to construct double mutants in which the deletion of an intergenic SUT (*sutΔ*) is systematically combined with individual deletions of non-essential genes in budding yeast. Genetic interactions are scored in double mutants that show significant deviation in fitness compared to the growth of the corresponding single gene deletion strains generated during the control SGA screen (Chapter 2 - Methodology). Specifically, a negative genetic interaction (NGI) refers to a more severe fitness defect in the double mutant compared to the corresponding single gene deletion mutants. Conversely, a positive genetic interaction (PGI) refer to double mutants with less severe fitness defect than the expected. Usually, double mutant strains with similar growth to one of the two corresponding single deletion strains are indicative of positive genetic interactions. The precise stepwise procedure used for the SGA screens and the deviations from a conventional approach [173] are shown in Chapter 2 - Methodology.

3.1.1 *TLC1* validates the SGA approach for interrogating the function of lincRNAs

To demonstrate proof of concept for the aforementioned rationale, we initially applied the SGA procedure to the yeast lincRNA *TLC1,* which has a well-defined cellular role in telomere maintenance [130,131]. The SGA screen was carried out in duplicate by combining the *tlc1Δ* strain against an ordered array of approximately 4500 viable protein-coding gene deletion strains. A total of 116 NGIs and 261 PGIs of *TLC1* were identified within the two SGA screens (Chapter 6 - Appendices). We identified NGIs with Ku complex components (*YKU70/80*) whose synthetic lethal interactions with *TLC1* were previously reported [179]. Moreover, *TLC1* showed NGIs with *RAD51, RAD52, RAD54* and *RAD57* genes, whose proteins are integral components of the Rad52-mediated telomere recombination pathway [133] and with the Ino80 chromatin remodelling complex

that is also implicated in telomere lengthening via homologous recombination [140]. Since PGIs are typically detected among components of the same protein complex [172,180], we also found that *TLC1* has a positive genetic interaction with its co-factors *EST1* and *EST2,* which are subunits of the telomerase complex. We validated the GIs by analysing the growth of isogenic WT, single and double deletion strains in liquid cultures (**Figure 3.1**).

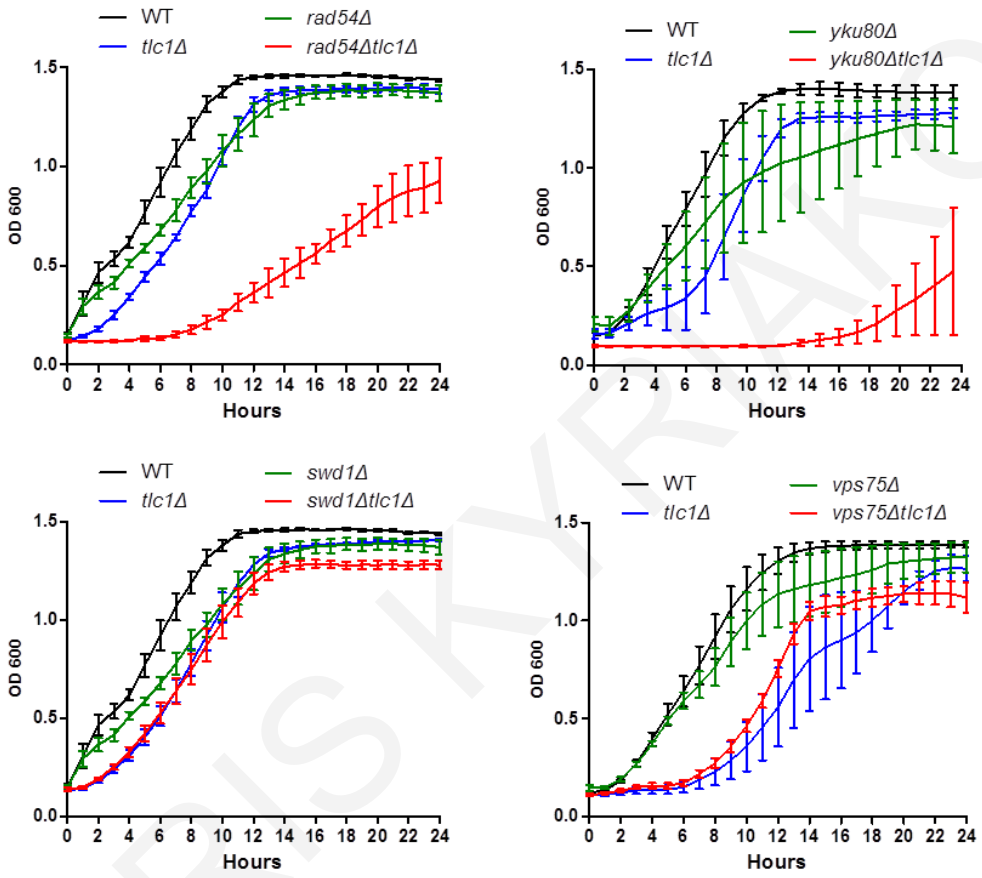

Figure 3.1 Growth curve analysis validates the negative GI of *TLC1* with *RAD54* and *YKU80 and* the positive GI with *SWD1* and *VPS75.* The growth curve of the indicated isogenic strains represents the optical density (y-axis) of liquid cultures per hour (x-axis) for 24 hours. Error bars represent SEM of 3 independent tetrads.

To further support the relevance of the identified GIs with the function of *TLC1*, we then performed Gene Ontology (GO) analysis of our SGA data, as an objective metric for deriving functional utility from GI datasets [181]. We chose to perform GO enrichment analysis using only NGIs, since the SGA technique demonstrates higher precision rate on detecting true NGIs compared to true PGIs and in addition, NGIs frequently occur between genes with overlapping functions [172,178,182]. In agreement with the individual genetic interactions mentioned above, GO analysis of all *TLC1* NGIs significantly enriched the biological process terms, telomere organization (p-value=0.00081) and DNA

recombination (p-value=0.0049). Furthermore, *TLC1* NGIs significantly enriched the term chromatin remodelling (p-value=0.0027) (**Figure 3.2**).

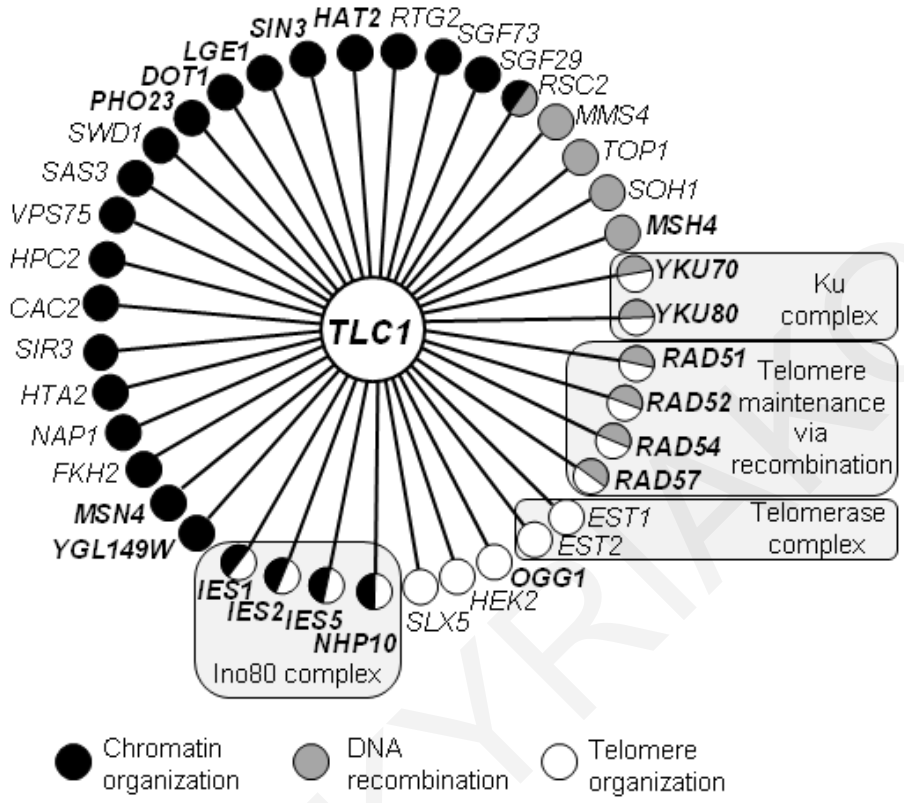

Figure 3.2: The genetic interaction network of *TLC1* corresponds to its cellular functions. Genetic interactions (GIs) of *TLC1* associated with the three indicated Gene Ontology (GO) biological processes. Gene nodes are coloured according to their assigned GO annotation. Negative (bold letters) and positive (regular font) genetic interactions that belong to the three GO terms are shown. Previously established *TLC1* cofactors are highlighted in light grey boxes.

Chromatin remodelling has been associated with telomere maintenance, however the underlying mechanism supporting this link is not well-understood yet. For example, telomere length changes are directly associated with chromatin remodelling changes which affect the expression of subtelomeric genes by a procedure generally known as telomere position effect. Additionally, chromatin remodelling factors such as Ino80 complex could promote telomere maintenance via DNA recombination by altering chromatin structure on the telomeres. Finally, genetic studies have revealed a large number of genetic interactions between chromatin remodelling genes and protein-coding gene that encode the members of telomerase complex [140,183–185].

In order to analyse further the observed *TLC1* correlation to chromatin remodelling we examined gene expression changes at genome-wide level in *tlc1Δ* cells. We have revealed an enormous number of genes, which are upregulated (482 genes) or downregulated (92 genes) by at least 1,7 fold in *tlc1Δ* cells (**Figure 3,3**). This evidence

supports the connection between *TLC1* and various chromatin remodelers that were obtained through SGA-derived genetic interactions. These results lay down the foundation for future study of *TLC1* involvement in chromatin organization.

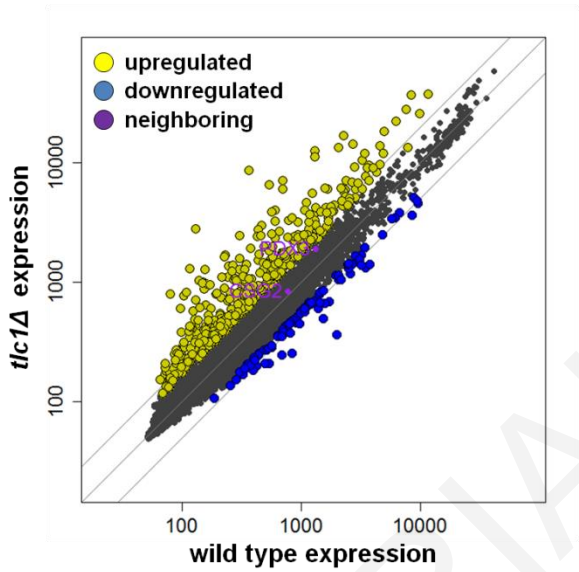

Figure 3.3: Deletion of *TLC1* exhibits gene expression changes in a number of yeast genes. Scatter plot comparing expression values in libraries derived from wild type *TLC1* (x-axis) and *tlc1Δ* (y-axis) yeast cells. According to van Wageningen et al. [186], 1,7-fold was set as a threshold for significant gene expression change. Points displayed in yellow are genes that are 1,7-fold upregulated in *tlc1Δ.* Points in blue are genes that are 1,7-fold-downregulated in *tlc1Δ*. The black points represent genes where no significant difference in expression was observed between wild-type and *tlc1Δ* cells. The two neighbouring genes of *TLC1* (*PDX3* and *CSG2*) are shown by purple dots. The expression profile of *tlc1Δ* cell was generated by Dr. Thanasis Margaritis (Frank Holstege Lab, Princess Máxima Center for pediatric oncology, Utrecht, Netherlands) using DNA microarrays as described in [186].

It was previously demonstrated that genes with highly similar genetic interaction profiles have strong functional relationship to the extent that they can be physical partners within the same complex [178]. Hence, we hypothesized that *TLC1* should have a genetic interaction profile that is highly correlated to the profile of other components of the telomerase complex. To test this hypothesis and support the validity of our *TLC1* SGA screens, we performed an independent SGA screen for the protein-coding gene *EST1* which encodes a subunit of the telomerase complex. We identified 34 NGIs for *EST1* of which 22 were common with *TLC1* NGIs (p=2.004E-29), indicating that their GI profiles are highly related (**Figure 3.4A**). The shared GIs between *EST1* and *TLC1* enrich for the GO terms telomere organization and DNA recombination that are related to their cellular function (**Figure 3.4A**). To further examine the validity of our SGA screens, we also compared our identified *TLC1* GIs to *EST1* GIs reported in previous studies. Notably, about 40% of *TLC1* NGIs identified in this study were also revealed as *EST1* negative

genetic interactions by two independent SGA studies [178,187]. Once again, the common NGIs between *TLC1* and *EST1* enrich the GO terms telomere organisation and DNA recombination (**Figure 3.4B and C**). Overall, these findings demonstrate that SGA-derived GIs can illuminate the biological role of *TLC1*, and support the utility of this approach in identifying the function of other uncharacterised yeast lincRNAs.

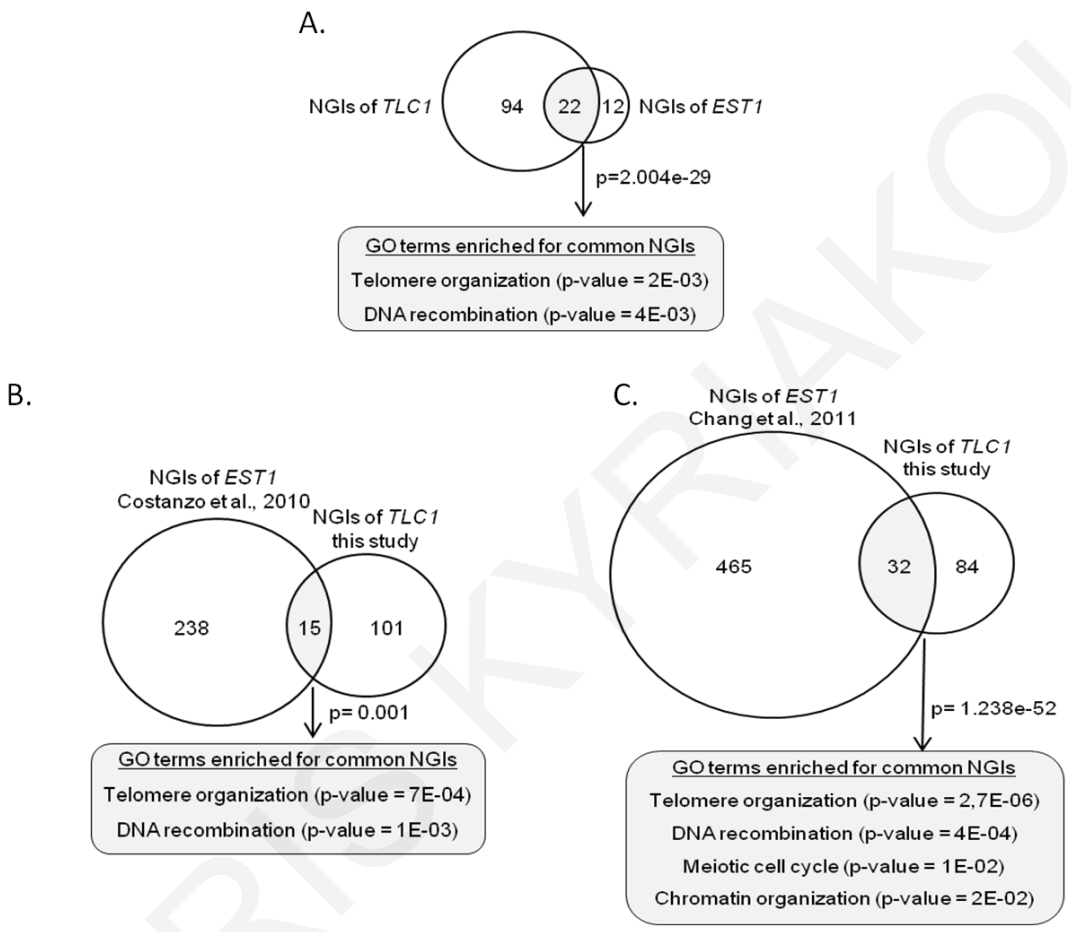

Figure 3.4: *TLC1* genetic interaction profile validates the established relationship with its telomerase partner, *EST1*. A. Venn diagram showing the significant overlap (p=2E-29) between genes classified as having a negative genetic interaction with *TLC1* and *EST1* in this study. **B.** Venn diagram showing the significant overlap (p-value=0.001, generated using the hypergeometric test) between genes whose deletions result in negative genetic interactions with *TLC1* in this study and with *EST1* as reported in [178]. GO terms enriched by common NGIs with p-value<0.05 (generated using the Fisher exact test) are indicated below the Venn diagram. **C.** Same analysis as in (**A**) between negative genetic interactions identified for *TLC1* in this study and those reported for *EST1* in [187]. The p-value was generated using the hypergeometric test (phyper).

3.1.2 SGA analysis implicates intergenic SUTs in diverse cellular processes

The *S. cerevisiae* genome encodes approximately 850 SUTs [7] of which 95 are intergenic (**Table 3.1**) since they do not overlap any other known genomic features (Chapter 2 - Methodology). We then applied the SGA procedure to six intergenic SUTs that differ in size, distance from adjacent genes and level of expression (**Table 3.1 and Appendix 16**) [7,107]. Before proceeding with SGA we initially examined the growth of the single deletion mutants of each individual intergenic SUT and did not find any significant growth changes compared to wild-type cells (**Figure 3.5**). As explained above, this finding supports the need of exploring globally double deletion mutants for these lincRNAs in order to illuminate possible cellular functions.

Table 3.1: Intergenic SUTs identified in Xu et al., 2009. Gene boundaries were considered the UTR, ORF or any other feature at the start or end of a gene as annotated in the S. cerevisiae strain S288C reference genome which was used by [7].

	Unannotated Transcript ID	Start (bp)	End (bp)	Chr.	Strand	Left gene	*Distance from left gene's boundary	Right gene	*Distance from left gene's boundary
1	**SUT001**	9369	9601	1	+	NA	NA	CUT001	20472
2	**SUT004**	198775	199895	1	+	YAR042W	2520	NA	NA
3	**SUT007**	196311	196735	2	+	YBL015W	448	YBL013W	5280
4	**SUT010**	251616	252104	2	+	YBR006W	3016	SUT011	2536
5	**SUT014**	362864	364592	2	+	CUT018	1896	CUT019	1304
6	**SUT019**	532512	533192	2	+	YBR142W	1712	YBR145W	408
7	**SUT035**	205762	205938	3	+	SUT034	1320	SUT036	888
8	**SUT042**	80713	82585	4	+	YDL212W	1464	YDL210W	1952
9	**SUT054**	542179	542523	4	+	YDR041W	1608	CUT065	24
10	**SUT055**	544043	544730	4	+	CUT065	800	YDR044W	1681
11	**SUT058**	680212	680420	4	+	YDR110W	2224	YDR115W	1712
12	**SUT067**	1140661	1140701	4	+	YDR334W	152	YDR335W	104
13	**SUT083**	1500709	1501021	4	+	YDR531W	1304	YDR536W	6920
14	**SUT085**	1521093	1522253	4	+	YDRWdelta31	2344	NA	NA
15	**SUT087**	11545	11929	5	+	CUT103	1048	YEL072W	1640
16	**SUT098**	504001	504945	5	+	CUT119	2672	YER164W	144
17	**SUT105**	110185	110553	6	+	YFL014W	2440	YFL009W	5416
18	**SUT107**	256457	257401	6	+	YFR052W	2984	CUT123	4072
19	**SUT111**	74442	76698	7	+	YGL226W	624	YGL225W	104
20	**SUT123**	622051	622283	7	+	CUT151	4472	SUT124	2952
21	**SUT125**	650859	651163	7	+	YGR082W	6128	YGR088W	3456
22	**SUT126**	660091	661403	7	+	YGR089W	264	YGR090W	680
23	**SUT129**	738427	738883	7	+	YGR122W	2936	CUT155	520
24	**SUT135**	856683	857035	7	+	SUT134	6272	YGR181W	1192
25	**SUT142**	994314	994954	7	+	YGR249W	4384	CUT165	80
26	**SUT173**	516596	517260	8	+	YHR206W	1712	YHR208W	224
27	**SUT174**	522204	522596	8	+	YHR209W	1888	YHR211W	464
28	**SUT193**	387001	388449	9	+	YIR018W	1120	SUT194	792
29	**SUT211**	415136	415384	10	+	CUT213	1048	YJL	6528

30	**SUT234**	321955	322451	11	+	YKL064W	1528	YKL062W	256
31	**SUT242**	618510	619150	11	+	YKR093W	1128	YKR095W	128
32	**SUT249**	222321	222617	12	+	YLR033W	11840	SUT250	1536
33	**SUT285**	13521	14065	13	+	YML131W	2072	CUT280	912
34	**SUT298**	297121	297193	13	+	YMR012W	2064	snR78	80
35	**SUT303**	432137	433041	13	+	SUT302	1160	YMR083W	1088
36	**SUT305**	480873	481209	13	+	YMR100W	12512	YMR107W	1744
37	**SUT311**	610425	610897	13	+	YMR173W,	280	YMR175W	80
38	**SUT339**	724500	725972	14	+	CUT351	424	SUT340	1864
39	**SUT340**	727836	728060	14	+	SUT339	1864	SUT341	424
40	**SUT347**	8665	9065	15	+	YOL164W	416	SUT348	6624
41	**SUT348**	15689	16401	15	+	SUT347	6624	SUT349	5464
42	**SUT354**	40321	40569	15	+	SUT353	1152	YOL152W	136
43	**SUT363**	408138	408218	15	+	YOR040W	248	YOR042W	160
44	**SUT367**	444098	444538	15	+	YOR061W	1352	YOR063W	112
45	**SUT370**	570970	571786	15	+	YOR127W	6552	tD(GUC)O	176
46	**SUT375**	672610	673186	15	+	CUT388	1976	YOR181W	2272
47	**SUT398**	286625	287009	16	+	YPL143W	3512	SUT399	2400
48	**SUT414**	544035	544323	16	+	YPL008W	1984	YPL006W	272
49	**SUT431**	937283	937955	16	+	YPR198W	1416	CUT435	1256
50	**SUT432**	5076	6237	1	-	NA	NA	YAL067C	1040
51	**SUT433**	28085	29773	1	-	CUT436	16944	CUT437	760
52	**SUT437**	45285	45461	2	-	YBL093C	272	YBL091C-A	1064
53	**SUT444**	255772	256276	2	-	YBR009C	32	YBR011C	624
54	**SUT451**	786476	786868	2	-	YBR292C	624	SUT452	2208
55	**SUT457**	176598	176942	3	-	YCR030C	88	YCR031C	448
56	**SUT463**	411397	411565	4	-	YDL024C	1560	CUT491	2272
57	**SUT465**	443805	444197	4	-	YDL005C	1448	YDL002C	2512
58	**SUT467**	488934	489222	4	-	YDR022C	176	YDR026C	3248
59	**SUT469**	544983	545967	4	-	YDR043C	1416	CUT495	1696
60	**SUT471**	593223	593495	4	-	YDR072C	1688	CUT500	4928
61	**SUT477**	924281	924537	4	-	YDR228C	384	YDR231C	1696
62	**SUT479**	980065	980921	4	-	YDR261C	784	YDR263C	13136
63	**SUT480**	1018121	1019129	4	-	YDR277C	2240	CUT518	840
64	**SUT493**	1353241	1353553	4	-	YDR443C	3224	YDR447C	1216
65	**SUT495**	1476649	1476993	4	-	CUT537	16	YDR520C	3968
66	**SUT496**	1493649	1493945	4	-	snR84	536	YDR529C	2008
67	**SUT497**	1507393	1507489	4	-	YDR534C	320	CUT540	408
68	**SUT501**	10501	11341	5	-	SUT500	736	SUT502	3352
69	**SUT515**	363965	364309	5	-	YER101C	2112	YER105C	3200
70	**SUT518**	522869	522933	5	-	YER168C	152	SUT519	3999
71	**SUT526**	103277	103549	6	-	YFL018C	56	YFL017C	280
72	**SUT532**	17213	17709	7	-	YGL257C	2920	CUT583	4176
73	**SUT539**	165607	166127	7	-	YGL179C	528	CUT590	736
74	**SUT570**	958775	959687	7	-	YGR233C	360	YGR235C	1568
75	**SUT581**	249813	250989	8	-	YHR075C	112	YHR077C	1248
76	**SUT591**	406222	406766	8	-	YHR153C	3520	CUT652	3640
77	**SUT601**	28493	28789	9	-	NA	NA	YIL166C	1600
78	**SUT616**	427341	429437	9	-	SUT615	1976	YIR039C	904
79	**SUT617**	75557	75797	10	-	YJL190C	176	YJL187C	816
80	**SUT620**	90149	90517	10	-	YJL178C	24	YJL176C	1352
81	**SUT640**	524108	524572	10	-	YJR045C	2232	YJR047C	224
82	**SUT643**	605932	607420	10	-	YJR094C	128	CUT696	2056
83	**SUT710**	928244	928572	12	-	YLR401C	3752	CUT753	32
84	**SUT718**	146269	146301	13	-	YML064C	296	YML062C	1112
85	**SUT721**	258725	258965	13	-	YML006C	152	SUT722	512

86	**SUT722**	259477	260077	13	-	SUT721	512	YML004C	1448
87	**SUT725**	271701	271917	13	-	YMR001C	184	YMR006C	5552
88	**SUT733**	616045	616325	13	-	YMR174C	5640	SUT734	2568
89	**SUT756**	735848	736160	14	-	YNR056C	1664	CUT820	56
90	**SUT790**	832103	832295	15	-	YOR271C	32	YOR273C	1936
91	**SUT815**	443111	444271	16	-	SUT814	11480	CUT899	40
92	**SUT827**	619767	619983	16	-	SUT826	4488	CUT905	2720
93	**SUT830**	645415	645679	16	-	CUT907	176	YPR037C	776
94	**SUT834**	769743	770687	16	-	CUT914	2296	YPR120C	3032
95	**SUT847**	935951	937263	16	-	CUT925	2168	YPR199C	712

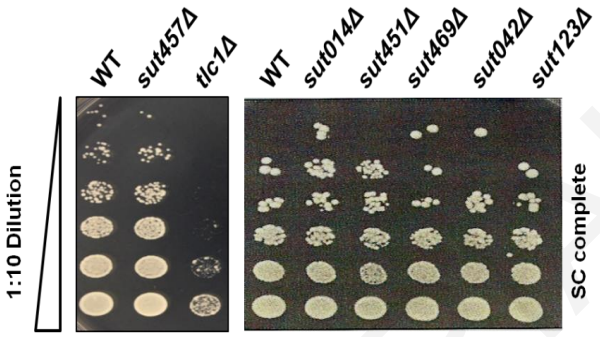

Figure 3.5: Cell growth is not affected by the single SUT deletions. Ten-fold serial spotting from meiotic spores isolated by tetrad analysis. The cells were spotted on SC complete media and let to grow at 30^0C for 48 hours. *tlc1Δ* cells show expected growth reduction.

The SGA screen for each deleted lincRNA was paired with a control SGA screen (Chapter 2 - Methodology) to minimize the 'batch effect' [172]. Specifically, screens conducted in a batch are influenced by common experimental factors such as differences in media and treatment of the cell cultures which can influence cell growth. Therefore, double mutants should be generated by SGA screens in the same batch with the control SGA screen that generates the corresponding single mutants in order to avoid variations between the screens.

We identified in total 606 negative genetic interactions and 1079 positive genetic interactions for all six tested SUTs. We subsequently analysed the NGIs of each SUT (Chapter 6 - Appendices) for the enrichment of GO biological process terms as described for *TLC1* above. Notably, all tested lincRNAs enriched at least one GO term (**Figure 3.6**) except *SUT123* which did not highlight any terms despite that it displayed 74 NGIs (Chapter 6 - Appendices). It is possible that *SUT123* is involved in multiple processes that are diluted among the identified genetic interactions. The other five SUTs exhibited NGIs which result in distinct GO enrichment profiles (**Figure 3.6**). In particular, the SGA screen using the *sut457Δ* strain enriched for the two GO terms, telomere organisation (p-value=0.022) and not-yet-annotated (p-value=0.046) (**Figure 3.6**). The latter term consists of functionally uncharacterised genes and therefore does not provide any insights into the

function of this lincRNA. Furthermore, *SUT042* also showed a specific profile since its screen enriched GO terms (membrane fusion p-value=0.039; organelle fusion p-value=0.020; vesicle organisation p-value=0.020) associated with vesicle function (**Figure 3.6**). However, the other three lincRNAs, *SUT014*, *SUT451* and *SUT469,* exhibited GO profiles that are more diverse in function. *SUT451* and *SUT469* SGA screens each enriched seven different biological processes, while *SUT014* showed the most varied profile with enrichment of ten different GO terms (**Figure 3.6**). The heterogeneous GO term profiles suggest that the latter three SUTs are pleiotropic or that the enriched cellular processes are interconnected [178]. Altogether, these results indicate that under physiological conditions intergenic SUTs are implicated in a broad spectrum of biological processes that are important for normal cell growth.

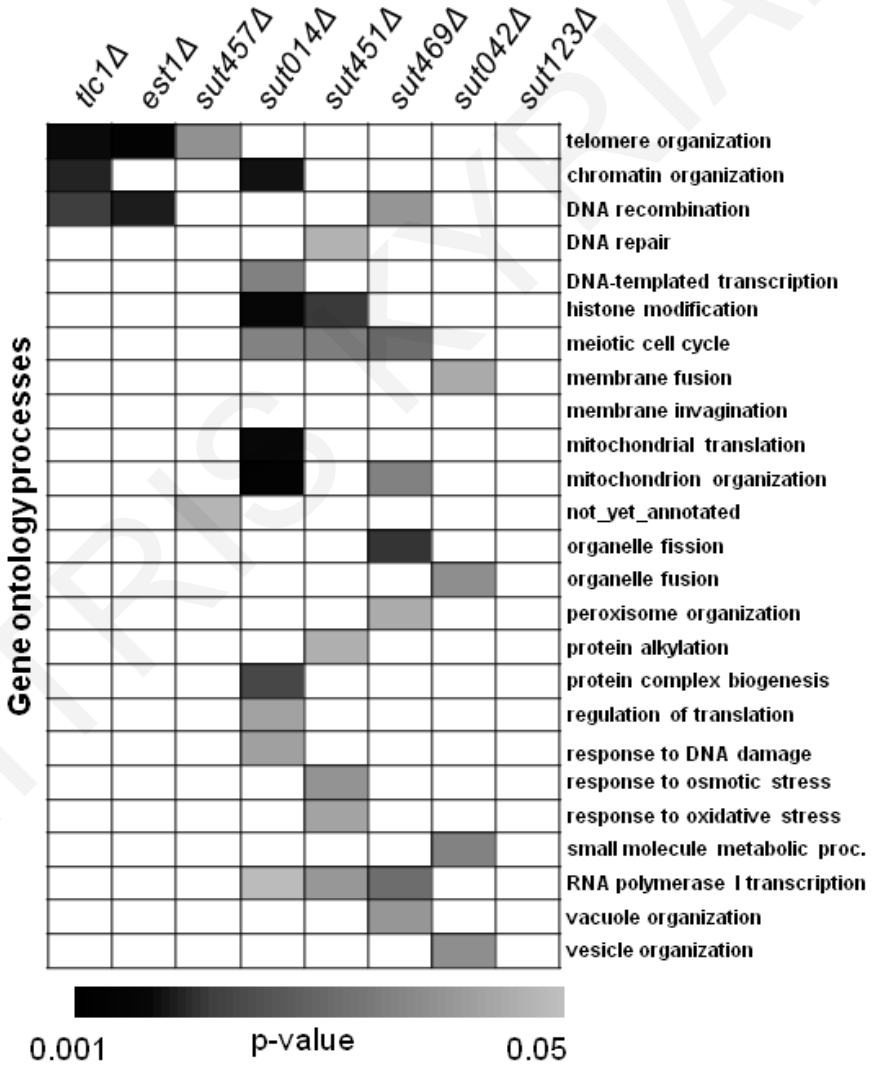

Figure 3.6: Genetic interactions link intergenic SUTs to diverse biological processes. Heatmap of GO terms enriched by genes whose deletions result in negative genetic interactions. The SGA procedure was performed for *TLC1*, *EST1* and six intergenic SUTs. The NGIs from the

different SGA screens were analysed as described in Chapter 2 - Methodology to identify enriched GO terms with p≤0.05 (generated using Fisher exact test).

Additionally, we performed high-throughput transcriptome analysis(DNA microarrays) for all the SGA-tested SUTs following the same procedure as for *tlc1Δ* described above. Interestingly, *sut451Δ* cells displayed up- and down-regulation (1,7 fold) of various genes compared to wild-type cells (**Figure 3.7**). This result is consistent with the fact that the SGA analysis of *SUT451* identified 'histone modification' as the most enriched biological process (**Figure 3.6**). Therefore, it is possible that *SUT451* might play a role in gene regulation. On the contrary, none of the other SUTs showed any changes in gene expression compared to wild-type cells, with the exception of *sut014Δ* which only upregulates its neighbouring gene, *ORC2* (>1,7 fold) (data not shown). This might indicate a neighbouring gene effect (NGE) since the expression of the antibiotic resistance cassette used for the substitution of *SUT014* for generating *sut014Δ* cells might affect the expression of neighbouring genes such as the *ORC2*. In contrary, if NGE is not the case here, *SUT014* could regulate *ORC2* expression by acting in *cis*.

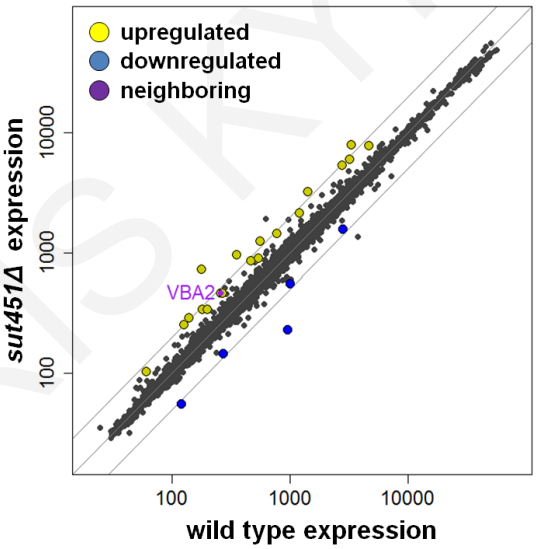

Figure 3.7: Deletion of *sut451Δ* exhibits gene expression changes in a various genes compared to wild-type cells. Scatter plot comparing expression values in libraries derived from wild type *SUT451* (x-axis) and *sut451Δ* (y-axis) yeast cells. Points displayed in yellow are genes that are 1,7-fold upregulated in *sut451Δ*. Points in blue are genes that are 1,7-fold-downregulated in *sut451Δ*. The black points represent genes where no significant difference in expression was observed between wild-type and *sut451Δ* cells. The upstream neighbouring gene of *SUT451*, *VBA2* is upregulated by less than 1,7 fold change and is shown by purple point. The downstream neighbouring gene of *SUT451*, *YBR292C* has no change in expression levels. The expression profile was generated by Dr. Thanasis Margaritis (Frank Holstege Lab, Princess Máxima Center for pediatric oncology, Utrecht, Netherlands) using DNA microarrays as described in Wageningen et al., 2010.

3.1.3 *SUT457* and *SUT042* exhibit distinct genetic interaction profiles in comparison to their adjacent genes

Previously characterised SUTs and other yeast non-coding RNAs have been linked to transcriptional regulation of their neighbouring genes [10]. Therefore, we reasoned that SGA analysis of a *cis*-acting lincRNA and of its cognate genes would most likely result in the identification of similar GIs. To compare the genetic interaction networks of the examined intergenic SUTs with those of their neighbouring genes, we exploited the genetic interaction data of protein-coding genes that are available on the DRYGIN dataset (http://drygin.ccbr.utoronto.ca/; accessed 29/02/2016) and those generated by Szappanos *et. al*. [188], which are compatible with the SGA approach used in this study. We first compared the GO enrichment profiles of *TLC1* with its upstream and downstream gene, *PDX3* and *CSG2* respectively, as controls since *TLC1* is not linked to the transcriptional control of its neighbours. As predicted, the genetic interactions of *TLC1* enrich GO terms that are distinct to those enriched by the genetic interactions of its flanking genes (**Figure 3.8**). Similarly to *TLC1*, two other lincRNAs, *SUT457* and *SUT042*, exhibit GO enrichment profiles that are completely different from those of their upstream and downstream neighbouring genes (**Figure 3.8**). In contrast, *SUT014*, *SUT451* and *SUT469,* whose GIs enrich diverse biological processes, display GO profiles that partially overlap those of their adjacent genes (**Figure 3.9**). These findings suggest that *SUT014*, *SUT451* and *SUT469* might have functions that are linked to the expression of their neighbouring genes (e.g. *SUT014* and *ORC2*) while the role of *SUT457 and SUT042* is independent to the function of their adjacent genes.

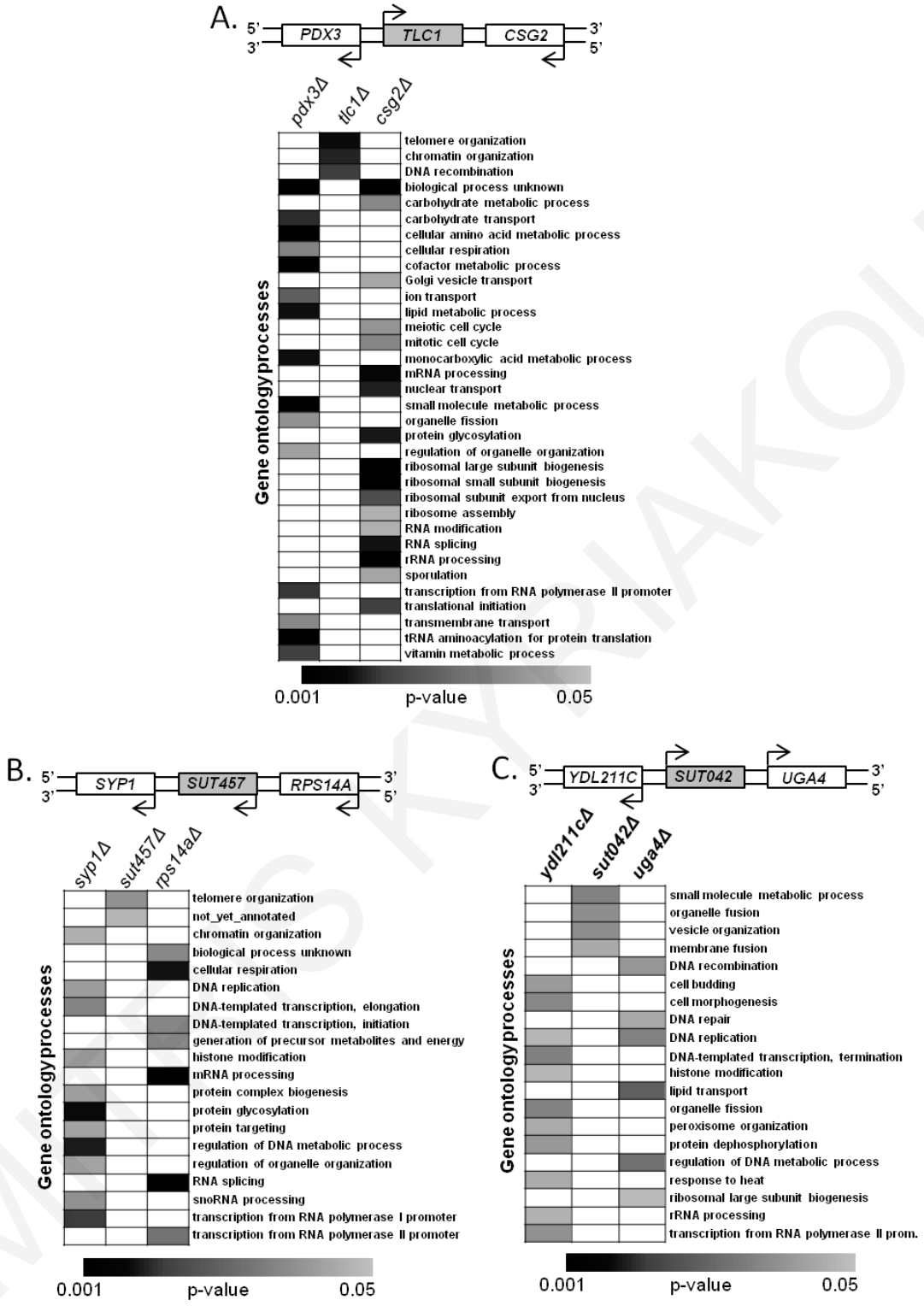

Figure 3.8: *SUT457* and *SUT042* GI profiles infer their *trans*-acting roles. Heatmap of GO terms enriched with p≤0.05 (generated using the Fisher exact test) by genes classified as having a negative genetic interaction with *TLC1* (**A**), *SUT457* (**B**), *SUT042* (**C**) or their corresponding flanking genes. The NGIs of the genes flanking the tested lincRNAs were extracted from the Drygin database (http://drygin.ccbr.utoronto.ca/) and Szappanos et al., 2011 [188]**.**

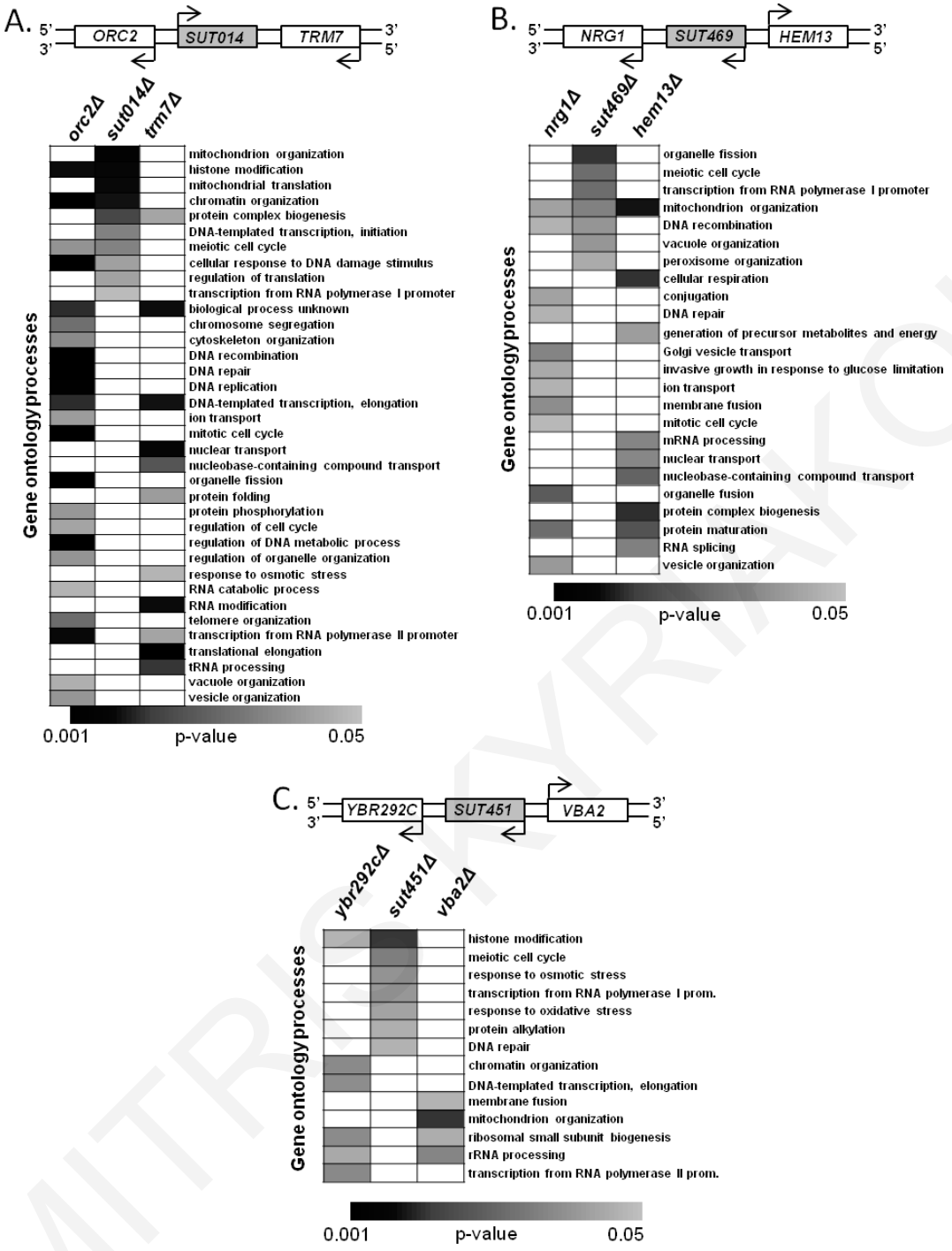

Figure 3.9: *SUT014*, *SUT469* and *SUT451* GI profiles suggest in-*cis* biological roles. Heatmap of GO terms enriched with p≤0.05 (generated using the Fisher exact test) by genes classified as having a negative genetic interaction with *SUT014* (**A**), *SUT469* (**B**), *SUT451* (**C**) or their corresponding flanking genes. The NGIs of the genes flanking the tested lincRNAs were extracted from the Drygin database (http://drygin.ccbr.utoronto.ca/) and Szappanos et al., 2011 [188]**.**

3.2 SUT457 is a novel telomere overhang homeostasis factor

3.2.1 Deletion of *SUT457* accelerates senescence in telomerase-deficient cells

Our previous findings suggest that *SUT014*, *SUT469* and *SUT451* might have in *cis* functions since their GO profiles partly overlap the GO profiles of their respective neighbouring gene. In the contrary, *SUT042* and *SUT457* GO profiles differ from those of their neighbouring genes, thus suggesting in *trans* activities in the enriched biological processes. Additionally, all the above SUTs, with the exception of *SUT457,* had shown enrichment in multiple biological processes making it difficult to pinpoint the biological process to follow with further experiments. Also, we expected that from the 9 or 10 enriched terms found in the GO profile of some of these SUTs (e.g. *SUT014*) only few (e.g. one or two) might be the direct outcome of SUT loss, while the rest could be secondary effects. Thus, despite the fact that *SUT457* GIs enriched for 'not-yet-annotated' and therefore we could not use this information for functional characterization, they also showed a very specific GO enrichment profile in telomere organization that was distinct from its flanking genes (**Figure 3.8**). Therefore, we decided to further characterise the cellular role of *SUT457* since it had the clearest enrichment profile and could possibly act in *trans*.

All SUTs tested were validated for their deletion using PCR. However, it was important to validate the deletion also at the RNA level before proceeding to further characterization. Therefore, we verified by northern blot analysis the loss of SUT457 transcript (345 bp) in the *sut457Δ* strain which was processed in the SGA screens (**Figure 3.10**). This analysis allowed us to also verify the size of this *SUT457* which was previously described in [7] and is really correct.

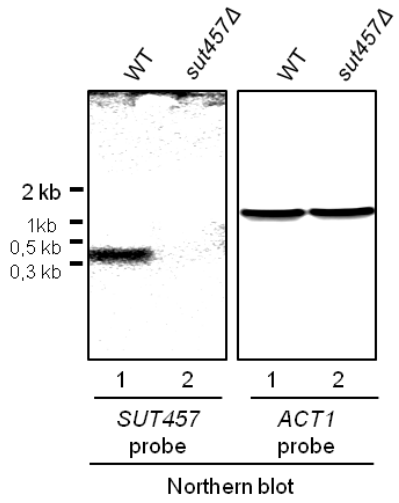

Figure 3.10: Detection of SUT457 RNA. Total RNA was isolated from wild-type and *sut457Δ* cells and analysed by northern blotting using a probe (**Chapter 2- Methodology**) against the *SUT457* sequence (**Appendix 16**). A band of 345 bp corresponding to the size of SUT457 is detected only in wild-type cells (left panel). A probe against actin (**Chapter 2- Methodology**) was used as a loading control (right panel).

Then, we examined whether construction of the *sut457Δ* strain genetically perturbs the expression of its neighbouring genes (**Figure 3.11A**). As shown in the global gene expression analysis we did not observe significant changes in the expression of any other genes. However, to confirm that there are no other changes in the vicinity of *SUT457* we used total RNA extracts from *sut457Δ* cells. Then, quantitative RT-PCR analysis showed that in *sut457Δ* cells the expression of *SUT457*-adjacent genes *SYP1*, *SNR65* and *RPS14A* remains unaffected compared to a WT control strain (**Figure 3.11B**). This result demonstrates that construction of *SUT457* deletion does not lead to the previously reported neighbouring gene effect (NGE) [189,190] and hence, it confirms that the genetic interaction network of *sut457Δ* is directly associated with *SUT457* itself and not with its adjacent genes.

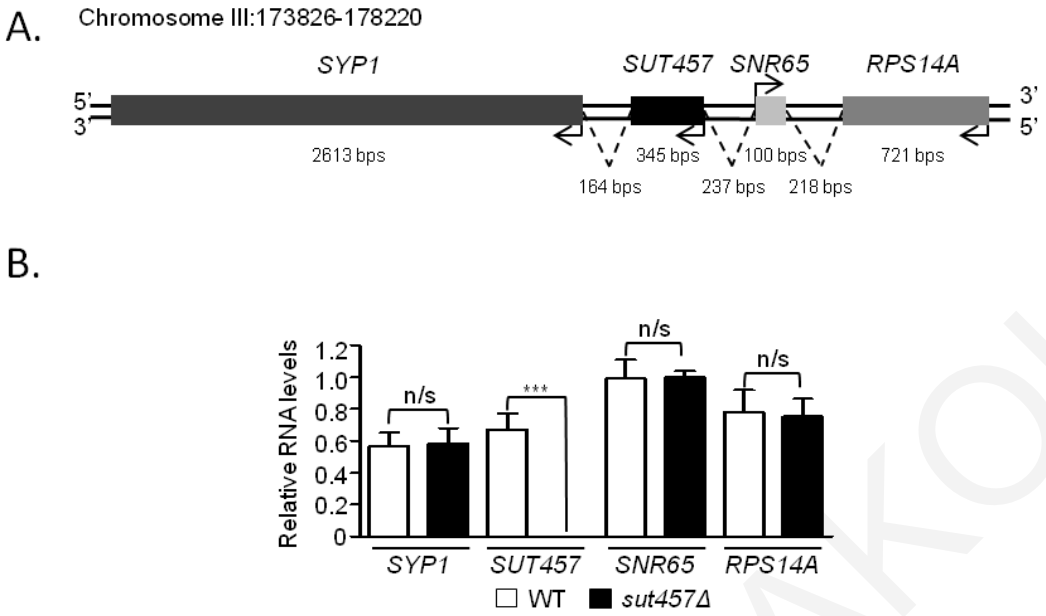

Figure 3.11: *SUT457* deletion does not change the expression of neighbouring genes. A. Schematic representation of the *SUT457* locus on Chromosome III. Arrows indicate direction of transcription. **B.** Expression levels of *SYP1*, *SUT457*, *SNR65* and *RPS14A* determined by qRT-PCR using total RNA extracted from isogenic WT and *sut457Δ* strains. The expression levels of each gene were normalised to the expression of *ACT1*. Error bars represent s.e.m resulting from three independent replicates. *** refers to p<0.001 and n/s to not-significant (generated by t-test).

SUT457 genetically interacts with 12 out of 42 telomere organisation genes (p-value=0.0145) found in the SGA deletion collection (**Figure 3.12A**). These genes are associated with roles in supporting telomerase function (*HEK2*, *PBP2*, *YKU70, TGS1*, *HSC82*) [191–194], modulating subtelomeric chromatin changes (*PBP2* and *HEK2*) [191], regulating telomere-end processing (*YKU70, GBP2, MRE11, CGI121, TGS1* and *HSC82*) [138,149,193,195–197] and controlling telomere maintenance via recombination (*RAD51*, *RAD52*, *RAD57*, *RAD59*, *MRE11*, *CGI121*) [133,140]. The genetic interactions were validated by growth assays of isogenic wild-type, single and double deletion strains (**Figure 3.12B**).

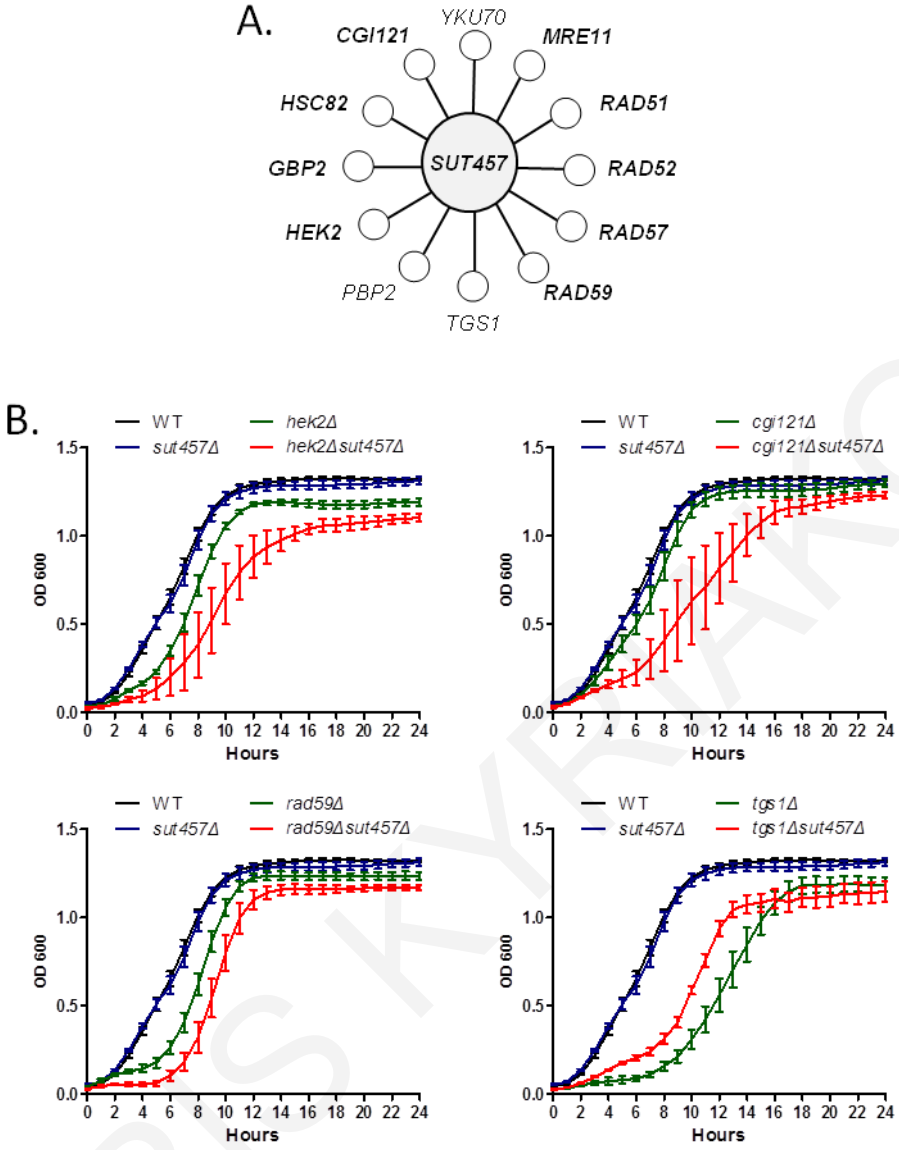

Figure 3.12: *SUT457* genetically interacts with telomere organization genes. A. SGA-derived genetic interactions (GIs) of *SUT457* with telomere regulators. Gene names in bold represent NGIs while gene names in regular font correspond to PGIs. **B.** Validation of *SUT457* GIs with four telomere organization genes (*HEK2, CGI121, RAD59* and *TGS1*). The growth curve of the indicated isogenic strains represents the optical density (y-axis) of liquid cultures per hour (x-axis) for 24 hours. Error bars represent SEM of 3 independent tetrads.

The genetic link between *SUT457* and telomere organisation initially prompted us to determine if loss of this lincRNA leads to changes in telomere length. To examine this, we used denaturing southern blot analysis and found that deletion of *SUT457* alone does not affect telomere length compared to isogenic wild-type strains (**Figure 3.13**, compare lanes 1 and 2, 28 and 29). Then we examined whether *sut457Δ* in combination with deletion of any of its 12 genetic interactors (**Figure 3.12**) affects telomere length. As expected, significantly shorter telomeres were detected in the *yku70Δ* and *mre11Δ* single mutants compared to WT cells, but telomere length was not further affected in the

yku70Δsut457Δ or *mre11Δsut457Δ* double mutants (**Figure 3.13**, compare lanes 3 and 4, 5 and 6). Consistently, *sut457Δ* in combination with deletion of the remaining telomere-related genetic interactors (**Figure 3.12**) does not have a significant change in telomere length compared to their isogenic single deletion mutants (**Figure 3.13**, lanes 7-14 and 16-27).

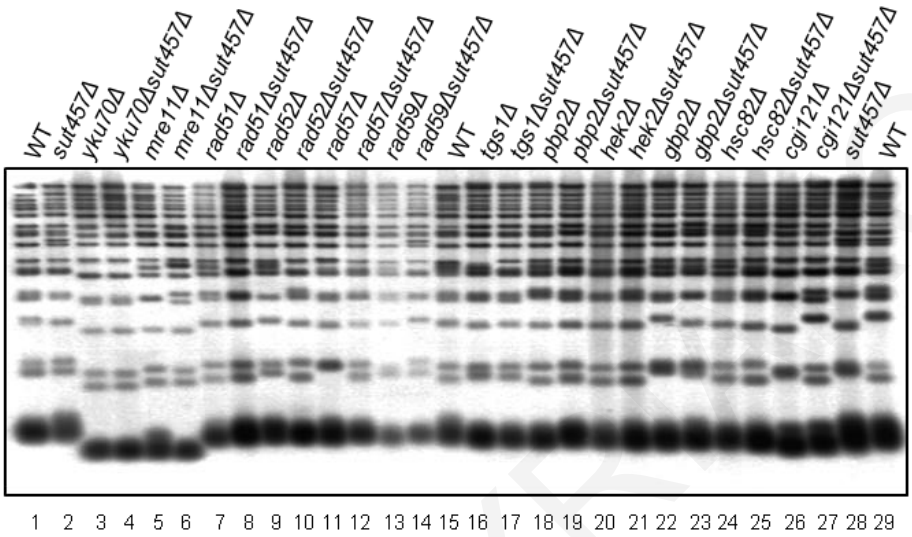

Figure 3.13: *SUT457* deletion does not affect telomere length. Telomere length analysis of genomic DNA isolated from the indicated wild-type and mutant strains at passage 1. The extracted DNA was fragmented with XhoI, analysed by Southern blotting under denaturising conditions and the telomeres where detected by a biotinylated probe against telomeric repeats.

Based on the fact that some of the telomere associated GIs of *SUT457* (e.g. *RAD51*, *RAD52, RAD57, MRE11*) are known to affect entry into senescence in telomerase-deficient cells [140,187], we next sought to determine if deletion of *SUT457* influences the rate of senescence in *TLC1* null cells. Therefore, we performed liquid senescence assays using the four isogenic strains; wild-type, *sut457Δ*, *tlc1Δ* and the double mutant *sut457Δtlc1Δ*. Consistent with the fact that single deletion of *SUT457* had wild-type telomeric length (**Figure 3.13**), we observed that *sut457Δ* and WT strains had a very similar growth profile in senescence assays (**Figure 3.14**). However, we found that the double mutant *sut457Δtlc1Δ* had an accelerated entry into senescence compared to the *tlc1Δ* single mutant (**Figure 3.14**).

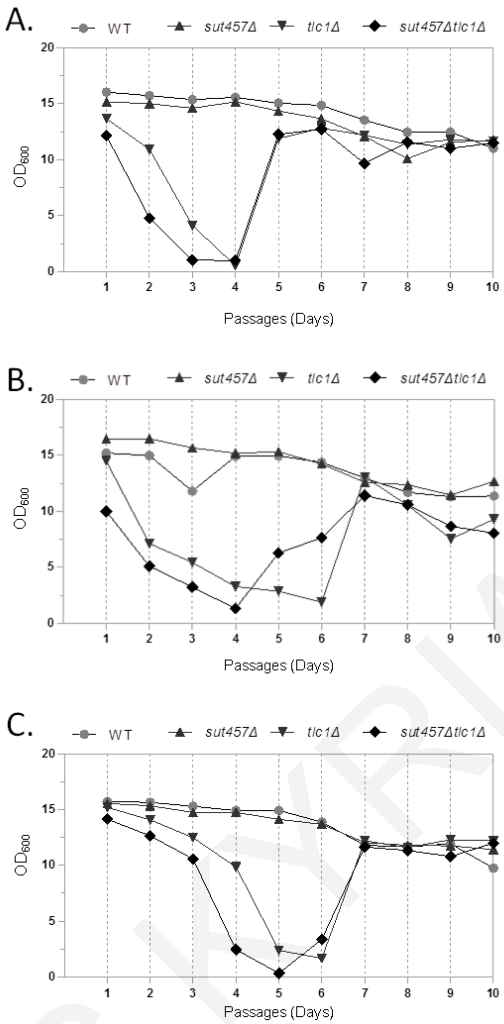

Figure 3.14: Depletion of *SUT457* in *tlc1Δ* cells accelerates senescence. Senescence assays performed using liquid cultures of the indicated isogenic wild-type and mutant strains. The strains were generated through tetrad dissection of the heterozygous diploid double mutant *SUT457/sut457ΔTLC1/tlc1Δ*. Senescence assays performed using liquid cultures of the indicated isogenic wild-type and mutant strains. Each plot (**A-C**) represents independent tetrads examined.

Since, senescence occurs due to telomere shortening in *tlc1Δ* cells, we decided to check whether the double mutant *tlc1Δsut457Δ* cells could have accelerated senescence due to faster telomere shortening. Interestingly, this faster induction of senescence correlates with the appearance of shorter telomeres in the *sut457Δtlc1Δ* double deletion strain compared to the *tlc1Δ* single mutant (**Figure 3.15**, left panel). Moreover, in the absence of telomerase complex the telomeres are maintained by backup pathways that fix the telomeres via DNA recombination. These backup pathways rescue the cells from the senescence state and allow them to divide again normally after senescence (survivors) as shown for *tlc1Δ* cells in **Figure 3.14**. Since, a lot of telomere organization genes are known to affect this process, we were interested in finding out whether *SUT457* is involved in the generation of survivor cells also. By testing the telomeric DNA with

Southern blotting we reveal that the deletion of *SUT457* did not affect the process of telomere recombination during survivors' development in strains lacking telomerase (**Figure 3.15**, right panel). Specifically, the telomeric footprint in both *tlc1Δ* and *tlc1Δsut457Δ* cells (**Figure 3.15**, right panel, last two lanes) was the same, therefore *SUT457* deletion did not affect this phenotype.

Altogether, these findings link the function of *SUT457* to telomere organization and specifically show that *SUT457* participates within a pathway that works in parallel to telomerase complex in order to maintain telomere integrity. However, *SUT457* is not involved in telomere maintenance via telomerase complex since in *sut457Δ* cells we did not observed any changes in telomere length. Also, *SUT457* is not involved in telomere maintenance via DNA recombination as observed by the telomere analysis of survivor cells.

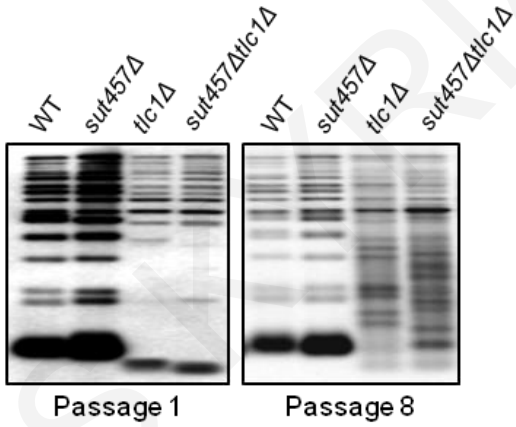

Figure 3.15: Loss of *SUT457* exacerbates telomere shortening in telomerase defective cells. Telomere length analysis of genomic DNA isolated from the indicated wild-type and mutant strains during passages 1 and 8. The extracted DNA was fragmented with XhoI, analysed by Southern blotting under denaturising conditions and the telomeres where detected by a biotinylated probe against telomeric repeats.

3.2.2 Loss of *SUT457* leads to accumulation of telomeric single-stranded DNA

It has been previously reported that faster senescence in telomerase-negative cells can be also attributed to abnormal accumulation of telomeric ssDNA [152,153]. Thus, we hypothesized that deletion of *SUT457* may lead to the accumulation of ssDNA at telomeres. This hypothesis was further supported by the SGA findings which show that *SUT457* genetically interacts with the genes *YKU70*, *MRE11*, *TGS1*, *CGI121, HSC82* and *GBP2* (**Figure 3.12A**) that encode for factors implicated in telomere-end protection and in the formation of telomeric ssDNA overhang [148]. To examine this hypothesis, we

extracted genomic DNA from isogenic wild-type and *sut457Δ* cells at an early passage and performed native southern blotting using a C-rich oligonucleotide probe. In addition, we extracted genomic DNA from a later passage to mimic the subculturing of cells resulting from the serial pinning steps performed during the SGA procedure. Absence of *SUT457* led to an increase in the signal of telomeric single strand DNA compared to wild-type cells in passage 1 (P1), which became even more intense after subculturing yeast cells for five passages (P5) (**Figure 3.16A and B**). In order to verify that the detected ssDNA signal is due to an increase in 3' terminal overhang and not due to accumulation of internal DNA replication intermediates, we treated the native DNA with bacterial Exonuclease I that can only degrade terminal ssDNA in a 3' to 5' direction. The ssDNA that accumulated in *sut457Δ* mutant was sensitive to bacterial Exonuclease I digestion (**Figure 3.16C**) indicating that the detected ssDNA indeed corresponds to telomeric 3' overhang. We also validated the increase in telomeric overhang by comparing the levels of ssDNA among 11 different *sut457Δ* mutant clones and their corresponding WT strains. As above, we observed statistically significant accumulation of telomeric ssDNA in *sut457Δ* strains at an early passage (P1) which became even more substantial at a later passage (P5) (**Figure 3.16B**).

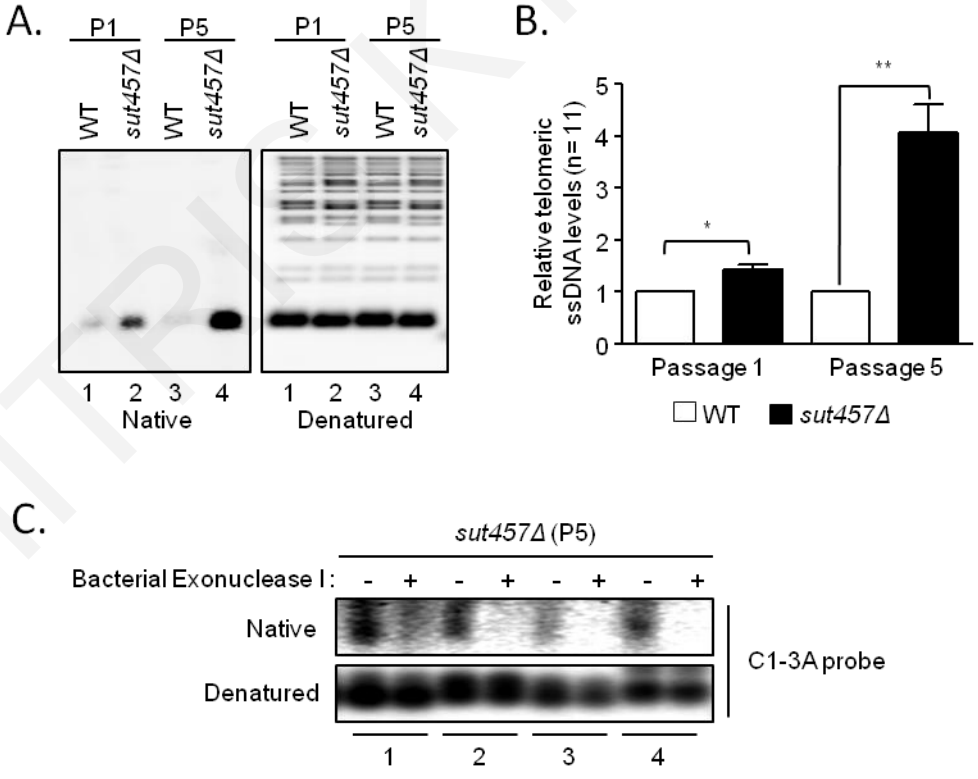

Figure 3.16: *SUT457* is involved in telomere-end homeostasis. A. Analysis of telomeric ssDNA overhangs in isogenic WT and *sut457Δ* strains. Yeast colonies were restreaked on agar plates and genomic DNA was extracted at passage 1 (lanes 1 and 2) and passage 5 (lanes 3 and 4), fragmented with XhoI and subjected to native southern blotting (left panel) using a biotinylated

probe against telomeric repeats. The southern blot was then treated with 0.4 N NaOH and the denatured DNA was re-probed to monitor equal loading (right panel). **B.** Accumulation of telomeric ssDNA in eleven sut457Δ strains compared to their respective wild-type strains during passages 1 and 5 (P1 & P5). The ssDNA signal for each wild-type and mutant strain detected in the native southern blot was normalised to the corresponding signal in the denatured southern blot. Error bars represent s.e.m. * refers to p<0.05, ** to p<0.01 and n/s to not-significant (generated by Nonparametric One-tailed Mann-Whitney t-test). **C.** Degradation of telomeric ssDNA by bacterial Exonuclease I. Genomic DNA extracted from four individual sut457Δ strains at passage five was either untreated (-) or digested with bacterial exonuclease I (+), which degrades telomeric overhang DNA in the 3' to 5' direction, before subjected to native southern analysis using a biotinylated probe against telomeric repeats (upper blot). The DNA on the membrane was then denatured with 0.4 N NaOH and re-probed to monitor equal loading (lower blot).

Accumulation of telomeric ssDNA has been proposed to be a signal for cell cycle arrest [151]. However, we did not observe a growth reduction in the *sut457Δ* mutant strain compared to WT cells (**Figure 3.17**). It was previously demonstrated that growth arrest associated with telomeric overhang accumulation is masked by telomeric ssDNA binding proteins, such as Gbp2 [195]. Interestingly *GBP2* was identified as a *SUT457* negative genetic interaction (**Figure 3.12A**) and therefore, we next examined how lack of Gbp2 can affect the growth of *sut457Δ* cells. We observed a strong growth arrest of *gbp2Δsut457Δ* cells at passage 5 (**Figure 3.17**), which coincides with the robust accumulation of telomeric ssDNA (**Figure 3.16 A and B**). Altogether, these data suggest that *SUT457* controls the levels of telomeric ssDNA overhang in order to maintain proper cellular growth.

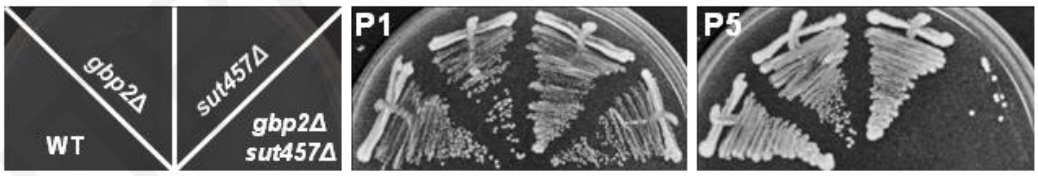

Figure 3.17: *GBP2* masks *sut457Δ*-associated cell-cycle arrest. Isogenic strains of the indicated genotype (right panel) were streaked repeatedly on solid rich medium and their growth at passage 1 and 5 is shown. This result was repeated with 3 different tetrads.

3.2.3 Exo1 nuclease is required for the accumulation of telomeric ssDNA in *sut457Δ* cells

Next, we sought to delve deeper into the mechanism of telomeric overhang accumulation in *sut457Δ* cells. It was known that the 5'-3' exonuclease Exo1 plays a key

role in telomere G-rich overhang formation in yeast by mediating C-rich strand degradation [198]. The action of Exo1 is blocked by the Ku complex since lack of Yku70 leads to unprotected telomere ends and results in Exo1-dependent accumulation of telomeric ssDNA [149,150,199]. Because *SUT457* genetically interacts with *YKU70* (**Figure 3.12A**), we hypothesized that Exo1 activity may be responsible for the accumulation of telomeric overhang in *sut457Δ* cells. To test this hypothesis, we initially wanted to generate an *exo1Δsut457Δ* double mutant strain by crossing the *exo1Δ* and *sut457Δ* single mutants but we realised that *EXO1* was not properly deleted in the *exo1Δ* strain found in the SGA knockout library. Therefore, we constructed a new *exo1Δ* deletion strain and mated it to the *sut457Δ* mutant, thus generating isogenic haploid strains that were analysed for telomeric ssDNA levels. Consistent with the above findings, we detected a strong signal in *sut457Δ* corresponding to the accumulation of telomeric ssDNA after subculturing yeast for 5 passages (**Figure 3.18A**). Notably, we observed that the telomeric overhang signal in the *exo1Δsut457Δ* double mutant cells is reduced back to WT levels (**Figure 3.18A**, compare lanes 1, 3 and 4). This result was verified by quantifying the levels of telomeric ssDNA in isogenic mutant strains generated from three independent tetrads (**Figure 3.18B**). Furthermore, to validate that EXO1 plays a role in the generation of increased telomeric ssDNA in *sut457Δ* cells we then examined if deletion of *exo1* could rescue the *gbp2Δsut457Δ* lethal phenotype. As expected, deletion of *EXO1* in *gbp2Δsut457Δ* cells rescued their growth arrest at passage 5 suggesting that *exo1Δ* suppresses the effect of *sut457Δ* (**Figure 3.18C**). Altogether, these findings show that *SUT457* functions within an Exo1-dependent pathway to affect telomeric overhang accumulation.

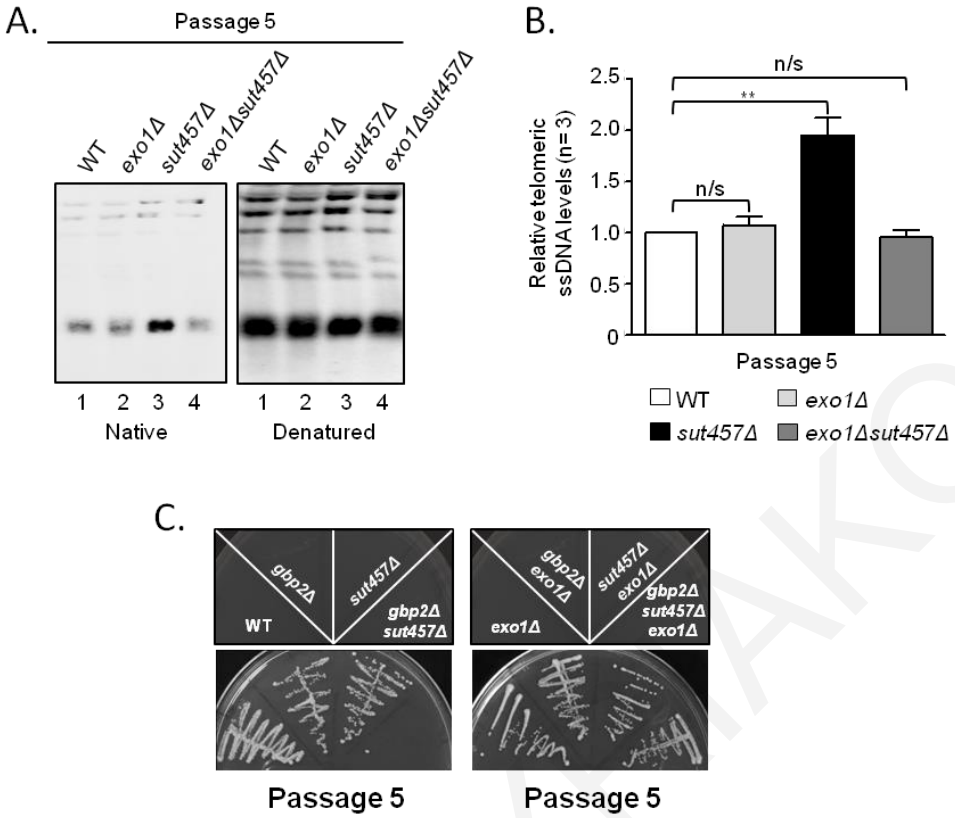

Figure 3.18: *SUT457* blocks Exo1-dependent telomeric C-strand degradation. A. Analysis of telomeric ssDNA levels at passage 5 of WT, *sut457Δ*, *exo1Δ* and *exo1Δsut457Δ* isogenic strains generated through dissection of the heterozygous diploid double mutant *EXO1/exo1ΔSUT457/sut457Δ*. Southern blotting was performed as in Figure 3.16A. **B.** Telomeric ssDNA levels analysed at passage 5 in the indicated isogenic wild-type and mutant strains generated from three independent tetrads (n=3). The quantification of the ssDNA signal for each wild-type and mutant strain was performed as in Figure 3.16B. Error bars represent s.e.m. ** refers to p<0.01 and n/s to not-significant. The statistical analysis was performed using One-Way ANOVA (Dunnett's test). **C.** Deletion of *EXO1* rescues the growth arrest of *gbp2Δ sut457Δ* mutant cells. Isogenic strains of the indicated genotype (top panels) were streaked repeatedly on solid rich medium and their growth at passage 5 is shown.

3.2.4 The lincRNA SUT457 acts in *trans* to regulate the levels of telomeric ssDNA

The genetic interaction profile of *SUT457* was distinct from that of its adjacent genes, (**Figure 3.8B**) which is consistent with the fact that loss of *SUT457* does not affect the expression of its neighbours (**Figure 3.11B**). Therefore, we hypothesized that unlike most characterised yeast lncRNAs, which control the expression of their cognate genes, *SUT457* may function in *trans* distant from its locus of synthesis. To address this hypothesis, we examined whether ectopic expression of *SUT457* could rescue the phenotype of telomeric overhang accumulation observed in *sut457Δ* cells (**Figure 3.16A**).

For this purpose, we deleted *SUT457* from its endogenous locus on chromosome III and re-introduced it on chromosome V under the control of the URA3 promoter (**Figure 3.19A**, *sut457Δ* [ectop*SUT457*]). We also constructed another strain in which *SUT457* was ectopically expressed at the URA3 locus in WT cells to serve as an additional control (**Figure 3.19A**, WT [ectop*SUT457*]). Native southern blot analysis indicated that deletion of *sut457Δ* from its endogenous locus results in robust increase in telomeric ssDNA at passage 5 as previously shown (**Figure 3.19B**, compare lanes 1 and 3), but, interestingly, concomitant ectopic expression of *SUT457* reduces the telomeric overhang signal to corresponding WT levels (**Figure 3.19B**). This result was verified by quantifying the levels of telomeric ssDNA in five independent constructed strains (**Figure 3.19C**). Collectively, these findings demonstrate that SUT457 can control the levels of telomeric ssDNA overhang regardless of its genomic location, indicating that this lincRNA functions in *trans*.

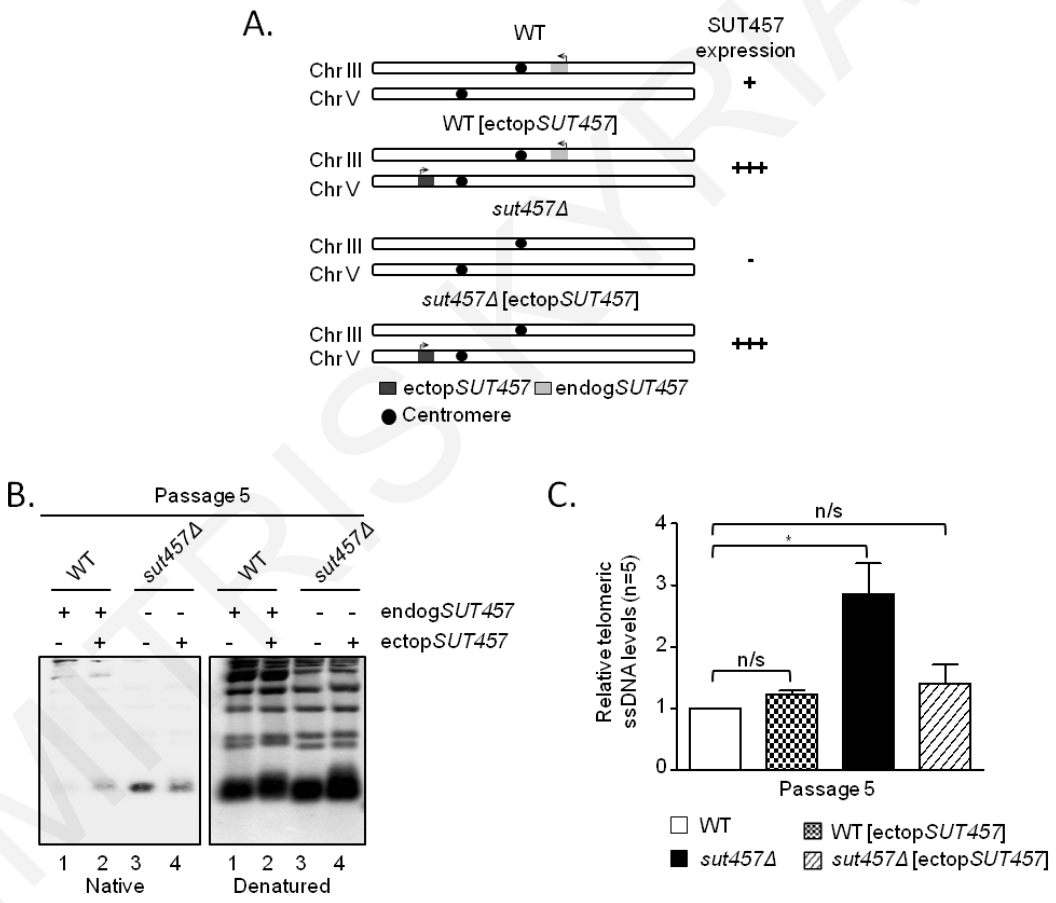

Figure 3.19: SUT457 regulates the levels of telomeric ssDNA by acting in *trans*. A. Schematic illustration indicating the presence of endogenous (endogSUT457, light grey box) and ectopic SUT457 (ectopSUT457, dark grey box) in WT and sut457Δ strains. The level of SUT457 expression for each constructed strain is indicated on the right: + (WT levels of expression), +++ (higher expression than WT), and - (no expression). Arrows indicate the direction of SUT457 transcription at each locus. **B.** Analysis of telomeric ssDNA levels in WT (lane 1), WT [ectopSUT457] (lane 2), sut457Δ (lane 3) and sut457Δ [ectopSUT457] (lane 4) strains at passage

5. Genomic DNA was extracted, fragmented with XhoI and subjected to native southern blotting using a biotinylated probe against telomeric repeats (left panel). The southern blot was then treated with 0.4 N NaOH and the denatured DNA was re-probed to monitor equal loading (right panel). **C.** Telomeric ssDNA levels were analysed in five independent clones of the indicated wild-type and mutant strains at passage 5. The ssDNA signal for each strain detected in the native southern blot was normalised to the corresponding signal in the denatured southern blot. Error bars represent s.e.m. * refers to $p<0.05$ and n/s to not-significant. The statistical analysis was performed using One-Way ANOVA (Dunnett's test).

Chapter 4 – Discussion

Despite the plethora of lincRNAs identified by genome-wide approaches, only few have been characterised so far and these have been implicated in important biological processes such as gene transcription, cell-cycle regulation and apoptosis as well as in disease development [13,167,200]. Therefore, functional characterization of the majority of lincRNAs is still work in progress, which is often hampered by the unavailability of appropriate research methodologies [10]. For example, rigorous genetic studies that could aid in the functional characterisation of individual lncRNAs are still underdeveloped [10]. Here, we utilised for the first time the high-throughput SGA method to systematically catalogue the genetic interactions of intergenic SUTs. Initially, we verified the utility of the approach by demonstrating that genetic interactions identified for the telomerase RNA *TLC1* enrich GO terms that correspond to its known cellular function. Subsequent SGA screens and analysis of genetic interaction profiles implicated the six tested intergenic SUTs in diverse biological processes. One of these lincRNAs, *SUT457*, exhibited genetic interactions that enriched a definitive GO annotation linking it to telomere biology. Further functional characterisation unveiled the role of *SUT457* in preventing the accumulation of telomeric ssDNA. Moreover, phenotypic rescue experiments showed that *SUT457* acts in *trans* to maintain physiological levels of telomeric ssDNA. Our work reveals that systematic mapping of the genetic interactions of lncRNAs could associate these molecules with specific biological processes and pinpoint their individual functions.

4.1 The genetic interaction profiles of lincRNAs reveal their biological function

In yeast, the function of identified lncRNAs has been mainly linked to the regulation of gene expression. Most lncRNAs characterised so far regulate their cognate genes either through transcriptional interference [58,119,201] or by modulating their local chromatin structure [61,62,118,202]. Accordingly, two of the six SGA-tested lincRNAs, *SUT014* and *SUT451* genetically interact with a variety of chromatin remodelling and histone modifying genes respectively (**Figure 3.6**). The GI-profiles of *ORC2* and *YBR292C*, which are *SUT014* and *SUT451* neighbouring genes respectively, also showed enrichment of the biological processes chromatin remodelling and histone modification, thus suggesting that these SUTs might have *in-cis* function (**Figure 3.9**). In fact, *SUT014* deletion leads to upregulation of its neighbouring gene, *ORC2* (**Chapter 3.1.2**). *SUT451* loss resulted in expression changes of several genes compared to wild-type cells (**Figure 3.7**). In summary, both *SUT014* and *SUT451* are associated to gene expression

regulation, although future functional studies are necessary to reveal their precise molecular mode of action.

Emerging evidence suggests that lncRNAs could have roles beyond gene regulation [177]. The GO enrichment profiles of the tested intergenic SUTs have linked them to nuclear functions such as DNA repair, meiosis and telomere organisation but also to cytoplasmic processes including membrane fusions and vesicle formation, as for example in the case of *SUT042* (**Figure 3.6**). The latter is consistent with the fact that a large number of SUTs are transported to the cytoplasm and have been proposed to represent functional transcripts within this cell compartment [117]. Therefore, further studies of the tested SUTs, which are linked to membrane fusion and vesicle organization such as *SUT042*, could shed light on the molecular mechanisms connecting lincRNAs with vesicle formation and trafficking.

The biological role of lncRNAs in regulating adjacent genes is tightly linked with acting in *cis* [10]. However, increasing evidence reveals *trans*-acting lncRNAs in various biological processes such as gene expression, genomic imprinting, X-chromosome inactivation [203] and also in cancer development [204,205]. We hypothesized that the GI-profile of *trans*-acting SUTs would differ from the GI profile of their neighbouring genes. For example, *TLC1* has a genetic interaction network that varies from that of its upstream and downstream genes (**Figure 3.8A**), which is in line with the fact that *TLC1* has a function unrelated to its neighbours and acts in *trans* at chromosome ends [206]. We observed a significant correlation between the GO enrichment profiles for three of the tested SUTs (*SUT014*, *SUT451* and *SUT469)* with the GO enrichment profiles of their respective neighbouring genes (**Figure 3.9**). The observations suggest that these SUTs may regulate the expression of their neighbouring genes, in *cis*. It is important to note that we cannot exclude the likelihood that construction of these three SUT deletions leads to a neighbouring gene effect (NGE) [189,190], which might be responsible for the observed overlap among enriched GO profiles (**Figure 3.9**). Contrary, *SUT457* and *SUT042* showed a completely different GO enrichment profile compared to the profile of their neighbouring genes (**Figure 3.8 B and C**), suggesting in *trans* roles for these SUTs in the biological processes enriched by their GIs. Consistently, *SUT457* deletion does not change the expression levels of its neighbouring genes (**Figure 3.11B**). We also verified that *SUT457* is indeed *trans*-acting since its ectopic expression was able to rescue a telomere defective phenotype in *sut457Δ* cells (**Figure 3.19**). In summary, two of the six tested SUTs are putative *trans*-acting lncRNAs, implying that the number of *trans*-acting lncRNAs could be higher than previously suggested by other studies.

4.2 Functional characterization of *SUT457* elaborates its GI-inferred role in telomere overhang regulation

SUT457 has a clear GO enrichment profile pointing its role towards telomere organization (**Figure 3.6**). Specifically, *SUT457* genetically interacts with genes (*RAD51, RAD52, RAD57, RAD59* and *MRE11*) (**Figure 3.12A**), which are involved in telomere maintenance when telomere synthesis by telomerase complex is impaired (**Figure 1.12**). Thus, we first hypothesised that *SUT457* could be used as a template for telomere synthesis by the telomerase complex. Thus, we examined the nucleotide sequence of *SUT457* (**Appendix 16**) to determine if it resembles the sequence of telomerase RNA, *TLC1*. *SUT457* sequence (**Appendix 16**) does not match with the *TLC1* fragment used as template for telomere synthesis [207] neither with *TLC1* fragments bound by its physical interactors, YKU complex, Est1, Est2, or Sm7 proteins [208]. Consistently, *sut457Δ* cells did not show any obvious changes in telomere length before (**Figure 3.13)** or after (**Figure 3.15 compare P1 to P8 and 3.16A denatured southern blot compare P1 to P5)** subculturing, suggesting that *SUT457* is probably not necessary for telomere synthesis [133,140]. Also, deletion of *SUT457* alone was not enough to cause replicative senescence (**Figure 3.14**) or growth reduction (**Figure 3.5**) as it happens in *tlc1Δ* cells. Collectively, these data indicate that *SUT457* does not affect telomere synthesis.

Telomere organization is highly dependent on a conserved ssDNA fragment at G-rich telomeric ends called telomeric overhang (**Figure 1.13**). The telomeric overhang is an essential harbouring site for proteins that act to protect telomeres from degradation and orchestrate telomere maintenance mechanisms. Among the telomere organization genes which genetically interact with *SUT457* (**Figure 3.12A**), six genes (*YKU70, HSC82, CGI121, TGS1, MRE11* and *GBP2*) are involved in the maintenance of telomeric overhang in yeast [121,138,145,149,179,193,195–197,209]. Accordingly we showed that lack of *SUT457* exhibited an accumulation in telomeric ssDNA overhang (**Figure 3.16**). Consistent with the above observations, *SUT457* showed a positive genetic interaction with the telomere-capping factor *YKU70* (**Figure 3.12A**) implying that these two molecules affect the same molecular process [172]. Yku70 binds to and protects telomeres from Exo1 nucleolytic processing thus preventing the accumulation of telomeric ssDNA overhang [149,179,198]. We reveal that loss of *SUT457* causes telomeric overhang accumulation after cell subculturing by an Exo1-dependent procedure (**Figure 3.18**). Additionally, we show that loss of the telomeric ssDNA masking protein Gbp2 in *sut457Δ* cells results in growth inhibition after subculturing (**Figure 3.17**). Consistently, in agreement with the fact that *EXO1*-dependent accumulation of telomeric ssDNA induces

cell-cycle arrest [149,210], the growth arrest observed in *sut457Δgbp2Δ* is rescued by deletion of *EXO1* (**Figure 3.18B**).

In order to design a possible model that describes *SUT457* function in telomeric overhang regulation we have to keep in mind that it might affect telomeres by an indirect manner. Specifically, in an indirect model, *SUT457* deletion could deregulate a process which takes place away from telomeres and then a following cascade of events could lead to defects in the mechanisms that regulate telomere overhangs. Several studies have shown that lncRNAs could indirectly affect a biological process by controlling the expression of the genes involved in that process. Therefore, we tested if *SUT457* loss affects the expression of telomere maintenance genes, however we did not observe any gene expression changes compared to wild-type cells (**Figure 4.1**, indirect model). Subsequently, we believe that SUT457 might work directly on the telomeres to exert its functions. SUT457 probably functions in a pathway that it might be associated with Yku complex, Exo1 and other yet unidentified factors near telomere overhangs (**Figure 4.1**, direct model).

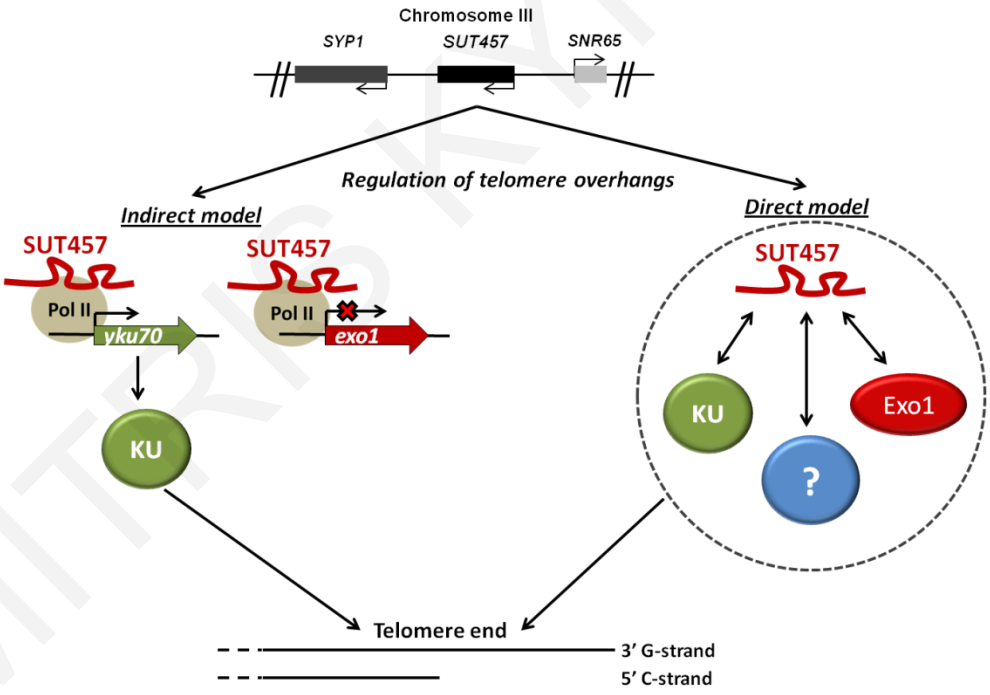

Figure 4.1 SUT457 could regulate telomere overhang homeostasis directly or indirectly. In the indirect model (left), SUT457 controls the expression of telomere organization genes. In this hypothetical example SUT457 allows the expression of the capping factor *YKU70* and blocks the expression of the exonuclease *EXO1*, thus indirectly controls the availability of these factors on the telomere end. In the direct model (right), SUT457 direct interplay with either Ku complex, Exo1 or other factors (blue circle) therefore affecting directly the telomere overhang maintenance pathways.

Based on the above evidence, as first scenario for the direct model, we can speculate that SUT457 functions in a pathway that protects telomere-ends from nucleolytic processing in order to regulate the levels of telomeric ssDNA overhangs. Specifically, we hypothesize that SUT457 supports telomere capping mediated by CST and YKU complexes [142,149,151]. Deregulation of telomere capping, due to *SUT457* deletion, might lead to extensive exonuclease degradation of telomeric C-strand by Exo1 [148] (**Figure 4.2A**). A second scenario is that *SUT457* might be involved in the process of telomeric C-strand fill-in by DNA polymerase α-primase (DNA polα-primase) [211–213]. Thus, loss of *SUT457* could lead to deregulation of telomeric C-strand synthesis, leading to accumulation of elongated G-strand telomeric overhangs (**Figure 4.2B**). The telomere-associated lncRNA TERRA has also been implicated in telomere overhang regulation [214,215], therefore the interplay between TERRAs and *SUT457* in the regulation of telomeric overhang homeostasis is also possible (**Figure 4.2C**). Specifically, TERRA binds on Yku complex and on LSD1 protein and promotes telomere resection of uncapped telomeres through an Exo1-dependent and Mre11-dependent manner respectively [214,215]. SUT457 could antagonize with TERRA for binding on these factors (e.g. on Yku70 or Yku80) therefore stopping telomere end resection by Exo1. All these suggested mechanisms are cell-cycle dependent, thus they are consistent with the fact that the telomeric overhangs accumulate after subculturing of *sut457Δ* cells (**Figure 3.16**).

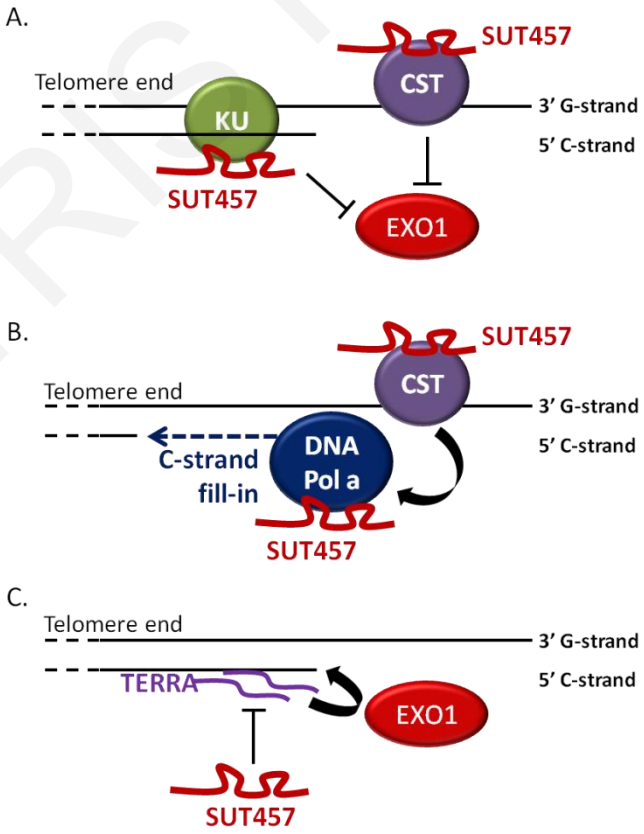

Figure 4.2 SUT457 potential molecular mechanisms. A. SUT457 physically interacts with key capping factors (YKU or CST complex) and supports their function against C-strand degradation by Exo1. **B.** During DNA replication Exo1 degrades C-strand and then DNA polymerase alpha is recruited on telomeres by CST complex in order to synthesize the missing fragment [130]. SUT457 could bind on CST complex or directly on DNA Pol alpha and affect the latter's localization and function. **C.** TERRA transcription supports Exo1 function toward degradation of the telomeric C-strand, so it is possible that SUT457 might bock their expression or cancel their effects on the Exo1-mediated telomere resection [214].

The telomere overhang regulation mechanisms are conserved between yeast and humans [148], thus a functionally equivalent lncRNA of *SUT457* could exist in human cells. Study of the primary and secondary structure of SUT457 RNA transcript can expose similarities with a potential human orthologue lncRNA. Interestingly, the 5'-end of *SUT457* begins with the 6-nucleotide sequence 5'-UUAGGG (**Appendix 16**) which represents the repeating sequence of human telomeres and is also found on the human lncRNA TERRA [216]. We speculate that a human orthologue of *SUT457* with these same structural features might exist. In fact, Azhibek et al., suggested that a yet unidentified RNA factor is responsible for switching telomerase binding from TERRA to the telomere end in human cells [216], thus a possible *SUT457* orthologue could be a potential candidate for this process.

4.3 Future directions

4.3.1 Perform genetic interaction analysis of all yeast lncRNAs

It remains unclear how many of the identified lncRNAs serve a biological function or are a mere result of transcriptional noise [154,156]**.** We proved here that the genetic interactions of unannotated lincRNAs with protein-coding genes infer their in *cis* and in *trans* functions. Based on the effectiveness of this approach, demonstrated by the results of the present study, we propose that SGA analysis can be performed for the functional characterization of a plethora, if not for all, stable lincRNAs described in yeast.

Although the present study focuses on long intergenic ncRNAs, future work could also analyse genetic interactions for yeast intragenic lncRNAs since methodologies are being developed that abrogate the transcription of a specific non-coding RNA without disrupting the expression of its associated sense mRNA [217]. Specifically, unidirectional transcriptional terminators can be used to block the expression of antisense lncRNAs only. It is estimated that approximately 25% of the antisense SUTs in yeast affect the expression of their overlapping gene [78], thus it will be expected that their GI network might be similar to the GI network of that gene. On the other hand the GI network of

intragenic SUTs that do not affect the expression of the overlapping gene will reveal novel functions for this group of lncRNAs.

Overall, this study can reveal a global map of genetic interactions for lncRNAs which will not only reveal their individual biological roles but it will indicate functional relationships between lncRNAs and protein-coding genes through similarities in their GI profiles.

4.3.2 Unveil the function of human lincRNAs by systematic analysis of their GIs with human protein-coding genes

Single deletions of most lncRNAs have proven inefficient for exposing any phenotypes [218]**,** possibly due to functional redundancy by other genes. Here, we show that genetic interaction profiling can be used for studying non-essential lincRNAs because double mutants overcome functional redundancy. Thus, we propose that the same double mutant approach can be employed for functional characterization of human lincRNAs. Thus, building upon the SGA approach, we propose to generate libraries of double knockdown human cells in order to study genetic interactions. Depleting multiple genes in human cells is now doable by technologies such as CRISPR and RNA-interference which allow simultaneous pairwise knockdowns to be performed in a high-throughput manner [219–222]. Specifically, the CRISPR interference (CRISPRi) technique has already been used for silencing lncRNAs in 7 different human cell lines. CRISPRi blocks the expression of a lncRNA via targeted recruitment of a transcriptional repressor (KRAB) to the lncRNA's transcriptional start site (TSS) [223]. CRISPRi can therefore reduce the risk of affecting genes after depleting the expression of their overlapping lncRNAs. Thus, we propose that CRISPRi is the approach to use for simultaneous double knockdown of lncRNAs and protein-coding genes.

Specifically, we propose that each human cell line in a double knockdown library will carry the depletion of a lncRNA of interest with the depletion of a protein-coding gene. The generation of double knockdowns can be performed in a high-throughput manner in 96-well or 384-well human cell cultures [219–222] and the loss of any targeted RNA in double and single knockdowns can be validated by RNA-sequencing of each cell line. The growth of double knockdown cells can be then tested by measuring fluorescently labelled nuclei in each cell culture by automated fluorescent cytometry, therefore counting the number of cells. Then, the measured number of double mutant cells can be compared to the number of the corresponding single knockdown cells in order to reveal genetic interactions.

A new bottleneck problem arises due to the fact that human genomes transcribe tens of thousands of protein-coding genes and lncRNAs making it very difficult to perform all the double knockdown combinations. Subsequently, we have to perform the genetic interaction analysis to selected groups of lncRNAs. Thus, we propose that lncRNAs which already affect cell growth in a certain degree when depleted [223], can be the first candidates to be tested by a genetic interaction screen in human cells. Specifically, 499 lncRNAs were found to be required for robust cellular growth after their depletion from human cells [223], thus they have a function that still remain unexplored. Double knockdowns of each such lncRNA with human protein-coding genes may reveal their individual biological roles. Additionally, the number of query lncRNAs can be significantly reduced based on the fact that most of the lncRNAs are cell-type specific, so they must be tested in certain cells lines. Accordingly, we propose that lncRNAs which affect the growth of pluripotent cells such as induced pluripotent stem cells (iPSCs) or embryonic stem cells (ESCs) can be the ones to be tested first as they might have interesting developmental properties.

The number of protein-coding genes can be also narrowed down by selecting only certain groups of them instead of all the 25000 human genes. One option is to use only protein-coding genes associated with cell growth, differentiation and development if pluripotent cells are used. Another option is to perform the GI analysis with gene groups which express chromatin remodelers and transcription factors since a lot of lncRNAs are associated to gene expression regulation. Unannotated genes should not be tested in the screens since based on our SGA findings, they cannot not provide useful information necessary for the functional characterization of lncRNAs (e.g. 'Not-yet-annotated' enriched GI group of *SUT457*). Finally, genes which are involved in human diseases might be interesting to use in such genetic interaction tests in order to reveal which lncRNAs contribute to the pathogenicity, thus leading to new drug discovery.

Such analyses may unveil the function of multiple human lncRNAs at individual level. Also, interspecies conservation of genetic interaction maps [224] could shed light on the evolution and functional conservation of lncRNAs since conserved GI profiles might reveal homology among them [41,225].

4.3.3 Describe the molecular pathway of *SUT457* on telomere homeostasis and uncover a potential human functional orthologue

This study has revealed *SUT457* association with telomere overhang regulation, however the precise molecular mechanism underlying the function of *SUT457* remains

elusive. Since *SUT457* is a *trans*-acting lncRNA it is possible to be localized near telomeres in order to exert its function. Thus, RNA-FISH (Fluorescence In Situ Hybridization) experiments can be performed initially in order to study the localization of fluorescently labelled SUT457 molecules compared to the telomeres, which will be marked by a different dye. SUT457 molecules can be quantified in each cell by a technique called single-molecule RNA FISH (smFISH) [226]. Specifically, multiple short DNA or RNA probes against the target RNA are used for smFISH in contrast to one large probe used during FISH in order to reduce background and increase the detection signal. SUT457 detection by smFISH will define its distribution across telomeres and will allow mechanistic questions, such as how many SUT457 molecules per cell or per telomere, to be addressed [227]. Additionally, Chromatin Isolation by RNA Purification (ChIRP) [28] can be used in order to precipitate SUT457 and pinpoint its genomic localization across the genome using deep sequencing. Additionally, the proteins that are co-precipitated with the SUT457 transcript during ChIRP can be analysed by mass spectrometry in order to be identified. Following experiments using *in vitro* pulldown assays will validate which of the physical interactions, found by mass spectrometry, binds directly on the SUT457 RNA. Next, mutations that disrupt SUT457-protein interactions may be linked to telomere overhang related phenotypes, thus suggesting that this interaction is important for the function of SUT457. Last but not least, it would be interesting to identify the phase in which *SUT457* physically interacts with its co-factors during the cell-cycle since telomere overhang regulation is a cell-cycle dependent procedure.

The primary nucleotide sequence of *SUT457* (**Appendix 16**) does not display significant sequence similarity with any other regions within the *S.cerevisiae* genome and lacks conservation, even amongst closely related yeast species ([7] and data not shown). Nevertheless, considering its unveiled role in the fundamental and conserved cellular process of telomere overhang homeostasis [148], we believe that functional analogues of *SUT457* may exist in other eukaryotes. Likewise, TLC1 is a lncRNA whose primary sequence is not evolutionarily conserved but it has functional analogues in other organisms [228]. We suspect that a human orthologue lncRNA of *SUT457* would have similar function. Therefore, finding the proteins that physically interact with *SUT457* in yeast can define which functionally equivalent human proteins might associate physically with a human orthologue lncRNA. Also, data defining the secondary structure of *SUT457* could be useful for discovering its human orthologous lncRNA based on structural similarities.

Chapter 5 - References

1. Jensen T, Jacquier A, Libri D. Dealing with pervasive transcription. Mol. Cell [Internet]. Elsevier Inc.; 2013;52:473–84. Available from: http://dx.doi.org/10.1016/j.molcel.2013.10.032

2. Mattick JS. RNA regulation: a new genetics? Nat. Rev. Genet. 2004;5:316–23.

3. Kapranov P, Cheng J, Dike S, Nix DA, Duttagupta R, Willingham AT, et al. RNA Maps Reveal New and a Possible Classes Pervasive Transcription RNA Function for. Science (80-.). 2007;316:1486.

4. Derrien T, Johnson R, Bussotti G, Tanzer A, Djebali S, Tilgner H, et al. The GENCODE v7 catalogue of human long non-coding RNAs : Analysis of their structure , evolution and expression. Genome Res. 2012;22:1775–89.

5. Bertone P, Stolc V, Royce TE, Rozowsky JS, Urban AE, Zhu X, et al. Global identification of human transcribed sequences with genome tiling arrays. Science (80-.). [Internet]. 2004;306:2242–6. Available from: http://www.sciencemag.org/cgi/doi/10.1126/science.1103388%5Cnhttp://www.ncbi.nlm.nih.gov/pubmed/15539566

6. Johnson JM, Edwards S, Shoemaker D, Schadt EE. Dark matter in the genome: Evidence of widespread transcription detected by microarray tiling experiments. Trends Genet. 2005;21:93–102.

7. Xu Z, Wei W, Gagneur J, Perocchi F, Clauder-Münster S, Camblong J, et al. Bidirectional promoters generate pervasive transcription in yeast. Nature [Internet]. 2009;457:1033–7. Available from: http://www.ncbi.nlm.nih.gov/pubmed/19169243

8. van Dijk EL, Chen CL, D'Aubenton-Carafa Y, Gourvennec S, Kwapisz M, Roche V, et al. XUTs are a class of Xrn1-sensitive antisense regulatory non-coding RNA in yeast. Nature [Internet]. Nature Publishing Group; 2011;475:114–7. Available from: /Users/yurikoharigaya/Documents/ReadCube Media/Nature 2011 van Dijk EL.pdf%5Cnhttp://dx.doi.org/10.1038/nature10118

9. Tisseur M, Kwapisz M, Morillon A. Pervasive transcription - Lessons from yeast. Biochimie [Internet]. Elsevier Masson SAS; 2011;93:1889–96. Available from: http://dx.doi.org/10.1016/j.biochi.2011.07.001

10. Quinn JJ, Chang HY. Unique features of long non-coding RNA biogenesis and function. Nat. Rev. Genet. [Internet]. Nature Publishing Group; 2016;17:47–62. Available from: http://www.nature.com/doifinder/10.1038/nrg.2015.10%5Cnhttp://www.ncbi.nlm.nih.gov/pubmed/26666209

11. Canella D, Praz V, Reina JH, Cousin P, Hernandez N. Defining the RNA polymerase III transcriptome: Genome-wide localization of the RNA polymerase III transcription machinery in human cells. Genome Res. 2010;20:710–21.

12. Yin QF, Yang L, Zhang Y, Xiang JF, Wu YW, Carmichael GG, et al. Long Noncoding RNAs with snoRNA Ends. Mol. Cell [Internet]. Elsevier Inc.; 2012;48:219–30. Available from: http://dx.doi.org/10.1016/j.molcel.2012.07.033

13. Geisler S, Coller J. RNA in unexpected places: long non-coding RNA functions in diverse cellular contexts. Nat. Rev. Mol. Cell Biol. [Internet]. Nature Publishing Group; 2013;14:699–712. Available from: http://www.ncbi.nlm.nih.gov/pubmed/24105322

14. Chen L. Linking Long Noncoding RNA Localization and Function. Trends Biochem. Sci. [Internet]. Elsevier Ltd; 2016;1–12. Available from: http://dx.doi.org/10.1016/j.tibs.2016.07.003

15. Esteller M. Non-coding RNAs in human disease. Nat. Rev. Genet. [Internet]. Nature Publishing Group; 2011;12:861–74. Available from: http://www.nature.com/doifinder/10.1038/nrg3074%5Cnhttp://www.ncbi.nlm.nih.gov/pubmed/22094949

16. Descostes N, Heidemann M, Spinelli L, Sch??ller R, Maqbool MA, Fenouil R, et al. Tyrosine phosphorylation of RNA Polymerase II CTD is associated with antisense promoter transcription and active enhancers in mammalian cells. Elife. 2014;2014:1–19.

17. Hsin JP, Li W, Hoque M, Tian B, Manley JL. RNAP II CTD tyrosine 1 performs diverse functions in vertebrate cells. Elife. 2014;2014:1–10.

18. Almada AE, Wu X, Kriz AJ, Burge CB, Sharp PA. Promoter directionality is controlled by U1 snRNP and polyadenylation signals. Nature [Internet]. 2013;499:360–3. Available from: http://eutils.ncbi.nlm.nih.gov/entrez/eutils/elink.fcgi?dbfrom=pubmed&id=23792564&retmode=ref&cmd=prlinks%5Cnpapers3://publication/doi/10.1038/nature12349

19. Zheng GXY, Do BT, Webster DE, Khavari PA, Chang HY. Dicer-microRNA-Myc circuit promotes transcription of hundreds of long noncoding RNAs. Nat. Struct. Mol. Biol. [Internet]. Nature Publishing Group; 2014;21:585–90. Available from: http://dx.doi.org/10.1038/nsmb.2842

20. Marvin MC, Clauder-Münster S, Walker SC, Sarkeshik A, Yates JR, Steinmetz LM, et al. Accumulation of noncoding RNA due to an RNase P defect in Saccharomyces cerevisiae. RNA [Internet]. 2011;17:1441–50. Available from: http://rnajournal.cshlp.org/cgi/doi/10.1261/rna.2737511%5Cnhttp://www.ncbi.nlm.nih.gov/pubmed/21665995%5Cnhttp://www.pubmedcentral.nih.gov/articlerender.fcgi?artid=PMC3153969

21. Salzman J, Gawad C, Wang PL, Lacayo N, Brown PO. Circular RNAs are the predominant transcript isoform from hundreds of human genes in diverse cell types. PLoS One. 2012;7.

22. Dhir A, Dhir S, Proudfoot NJ, Jopling CL. Microprocessor mediates transcriptional termination in genes encoding long noncoding microRNAs. Nat. Struct. Mol. Biol. [Internet]. 2015;22:319–27. Available from: http://www.ncbi.nlm.nih.gov/pubmed/25730776

23. Lai F, Gardini A, Zhang A, Shiekhattar R. Integrator mediates the biogenesis of enhancer RNAs. Nature [Internet]. 2015;525:399–403. Available from: http://www.ncbi.nlm.nih.gov/pubmed/26308897

24. van Heesch S, van Iterson M, Jacobi J, Boymans S, Essers PB, de Bruijn E, et al. Extensive localization of long noncoding RNAs to the cytosol and mono- and polyribosomal complexes. Genome Biol. [Internet]. 2014;15:R6. Available from: http://www.pubmedcentral.nih.gov/articlerender.fcgi?artid=4053777&tool=pmcentrez&rendertype=abstract

25. Xiang J, Yin Q, Chen T, Zhang Y, Zhang X-O, Wu Z, et al. Human colorectal cancer-specific CCAT1-L lncRNA regulates long-range chromatin interactions at the MYC locus. Cell Res. [Internet]. Nature Publishing Group; 2014;24:513–31. Available from: http://dx.doi.org/10.1038/cr.2014.35

26. Hacisuleyman E, Goff LA, Trapnell C, Williams A, Henao-Mejia J, Sun L, et al. Topological Organization of Multi-chromosomal Regions by Firre HHS Public Access. Nat Struct Mol Biol [Internet]. 2014;21:198–206. Available from: http://www.nature.com/authors/editorial_policies/license.html#terms

27. Rinn JL, Kertesz M, Wang JK, Squazzo SL, Xu X, Brugmann SA, et al. Functional Demarcation of Active and Silent Chromatin Domains in Human HOX Loci by Noncoding RNAs. Cell. 2007;129:1311–23.

28. Chu C, Qu K, Zhong FL, Artandi SE, Chang HY. Genomic Maps of Long Noncoding RNA Occupancy Reveal Principles of RNA-Chromatin Interactions. Mol. Cell [Internet]. Elsevier Inc.; 2011;44:667–78. Available from: http://dx.doi.org/10.1016/j.molcel.2011.08.027

29. Ishizuka A, Hasegawa Y, Ishida K, Yanaka K, Nakagawa S. Formation of nuclear bodies by the lncRNA Gomafu-associating proteins Celf3 and SF1. Genes to Cells. 2014;19:704–21.

30. Arigo JT, Eyler DE, Carroll KL, Corden JL. Termination of Cryptic Unstable Transcripts Is Directed by Yeast RNA-Binding Proteins Nrd1 and Nab3. Mol. Cell. 2006;23:841–51.

31. LaCava J, Houseley J, Saveanu C, Petfalski E, Thompson E, Jacquier A, et al. RNA degradation by the exosome is promoted by a nuclear polyadenylation complex. Cell. 2005;121:713–24.

32. Thiebaut M, Kisseleva-Romanova E, Rougemaille M, Boulay J, Libri D. Transcription Termination and Nuclear Degradation of Cryptic Unstable Transcripts: A Role for the Nrd1-Nab3 Pathway in Genome Surveillance. Mol. Cell. 2006;23:853–64.

33. Wyers F, Rougemaille M, Badis G, Rousselle JC, Dufour ME, Boulay J, et al. Cryptic Pol II transcripts are degraded by a nuclear quality control pathway involving a new poly(A) polymerase. Cell. 2005;121:725–37.

34. Preker P, Nielsen J, Kammler S, Lykke-Andersen S, Christensen MS, Mapendano CK, et al. RNA Exosome Depletion Reveals Transcription Upstream of Active Human Promoters. Cell Proc. Natl. Acad. Sci. U.S.A. Cell Sci. Nat. Cell Sci. Sci. Nat. Rev. Mol. Cell Biol. Genes Dev. Cell A. Barski al. Cell Nat. A. R. Kays, A. Schepartz, Chem. Biol. Nucleic Acids Res [Internet]. 2002;108:1559–601. Available from: www.sciencemag.org/cgi/content/full/1162253/DC1

35. Berretta J, Morillon A. Pervasive transcription constitutes a new level of eukaryotic genome regulation. EMBO Rep. [Internet]. 2009;10:973–82. Available from: http://www.pubmedcentral.nih.gov/articlerender.fcgi?artid=2750061&tool=pmcentrez&rendertype=abstract

36. Houseley J. Form and function of eukaryotic unstable non-coding RNAs. Biochem. Soc. Trans. [Internet]. 2012;40:836–41. Available from: http://www.ncbi.nlm.nih.gov/pubmed/22817744

37. Ruiz-Orera J, Messeguer X, Subirana JA, Alba MM, Albà M, Castresana J, et al. Long non-coding RNAs as a source of new peptides. Elife [Internet]. 2014;3:e03523. Available from: http://www.ncbi.nlm.nih.gov/pubmed/25233276%5Cnhttp://www.pubmedcentral.nih.gov/articlerender.fcgi?artid=PMC4359382

38. Marquardt S, Hazelbaker DZ, Buratowski S. Distinct RNA degradation pathways and 3’ extensions of yeast non-coding RNA species. Transcription. 2011;2:145–54.

39. Ulitsky I. Evolution to the rescue: using comparative genomics to understand long non-coding RNAs. Nat Rev Genet [Internet]. Nature Publishing Group; 2016;17:601–14. Available from: http://dx.doi.org/10.1038/nrg.2016.85

40. Ulitsky I, Shkumatava A, Jan CH, Sive H, Bartel DP. Conserved function of lincRNAs in vertebrate embryonic development despite rapid sequence evolution. Cell [Internet]. Elsevier Inc.; 2011;147:1537–50. Available from: http://dx.doi.org/10.1016/j.cell.2011.11.055

41. Hezroni H, Koppstein D, Schwartz MG, Avrutin A, Bartel DP, Ulitsky I. Principles of Long Noncoding RNA Evolution Derived from Direct Comparison of Transcriptomes in 17 Species. Cell Rep. [Internet]. The Authors; 2015;11:1110–22. Available from: http://dx.doi.org/10.1016/j.celrep.2015.04.023

42. Chu C, Spitale RC, Chang HY. Technologies to probe functions and mechanisms of long noncoding RNAs. Nat. Struct. Mol. Biol. [Internet]. Nature Publishing Group; 2015;22:29–35. Available from: http://dx.doi.org/10.1038/nsmb.2921

43. Dinger ME, Pang KC, Mercer TR, Mattick JS. Differentiating protein-coding and noncoding RNA: Challenges and ambiguities. PLoS Comput. Biol. 2008.

44. Housman G, Ulitsky I. Methods for distinguishing between protein-coding and long noncoding RNAs and the elusive biological purpose of translation of long noncoding RNAs [Internet]. Biochim. Biophys. Acta - Gene Regul. Mech. Elsevier B.V.; 2016. p. 31–40. Available from: http://dx.doi.org/10.1016/j.bbagrm.2015.07.017

45. Guttman M, Russell P, Ingolia NT, Weissman JS, Lander ES. Ribosome profiling provides evidence that large noncoding RNAs do not encode proteins. Cell [Internet]. Elsevier Inc.; 2013;154:240–51. Available from: http://dx.doi.org/10.1016/j.cell.2013.06.009

46. Ingolia NT. Ribosome profiling: new views of translation, from single codons to genome scale. Nat. Rev. Genet. [Internet]. Nature Publishing Group; 2014;15:205–13. Available from: http://www.ncbi.nlm.nih.gov/pubmed/24468696

47. Anderson DM, Anderson KM, Chang CL, Makarewich CA, Nelson BR, McAnally JR, et al. A micropeptide encoded by a putative long noncoding RNA regulates muscle performance. Cell [Internet]. Elsevier Inc.; 2015;160:595–606. Available from: http://dx.doi.org/10.1016/j.cell.2015.01.009

48. Nelson BR, Makarewich CA, Anderson DM, Winders BR, Troupes CD, Wu F, et al. A peptide encoded by a transcript annotated as long noncoding RNA enhances SERCA activity in muscle. Science (80-.). 2016;351:271–5.

49. Ulveling D, Francastel C, Hubé F. When one is better than two: RNA with dual functions [Internet]. Biochimie. Elsevier Masson SAS; 2011. p. 633–44. Available from: http://dx.doi.org/10.1016/j.biochi.2010.11.004

50. Gupta R a, Shah N, Wang KC, Kim J, Horlings HM, David J, et al. Long noncoding RNA HONTAIR reprograms chromatin state to promote cancer metastasis. Nature. 2010;464:1071–6.

51. Sleutels F, Zwart R, Barlow DP. The non-coding Air RNA is required for silencing autosomal imprinted genes. Nature. 2002;415:810–3.

52. Sibly R, Beverton RJH, Hill WG, Contributions IS, Casper BC, Baudisch A, et al. References and Notes 1. 2012;338:619–21.

53. Yue M, Charles Richard JL, Ogawa Y. Dynamic interplay and function of multiple noncoding genes governing X chromosome inactivation. Biochim. Biophys. Acta - Gene Regul. Mech. 2016.

54. Mariner PD, Walters RD, Espinoza CA, Drullinger LF, Wagner SD, Kugel JF, et al. Human Alu RNA Is a Modular Transacting Repressor of mRNA Transcription during Heat Shock. Mol. Cell. 2008;29:499–509.

55. Shamovsky I, Ivannikov M, Kandel ES, Gershon D, Nudler E. RNA-mediated response to heat shock in mammalian cells. Nature [Internet]. 2006;440:556–60. Available from: http://www.ncbi.nlm.nih.gov/pubmed/16554823

56. Martianov I, Ramadass A, Serra Barros A, Chow N, Akoulitchev A. Repression of the human dihydrofolate reductase gene by a non-coding interfering transcript. Nature. 2007;445:666–70.

57. Shearwin KE, Callen BP, Egan JB. Transcriptional interference - A crash course. Trends Genet. 2005. p. 339–45.

58. Hongay CF, Grisafi PL, Galitski T, Fink GR. Antisense Transcription Controls Cell Fate in Saccharomyces cerevisiae. Cell. 2006;127:735–45.

59. Kornienko AE, Guenzl PM, Barlow DP, Pauler FM. Gene regulation by the act of long non-coding RNA transcription. BMC Biol. [Internet]. 2013;11:59. Available from: http://www.biomedcentral.com/1741-7007/11/59

60. Carrozza MJ, Li B, Florens L, Suganuma T, Swanson SK, Lee KK, et al. Histone H3 methylation by Set2 directs deacetylation of coding regions by Rpd3S to suppress spurious intragenic transcription. Cell. 2005;123:581–92.

61. Houseley J, Rubbi L, Grunstein M, Tollervey D, Vogelauer M. A ncRNA Modulates Histone Modification and mRNA Induction in the Yeast GAL Gene Cluster. Mol. Cell [Internet]. Elsevier Inc.; 2008;32:685–95. Available from: http://dx.doi.org/10.1016/j.molcel.2008.09.027

62. van Werven FJ, Neuert G, Hendrick N, Lardenois A, Buratowski S, Van Oudenaarden A, et al. Transcription of two long noncoding RNAs mediates mating-type control of gametogenesis in budding yeast. Cell. 2012;150:1170–81.

63. Krystal GW, Armstrong BC, Battey JF. N-myc mRNA forms an RNA-RNA duplex with endogenous antisense transcripts. Mol. Cell. Biol. 1990;10:4180–91.

64. Munroe SH, Lazar MA. Inhibition of c-erbA mRNA splicing by a naturally occurring antisense RNA. J. Biol. Chem. 1991;266:22083–6.

65. Tripathi V, Ellis JD, Shen Z, Song DY, Pan Q, Watt AT, et al. The nuclear-retained noncoding RNA MALAT1 regulates alternative splicing by modulating SR splicing factor phosphorylation. Mol. Cell [Internet]. Elsevier Ltd; 2010;39:925–38. Available from: http://dx.doi.org/10.1016/j.molcel.2010.08.011

66. Hundley HA, Bass BL. ADAR editing in double-stranded UTRs and other non-coding RNA sequences.

67. Carrieri C, Cimatti L, Biagioli M, Beugnet A, Zucchelli S, Fedele S, et al. Long non-coding antisense RNA controls Uchl1 translation through an embedded SINEB2 repeat. Nature [Internet]. Nature Publishing Group; 2012;491:454–7. Available from: http://dx.doi.org/10.1038/nature11508

68. Gong C, Maquat LE. lncRNAs transactivate Staufen1-mediated mRNA decay by duplexing with 3'UTRs via Alu elements.

69. Faghihi M, Wahlestedt C. Regulatory roles of natural antisense transcripts. Nat. Rev. Mol. cell Biol. [Internet]. 2009;10:637–43. Available from: http://www.nature.com/nrm/journal/v10/n9/abs/nrm2738.html

70. Franco-Zorrilla JM, Valli A, Todesco M, Mateos I, Puga MI, Rubio-Somoza I, et al. Target mimicry provides a new mechanism for regulation of microRNA activity.

71. Hellwig S, Bass BL. A starvation-induced noncoding RNA modulates expression of Dicer-regulated genes. Proc. Natl. Acad. Sci. U. S. A. [Internet]. 2008;105:12897–902. Available from: http://www.ncbi.nlm.nih.gov/pubmed/18723671%5Cnhttp://www.pubmedcentral.nih.gov/articlerender.fcgi?artid=PMC2519042

72. Pijlman GP, Funk A, Kondratieva N, Leung J, Torres S, van der Aa L, et al. A Highly Structured, Nuclease-Resistant, Noncoding RNA Produced by Flaviviruses Is Required for Pathogenicity. Cell Host Microbe [Internet]. Elsevier Inc.; 2008;4:579–91. Available from: http://dx.doi.org/10.1016/j.chom.2008.10.007

73. Spitale RC, Tsai MC, Chang HY. RNA templating the epigenome: Long noncoding RNAs as molecular scaffolds. Epigenetics. 2011;6:539–43.

74. Zappulla DC. From The Cover: Yeast telomerase RNA: A flexible scaffold for protein subunits. Proc. Natl. Acad. Sci. 2004;101:10024–9.

75. Halic M, Becker T, Pool MR, Spahn CMT, Grassucci RA, Frank J, et al. Structure of the signal recognition particle interacting with the elongation-arrested ribosome. Nature [Internet]. 2004;427:808–14. Available from: http://dx.doi.org/10.1038/nature02342

76. Rinn JL, Chang HY. Genome regulation by long noncoding RNAs. Annu. Rev. Biochem. [Internet]. 2012;81:145–66. Available from: http://www.pubmedcentral.nih.gov/articlerender.fcgi?artid=3858397&tool=pmcentrez&rendertype=abstract

77. Derrien T, Johnson R, Bussotti G, Tanzer A, Djebali S, Tilgner H, et al. The GENCODE v7 catalog of human long noncoding RNAs: Analysis of their gene structure, evolution, and expression. Genome Res. 2012;

78. Batista PJ, Chang HY. Long noncoding RNAs: Cellular address codes in development and disease [Internet]. Cell. Elsevier Inc.; 2013. p. 1298–307. Available from: http://dx.doi.org/10.1016/j.cell.2013.02.012

79. Lee JT. Disruption of Imprinted X Inactivation by Parent-of-Origin Effects at Tsix expression implicates the existence of a maternally ex. Cell. 2000;103:17–27.

80. Sado T, Wang Z, Sasaki H LE. Regulation of imprinted X-chromosome inactivation in mice by Tsix. Development. 2001;1286:1275–86.

81. Yildirim E, Kirby JE, Brown DE, Mercier FE, Sadreyev RI, Scadden DT, et al. Xist RNA is a potent suppressor of hematologic cancer in mice. Cell [Internet]. Elsevier Inc.; 2013;152:727–42. Available from: http://dx.doi.org/10.1016/j.cell.2013.01.034

82. Wang KC, Yang YW, Liu B, Sanyal A, Corces-Zimmerman R, Chen Y, et al. A long noncoding RNA maintains active chromatin to coordinate homeotic gene expression. Nature [Internet]. Nature Publishing Group; 2011;472:120–4. Available from:

http://www.pubmedcentral.nih.gov/articlerender.fcgi?artid=3670758&tool=pmcentrez&rendertype=abstract

83. Maamar H, Cabili MN, Rinn J, Raj A. linc-HOXA1 is a noncoding RNA that represses HoXa1 transcription in cis. Genes Dev. 2013;

84. Giakountis A, Moulos P, Zarkou V, Oikonomou C, Harokopos V, Hatzigeorgiou AG, et al. A Positive Regulatory Loop between a Wnt-Regulated Non-coding RNA and ASCL2 Controls Intestinal Stem Cell Fate. Cell Rep. 2016;

85. Dinger M, Amaral P, Mercer T. Long noncoding RNAs in mouse embryonic stem cell pluripotency and differentiation. Genome Res. [Internet]. 2008;1433–45. Available from: http://genome.cshlp.org/content/18/9/1433.short

86. Guttman M, Amit I, Garber M, French C, Lin MF, Feldser D, et al. Chromatin signature reveals over a thousand highly conserved large non-coding RNAs in mammals. Nature [Internet]. Nature Publishing Group; 2009;458:223–7. Available from: http://www.pubmedcentral.nih.gov/articlerender.fcgi?artid=2754849&tool=pmcentrez&rendertype=abstract

87. Guttman M, Donaghey J, Carey BW, Garber M, Grenier JK, Munson G, et al. lincRNAs act in the circuitry controlling pluripotency and differentiation. Nature. 2011;477.

88. Ng S, Johnson R, Stanton LW. Human long non-coding RNAs promote pluripotency and neuronal differentiation by association with chromatin modifiers and transcription factors. EMBO J. [Internet]. Nature Publishing Group; 2012;31:522–33. Available from: http://dx.doi.org/10.1038/emboj.2011.459

89. Zhang B, Arun G, Mao YS, Lazar Z, Hung G, Bhattacharjee G, et al. The lncRNA malat1 is dispensable for mouse development but its transcription plays a cis-regulatory role in the adult. Cell Rep. [Internet]. Elsevier; 2012;2:111–23. Available from: http://dx.doi.org/10.1016/j.celrep.2012.06.003

90. Pollard KS, Salama SR, Lambert N, Lambot M, Coppens S, Pedersen JS, et al. An RNA gene expressed during cortical development evolved rapidly in humans. Nature. 2006;443:167–72.

91. Feng J, Bi C, Clark BS, Mady R, Shah P, Kohtz JD. The Evf-2 noncoding RNA is transcribed from the Dlx-5/6 ultraconserved region and functions as a Dlx-2 transcriptional coactivator. Genes Dev. 2006;

92. Fatica A, Bozzoni I. Long non-coding RNAs: new players in cell differentiation and development. Nat Rev Genet [Internet]. Nature Publishing Group; 2014;15:7–21. Available from: http://dx.doi.org/10.1038/nrg3606

93. Hindorff LA, Sethupathy P, Junkins HA, Ramos EM, Mehta JP, Collins FS, et al. Potential etiologic and functional implications of genome-wide association loci for human diseases and traits.

94. Sahu A, Singhal U, Chinnaiyan AM. Long noncoding RNAs in cancer: from function to translation The emergence of lncRNAs in cancer.

95. Audas TE, Lee S. Stressing out over long noncoding RNA ☆. BBA - Gene Regul. Mech. 2016;1859:184–91.

96. Huarte M. The emerging role of lncRNAs in cancer. Nat. Med. 2015;21.

97. Xue S, Li Q, Che J, Guo Y, Yang F, Zheng J. Decreased expression of long non-coding RNA NBAT-1 is associated with poor prognosis in patients with clear cell renal cell carcinoma. Int J Clin Exp Pathol. 2015;8:3765–74.

98. Wang X, Ruan Y, Wang X, Zhao W, Jiang Q, Jiang C, et al. Long intragenic non- - coding RNA lincRNA- - p21 suppresses development of human prostate cancer. Cell Prolif. 2016;1–10.

99. Liu B, Pan C, He Z, Wang J, Wang P, Ma T, et al. Long Noncoding RNA-LET Suppresses Tumor Growth and EMT in Lung Adenocarcinoma. Biomed Res. Int. [Internet]. 2016;2016:4693471. Available from: http://www.ncbi.nlm.nih.gov/pubmed/27896272%0Ahttp://www.pubmedcentral.nih.gov/articlerender.fcgi?artid=PMC5118531

100. Huang W, Cui X, Chen J, Feng Y, Song E, Li J, et al. Long non-coding RNA NKILA inhibits migration and invasion of tongue squamous cell carcinoma cells via suppressing epithelial- mesenchymal transition. Oncotarget [Internet]. 2016;7. Available from: www.impactjournals.com/oncotarget

101. Quagliata L, Matter MS, Piscuoglio S, Arabi L, Ruiz C, Procino A, et al. lncRNA HOTTIP / HOXA13 expression is associated with disease progression and predicts outcome in hepatocellular carcinoma patients. Hepatology. 2014;59:911–23.

102. Zhang D, Sun G, Zhang H, Tian J, Li Y. ScienceDirect Long non-coding RNA ANRIL indicates a poor prognosis of cervical cancer and promotes carcinogenesis via PI3K / Akt pathways. Biomed. Pharmacother. [Internet]. Elsevier Masson SAS; 2017;85:511–6. Available from: http://dx.doi.org/10.1016/j.biopha.2016.11.058

103. Mcgrath S, Christidis D, Perera M, Hong SK, Manning T, Vela I, et al. Prostate cancer biomarkers: Are we hitting the mark? 2016;

104. Pan W, Liu L, Wei J, Ge Y, Zhang J, Chen H, et al. A functional lncRNA HOTAIR genetic variant contributes to gastric cancer susceptibility. Mol. Carcinog. 2016;55:90–6.

105. Gupta SC, Tripathi YN. Potential of Long Non-coding RNAs in Cancer Patients: From Bio-markers to Therapeutic Targets.

106. Kaplan CD. Transcription Elongation Factors Repress Transcription Initiation from Cryptic Sites. Science (80-.). [Internet]. 2003;301:1096–9. Available from: http://www.sciencemag.org/cgi/doi/10.1126/science.1087374

107. David L, Huber W, Granovskaia M, Toedling J, Palm CJ, Bofkin L, et al. A high-resolution map of transcription in the yeast genome. PNAS. 2006;103:5320–5.

108. Nagalakshmi U, Wang Z, Waern K, Shou C, Raha D, Gerstein M, et al. The transcriptional landscape of the yeast genome defined by RNA sequencing. Science [Internet]. 2008;320:1344–9. Available from: http://www.ncbi.nlm.nih.gov/pmc/articles/PMC2951732/%5Cnhttps://www.ncbi.nlm.nih.gov/pmc/articles/PMC2951732/pdf/nihms229938.pdf%5Cnhttp://www.ncbi.nlm.nih.gov/pubmed/18451266%5Cnhttp://www.pubmedcentral.nih.gov/articlerender.fcgi?artid=PMC2951732

109. Davis CA, Ares M. Accumulation of unstable promoter-associated transcripts upon loss of the nuclear exosome subunit Rrp6p in Saccharomyces cerevisiae. Proc. Natl. Acad. Sci. U. S. A. [Internet]. 2006;103:3262–7. Available from: http://www.pnas.org/content/103/9/3262

110. Houalla R, Devaux F, Fatica A, Kufel J, Barrass D, Torchet C, et al. Microarray

detection of novel nuclear RNA substrates for the exosome. Yeast. 2006;23:439–54.

111. Luke B, Panza A, Redon S, Iglesias N, Li Z, Lingner J. The Rat1p 5' to 3' Exonuclease Degrades Telomeric Repeat-Containing RNA and Promotes Telomere Elongation in Saccharomyces cerevisiae. Mol. Cell [Internet]. Elsevier Inc.; 2008;32:465–77. Available from: http://dx.doi.org/10.1016/j.molcel.2008.10.019

112. Neil H, Malabat C, d'Aubenton-Carafa Y, Xu Z, Steinmetz LM, Jacquier A, et al. Widespread bidirectional promoters are the major source of cryptic transcripts in yeast. Nature [Internet]. Nature Publishing Group; 2009;457:1038–42. Available from: http://dx.doi.org/10.1038/nature07747%5Cnhttp://www.ncbi.nlm.nih.gov/pubmed/19169244

113. Lardenois A, Liu Y, Walther T, Chalmel F, Evrard B, Granovskaia M, et al. Execution of the meiotic noncoding RNA expression program and the onset of gametogenesis in yeast require the conserved exosome subunit Rrp6. Proc. Natl. Acad. Sci. U. S. A. 2011;108:1058–63.

114. Toesca I, Nery CR, Fernandez CF, Sayani S, Chanfreau GF. Cryptic transcription mediates repression of subtelomeric metal homeostasis genes. PLoS Genet. 2011;7.

115. Nadal-Ribelles M, Sole C, Xu Z, Steinmetz LM, DeNadal E, Posas F. Control of Cdc28 CDK1 by a Stress-Induced lncRNA. Mol. Cell. 2014;53:549–61.

116. Niederer RO, Papadopoulos N, Zappulla DC. Identification of novel noncoding transcripts in telomerase-negative yeast using RNA-seq. Sci. Rep. [Internet]. Nature Publishing Group; 2016;6:19376. Available from: http://www.nature.com/articles/srep19376

117. Tuck AC, Tollervey D. A transcriptome-wide atlas of RNP composition reveals diverse classes of mRNAs and lncRNAs. Cell [Internet]. Elsevier Inc.; 2013;154:996–1009. Available from: http://dx.doi.org/10.1016/j.cell.2013.07.047

118. Pinskaya M, Gourvennec S, Morillon A. H3 lysine 4 di- and tri-methylation deposited by cryptic transcription attenuates promoter activation. EMBO J. [Internet]. 2009;28:1697–707. Available from: http://www.pubmedcentral.nih.gov/articlerender.fcgi?artid=2699354&tool=pmcentrez&rendertype=abstract

119. Martens J a, Laprade L, Winston F. Intergenic transcription is required to repress the Saccharomyces cerevisiae SER3 gene. Nature. 2004;429:571–4.

120. Rathmell WK, Chu G. Involvement of the Ku autoantigen in the cellular response to DNA double-strand breaks. Proc. Natl. Acad. Sci. U. S. A. [Internet]. 1994;91:7623–7627. Available from: http://links.jstor.org/sici?sici=0027-8424(1994)91:16%3C7623:IOTKAI%3E2.0.CO;2-Z%5Cnhttp://www.jstor.org/journals/00278424.html

121. Gravel S, Larrivée M, Labrecque P, Wellinger RJ. Yeast Ku as a regulator of chromosomal DNA end structure. Science (80-.). 1998;280:741–4.

122. Grandin N, Damon C, Charbonneau M. Cdc13 cooperates with the yeast Ku proteins and Stn1 to regulate telomerase recruitment. Mol. Cell. Biol. [Internet]. 2000;20:8397–408. Available from: http://www.pubmedcentral.nih.gov/articlerender.fcgi?artid=102147&tool=pmcentrez&rendertype=abstract%5Cnfile:///C:/Users/Lab User/AppData/Local/Mendeley Ltd./Mendeley Desktop/Downloaded/Grandin, Damon, Charbonneau - 2000 - Cdc13 cooperates with the

yeast Ku

123. Fisher TS, Taggart AKP, Zakian VA. Cell cycle-dependent regulation of yeast telomerase by Ku. Nat. Struct. Mol. Biol. [Internet]. 2004;11:1198–205. Available from: http://www.ncbi.nlm.nih.gov/pubmed/15531893

124. Lopez CR, Ribes-Zamora A, Indiviglio SM, Williams CL, Haricharan S, Bertuch AA. Ku must load directly onto the chromosome end in order to mediate its telomeric functions. PLoS Genet. 2011;

125. Singer MS, Gottschling DE. TLC1: template RNA component of Saccharomyces cerevisiae telomerase. Science [Internet]. 1994;266:404–9. Available from: http://www.ncbi.nlm.nih.gov/pubmed/7545955

126. Feng J, Funk WD, Wang S-S, Weinrich SL, Avilion AA, Chiu C-P, et al. The RNA Component of Human Telomerase. Villeponteau Source Sci. New Ser. [Internet]. 1995;269:1236–41. Available from: http://www.jstor.org/stable/2888003

127. Young RS, Ponting CP. Identifi cation and function of long non-coding RNAs. Essays Biochem. 2013;54:113–26.

128. Wellinger RJ, Zakian VA. Everything you ever wanted to know about Saccharomyces cerevisiae telomeres: Beginning to end. Genetics. 2012.

129. Kupiec M. Biology of telomeres: Lessons from budding yeast. FEMS Microbiol. Rev. 2014.

130. Wellinger RJ, Zakian VA. Everything you ever wanted to know about Saccharomyces cerevisiae telomeres: Beginning to end. Genetics. 2012;191:1073–105.

131. Kupiec M. Biology of telomeres: Lessons from budding yeast. FEMS Microbiol. Rev. 2014;38:144–71.

132. Lundblad V, Szostak JW. A mutant with a defect in telomere elongation leads to senescence in yeast. Cell. 1989;57:633–43.

133. Chen Q, Ijpma A, Greider CW. Two survivor pathways that allow growth in the absence of telomerase are generated by distinct telomere recombination events. Mol. Cell. Biol. [Internet]. 2001;21:1819–27. Available from: http://www.ncbi.nlm.nih.gov/pubmed/11238918

134. Le S, Moore JK, Haber JE, Greider CW. RAD50 and RAD51 define two pathways that collaborate to maintain telomeres in the absence of telomerase. Genetics. 1999;

135. Teng SC, Zakian VA. Telomere-telomere recombination is an efficient bypass pathway for telomere maintenance in Saccharomyces cerevisiae. Mol. Cell. Biol. [Internet]. 1999;19:8083–93. Available from: http://www.ncbi.nlm.nih.gov/pubmed/10567534

136. Grandin N, Charbonneau M. The Rad51 pathway of telomerase-independent maintenance of telomeres can amplify TG1-3 sequences in yku and cdc13 mutants of Saccharomyces cerevisiae. Mol Cell Biol. 2003;23:3721–34.

137. Huang PH, Pryde FE, Lester D, Maddison RL, Borts RH, Hickson ID, et al. SGS1 is required for telomere elongation in the absence of telomerase. Curr. Biol. 2001;11:125–9.

138. Larrivée M, LeBel C, Wellinger RJ. The generation of proper constitutive G-tails on

yeast telomeres is dependent on the MRX complex. Genes Dev. 2004;18:1391–6.

139. Grandin N, Charbonneau M. Mrc1, a non-essential DNA replication protein, is required for telomere end protection following loss of capping by Cdc13, Yku or telomerase. Mol. Genet. Genomics. 2007;

140. Hu Y, Tang HB, Liu NN, Tong XJ, Dang W, Duan YM, et al. Telomerase-Null Survivor Screening Identifies Novel Telomere Recombination Regulators. PLoS Genet. 2013;9.

141. Cervantes RB, Lundblad V. Mechanisms of chromosome-end protection. Curr. Opin. Cell Biol. 2002.

142. Zubko MK, Guillard S, Lydall D. Exo1 and Rad24 differentially regulate generation of ssDNA at telomeres of Saccharomyces cerevisiae cdc13-1 mutants. Genetics. 2004;

143. Maringele L, Lydall D. EXO1 Plays a Role in Generating Type I and Type II Survivors in Budding Yeast. Genetics. 2004;166:1641–9.

144. Li S, Makovets S, Matsuguchi T, Blethrow JD, Shokat KM, Blackburn EH. Cdk1-Dependent Phosphorylation of Cdc13 Coordinates Telomere Elongation during Cell-Cycle Progression. Cell [Internet]. Elsevier Inc.; 2009;136:50–61. Available from: http://dx.doi.org/10.1016/j.cell.2008.11.027

145. Bonetti D, Martina M, Clerici M, Lucchini G, Longhese MP. Multiple Pathways Regulate 3′ Overhang Generation at *S. cerevisiae* Telomeres. Mol. Cell [Internet]. 2009;35:70–81. Available from: http://dx.doi.org/10.1016/j.molcel.2009.05.015%5Cnhttp://linkinghub.elsevier.com/retrieve/pii/S1097276509003487

146. Bonetti D, Clerici M, Anbalagan S, Martina M, Lucchini G, Longhese MP. Shelterin-like proteins and Yku inhibit nucleolytic processing of Saccharomyces cerevisiae telomeres. PLoS Genet. 2010;

147. Wu P, Takai H, De Lange T. Telomeric 3' overhangs derive from resection by Exo1 and apollo and fill-in by POT1b-associated CST. Cell [Internet]. Elsevier Inc.; 2012;150:39–52. Available from: http://dx.doi.org/10.1016/j.cell.2012.05.026

148. Bonetti D, Martina M, Falcettoni M, Longhese MP. Telomere-end processing: Mechanisms and regulation. Chromosoma. 2014;123:57–66.

149. Maringele L, Lydall D. EXO1-dependent single-stranded DNA at telomeres activates subsets of DNA damage and spindle checkpoint pathways in budding yeast yku70Δ mutants. Genes Dev. 2002;16:1919–33.

150. Bonetti D, Clerici M, Anbalagan S, Martina M, Lucchini G, Longhese MP. Shelterin-like proteins and Yku inhibit nucleolytic processing of Saccharomyces cerevisiae telomeres. PLoS Genet. 2010;6:1.

151. Garvik B, Carson M, Hartwell L. Single-stranded DNA arising at telomeres in cdc13 mutants may constitute a specific signal for the RAD9 checkpoint. Mol. Cell. Biol. [Internet]. 1995;15:6128–38. Available from: http://www.pubmedcentral.nih.gov/articlerender.fcgi?artid=230864&tool=pmcentrez&rendertype=abstract

152. Grandin N, Charbonneau M. Mrc1, a non-essential DNA replication protein, is required for telomere end protection following loss of capping by Cdc13, Yku or

telomerase. Mol. Genet. Genomics. 2007;277:685–99.

153. Luke-Glaser S, Luke B. The Mph1 helicase can promote telomere uncapping and premature senescence in budding yeast. PLoS One. 2012;7.

154. Ponjavic J, Ponting CP, Lunter G. Functionality or transcriptional noise ? Evidence for selection within long noncoding RNAs Functionality or transcriptional noise ? Evidence for selection within long noncoding RNAs. 2007;556–65.

155. Struhl K. Transcriptional noise and the fidelity of initiation by RNA polymerase II. Nat. Struct. Mol. Biol. 2007;14.

156. Marques AC, Ponting CP. Intergenic lncRNAs and the evolution of gene expression. Curr. Opin. Genet. Dev. [Internet]. Elsevier Ltd; 2014;27:48–53. Available from: http://dx.doi.org/10.1016/j.gde.2014.03.009

157. Ulitsky I, Bartel DP. XLincRNAs: Genomics, evolution, and mechanisms. Cell [Internet]. Elsevier Inc.; 2013;154:26–46. Available from: http://dx.doi.org/10.1016/j.cell.2013.06.020

158. Rinn JL, Kertesz M, Wang JK, Squazzo SL, Xu X, Brugmann SA, et al. Functional Demarcation of Active and Silent Chromatin Domains in Human HOX Loci by Noncoding RNAs. Cell. 2007;

159. Huarte M, Guttman M, Feldser D, Garber M, Koziol MJ, Kenzelmann-Broz D, et al. A large intergenic noncoding RNA induced by p53 mediates global gene repression in the p53 response. Cell. 2010;

160. Khalil AM, Guttman M, Huarte M, Garber M, Raj A, Rivea Morales D, et al. Many human large intergenic noncoding RNAs associate with chromatin-modifying complexes and affect gene expression. Proc. Natl. Acad. Sci. U. S. A. 2009;106:11667–72.

161. Hainer SJ, Pruneski JA, Mitchell RD, Monteverde RM, Martens JA. Intergenic transcription causes repression by directing nucleosome assembly. Genes Dev. 2011;

162. Van Werven FJ, Neuert G, Hendrick N, Lardenois A, Buratowski S, Van Oudenaarden A, et al. Transcription of two long noncoding RNAs mediates mating-type control of gametogenesis in budding yeast. Cell. 2012;

163. Koziol MJ, Rinn JL. RNA traffic control of chromatin complexes. Curr. Opin. Genet. Dev. 2010.

164. Geisler S, Coller J. RNA in unexpected places: long non-coding RNA functions in diverse cellular contexts. Nat. Publ. Gr. 2013;14.

165. Fatica A, Bozzoni I. Long non-coding RNAs: new players in cell differentiation and development. Nat. Publ. Gr. 2013;15.

166. Tsai MC, Spitale RC, Chang HY. Long intergenic noncoding RNAs: New links in cancer progression. Cancer Res. 2011;71:3–7.

167. Esteller M. Non-coding RNAs in human disease. Nat. Publ. Gr. 2011;12.

168. Sauvageau M, Goff LA, Lodato S, Bonev B, Groff AF, Gerhardinger C, et al. Multiple knockout mouse models reveal lincRNAs are required for life and brain development. Elife. 2013;2013:1–24.

169. Amândio AR, Necsulea A, Joye E, Duboule D. Hotair is dispensable for mouse

development. PLoS Genet. 2016;in press:1–27.

170. Li L, Helms JA, Chang HY, Amandio A, Necsulea A, Joye E, et al. Comment on "Hotair Is Dispensable for Mouse Development" PLOS Genet. [Internet]. 2016;12:e1006406. Available from: http://dx.plos.org/10.1371/journal.pgen.1006406

171. Quinn JJ, Chang HY. Unique features of long non-coding RNA biogenesis and function. Nat. Publ. Gr. 2016;17.

172. Baryshnikova A, Costanzo M, Kim Y, Ding H, Koh J, Toufighi K, et al. Quantitative analysis of fitness and genetic interactions in yeast on a genome scale. Nat. Methods [Internet]. 2010;7:1017–24. Available from: http://www.nature.com/doifinder/10.1038/nmeth.1534

173. Tong AHY, Evangelista M, Parsons AB, Xu H, Bader GD, Pagé N, et al. Systematic genetic analysis with ordered arrays of yeast deletion mutants. Science (80-.). 2001;294:2364–8.

174. Schmitt ME, Brown T a, Trumpower BL. A rapid and simple method for preparation of RNA from Saccharomyces cerevisiae. Nucleic Acids Res. 1990;18:3091–2.

175. Ortega LM, Hengartner CJ, Vega LR. Nonradioactive method to detect native single-stranded G-tails on yeast telomeres using a modified southern blot protocol. Biotechniques. 2011;50:407–10.

176. Kyriakou D, Stavrou E, Demosthenous P, Angelidou G, San Luis B-J, Boone C, et al. Functional characterisation of long intergenic non-coding RNAs through genetic interaction profiling in Saccharomyces cerevisiae. BMC Biol. [Internet]. BMC Biology; 2016;14:106. Available from: http://dx.doi.org/10.1186/s12915-016-0325-7

177. Yamashita A, Shichino Y, Yamamoto M. The long non-coding RNA world in yeasts. Biochim. Biophys. Acta [Internet]. Elsevier B.V.; 2015;1859:1–8. Available from: http://linkinghub.elsevier.com/retrieve/pii/S1874939915001716

178. Costanzo M, Baryshnikova A, Bellay J, Kim Y, Spear ED, Sevier CS, et al. The genetic landscape of a cell. Science (80-.). [Internet]. 2010;327:425–31. Available from: http://www.ncbi.nlm.nih.gov/entrez/query.fcgi?cmd=Retrieve&db=PubMed&dopt=Citation&list_uids=20093466

179. Lopez CR, Ribes-Zamora A, Indiviglio SM, Williams CL, Haricharan S, Bertuch AA. Ku must load directly onto the chromosome end in order to mediate its telomeric functions. PLoS Genet. 2011;7.

180. Dixon SJ, Costanzo M, Baryshnikova A, Andrews B, Boone C. Systematic mapping of genetic interaction networks. Annu. Rev. Genet. 2009;43:601–25.

181. Myers CL, Barrett DR, Hibbs M a, Huttenhower C, Troyanskaya OG. Finding function: evaluation methods for functional genomic data. BMC Genomics. 2006;7:187.

182. He X, Qian W, Wang Z, Li Y, Zhang J. Prevalent positive epistasis in Escherichia coli and Saccharomyces cerevisiae metabolic networks. Nat. Genet. [Internet]. Nature Publishing Group; 2010;42:272–6. Available from: http://dx.doi.org/10.1038/ng.524

183. Askree SH, Yehuda T, Smolikov S, Gurevich R, Hawk J, Coker C, et al. A genome-wide screen for Saccharomyces cerevisiae deletion mutants that affect telomere length. Proc. Natl. Acad. Sci. U. S. A. [Internet]. 2004;101:8658–63. Available from: http://www.ncbi.nlm.nih.gov/pubmed/15161972

184. Yu EY, Steinberg-Neifach O, Dandjinou AT, Kang F, Morrison AJ, Shen X, et al. Regulation of telomere structure and functions by subunits of the INO80 chromatin remodeling complex. Mol Cell Biol [Internet]. 2007;27:5639–49. Available from: http://www.ncbi.nlm.nih.gov/pmc/articles/PMC1952117/pdf/0418-07.pdf

185. Hass EP, Zappulla DC. The Ku subunit of telomerase binds Sir4 to recruit telomerase to lengthen telomeres in S. cerevisiae. Elife. 2015;4:1–19.

186. Van Wageningen S, Kemmeren P, Lijnzaad P, Margaritis T, Benschop JJ, De Castro IJ, et al. Functional overlap and regulatory links shape genetic interactions between signaling pathways. Cell. 2010;143:991–1004.

187. Chang H-Y, Lawless C, Addinall SG, Oexle S, Taschuk M, Wipat a., et al. Genome-Wide Analysis to Identify Pathways Affecting Telomere-Initiated Senescence in Budding Yeast. G3: Genes|Genomes|Genetics. 2011;1:197–208.

188. Szappanos B, Kovács K, Szamecz B, Honti F, Costanzo M, Baryshnikova A, et al. An integrated approach to characterize genetic interaction networks in yeast metabolism. Nat. Genet. [Internet]. Nature Publishing Group; 2011;43:656–62. Available from: http://dx.doi.org/10.1038/ng.846

189. Ben-Shitrit T, Yosef N, Shemesh K, Sharan R, Ruppin E, Kupiec M. Systematic identification of gene annotation errors in the widely used yeast mutation collections. Nat. Methods [Internet]. 2012;9:373–8. Available from: http://www.nature.com/nmeth/journal/vaop/ncurrent/full/nmeth.1890.html%5Cnhttp://www.ncbi.nlm.nih.gov/pubmed/22306811

190. Baryshnikova ABA. Neighboring-gene effect: a genetic uncertainty principle. Nat. Methods [Internet]. Nature Publishing Group; 2012;9:341–3. Available from: http://dx.doi.org/10.1038/nmeth.1900%5Cnpapers3://publication/doi/10.1038/nmeth.1900

191. Denisenko O, Bomsztyk K. Yeast hnRNP K-like genes are involved in regulation of the telomeric position effect and telomere length. Mol Cell Biol. 2002;22:286–97.

192. Bertuch AA, Lundblad V. The Ku heterodimer performs separable activities at double-strand breaks and chromosome termini. Mol. Cell. Biol. [Internet]. 2003;23:8202–15. Available from: http://www.ncbi.nlm.nih.gov/pubmed/14585978

193. Franke J, Gehlen J, Ehrenhofer-Murray AE. Hypermethylation of yeast telomerase RNA by the snRNA and snoRNA methyltransferase Tgs1. J. Cell Sci. 2008;121:3553–60.

194. Toogun OA, DeZwaan DC, Freeman BC. The Hsp90 Molecular Chaperone Modulates Multiple Telomerase Activities. Mol. Cell. Biol. [Internet]. 2008;28:457–67. Available from: http://mcb.asm.org/cgi/doi/10.1128/MCB.01417-07

195. Pang TL, Wang CY, Hsu CL, Chen MY, Lin JJ. Exposure of single-stranded telomeric DNA causes G2/M cell cycle arrest in Saccharomyces cerevisiae. J. Biol. Chem. 2003;278:9318–21.

196. Downey M, Houlsworth R, Maringele L, Rollie A, Brehme M, Galicia S, et al. A Genome-Wide Screen Identifies the Evolutionarily Conserved KEOPS Complex as a Telomere Regulator. Cell. 2006;124:1155–68.

197. DeZwaan DC, Toogun O a, Echtenkamp FJ, Freeman BC. The Hsp82 molecular chaperone promotes a switch between unextendable and extendable telomere states. Nat. Struct. Mol. Biol. [Internet]. Nature Publishing Group; 2009;16:711–6. Available from: http://www.pubmedcentral.nih.gov/articlerender.fcgi?artid=2744139&tool=pmcentrez&rend

ertype=abstract

198. Ngo HP, Lydall D. Survival and growth of yeast without telomere capping by Cdc13 in the absence of Sgs1, Exo1, and Rad9. PLoS Genet. 2010;6.

199. Vodenicharov MD, Laterreur N, Wellinger RJ. Telomere capping in non-dividing yeast cells requires Yku and Rap1. EMBO J. [Internet]. Nature Publishing Group; 2010;29:3007–19. Available from: http://dx.doi.org/10.1038/emboj.2010.155

200. Young RS, Ponting CP. Identification and function of long non-coding RNAs. Essays Biochem. [Internet]. 2013;54:113–26. Available from: http://essays.biochemistry.org/lookup/doi/10.1042/bse0540113

201. Ard R, Tong P, Allshire RC. Long non-coding RNA-mediated transcriptional interference of a permease gene confers drug tolerance in fission yeast. Nat. Commun. [Internet]. Nature Publishing Group; 2014;5:5576. Available from: http://www.pubmedcentral.nih.gov/articlerender.fcgi?artid=4255232&tool=pmcentrez&rendertype=abstract

202. Bumgarner SL, Dowell RD, Grisafi P, Gifford DK, Fink GR. Toggle involving cis-interfering noncoding RNAs controls variegated gene expression in yeast. TL - 106. Proc. Natl. Acad. Sci. U. S. A. [Internet]. 2009;106 VN-:18321–6. Available from: /Users/yurikoharigaya/Documents/ReadCube Media/bumgarner2009.pdf%5Cnhttp://dx.doi.org/10.1073/pnas.0909641106

203. Kanduri C. Long noncoding RNAs: Lessons from genomic imprinting ☆. BBA - Gene Regul. Mech. 2016;1859:102–11.

204. Garitano-Trojaola A, Agirre X, Prósper F, Fortes P. Long non-coding RNAs in haematological malignancies. Int. J. Mol. Sci. 2013;14:15386–422.

205. Li T, Mo X, Fu L, Xiao B, Guo J. Molecular mechanisms of long noncoding RNAs on gastric cancer. Oncotarget [Internet]. 2016;7:8601–12. Available from: http://www.impactjournals.com/oncotarget/index.php?journal=oncotarget&page=article&op=view&path%5B%5D=6926&path%5B%5D=19600

206. Lue NF. Sequence-specific and conformation-dependent binding of yeast telomerase RNA to single-stranded telomeric DNA. Nucleic Acids Res. 1999;27:2560–7.

207. Niederer RO, Zappulla DC. Refined secondary-structure models of the core of yeast and human telomerase RNAs directed by SHAPE. RNA [Internet]. 2015;21:254–61. Available from: http://www.pubmedcentral.nih.gov/articlerender.fcgi?artid=4338352&tool=pmcentrez&rendertype=abstract

208. Zappulla DC, Cech TR. Yeast telomerase RNA: A flexible scaffold for protein subunits. 2004;

209. Deng Y, Guo X, Ferguson DO, Chang S. Multiple roles for Mre11 at uncapped telomeres. Nature. 2009;460:914–8.

210. Zubko MK, Guillard S, Lydall D. Exo1 and Rad24 differentially regulate generation of ssDNA at telomeres of Saccharomyces cerevisiae cdc13-1 mutants. Genetics. 2004;168:103–15.

211. Qi H, Zakian VA. The Saccharomyces telomere-binding protein Cdc13p interacts with both the catalytic subunit of DNA polymerase ?? and the telomerase-associated Est1

protein. Genes Dev. 2000;14:1777–88.

212. Adams Martin a, Dionne I, Wellinger RJ, Holm C. The function of DNA polymerase alpha at telomeric G tails is important for telomere homeostasis. Mol. Cell. Biol. 2000;20:786–96.

213. Grossi S, Puglisi A, Dmitriev P V., Lopes M, Shore D. Pol12, the B subunit of DNA polymerase ??, functions in both telomere capping and length regulation. Genes Dev. 2004;18:992–1006.

214. Pfeiffer V, Lingner J. TERRA promotes telomere shortening through exonuclease 1-mediated resection of chromosome ends. PLoS Genet. 2012;8.

215. Porro A, Feuerhahn S, Lingner J. TERRA-Reinforced Association of LSD1 with MRE11 Promotes Processing of Uncapped Telomeres. Cell Rep. [Internet]. The Authors; 2014;6:765–76. Available from: http://dx.doi.org/10.1016/j.celrep.2014.01.022

216. Azhibek D, Skvortsov D, Andreeva A, Zatsepin T, Arutyunyan A, Zvereva M, et al. TERRA mimicking ssRNAs prevail over the DNA substrate for telomerase in vitro due to interactions with the alternative binding site. J. Mol. Recognit. 2015;

217. Huber F, Bunina D, Gupta I, Theer P, Steinmetz LM, Knop M. Protein Abundance Control by Non-coding Antisense Protein Abundance Control by Non-coding Antisense Transcription. CellReports [Internet]. The Author(s); 2016;15:1–12. Available from: http://dx.doi.org/10.1016/j.celrep.2016.05.043

218. Kapusta A, Feschotte C. Volatile evolution of long noncoding RNA repertoires: Mechanisms and biological implications. Trends Genet. 2014.

219. Cong L, Ran FA, Cox D, Lin S, Barretto R, Hsu PD, et al. Multiplex Genome Engineering Using CRISPR/VCas Systems. Science (80-.). 2013;339:819–23.

220. Roguev, Talbot, Negri, Shales, Cagney, Bandyopadhyay, et al. Quantitative genetic-interaction mapping in mammalian cells. Nat. Methods [Internet]. Nature Publishing Group; 2013;10:432–7. Available from: http://www.ncbi.nlm.nih.gov/entrez/query.fcgi?db=pubmed&cmd=Retrieve&dopt=AbstractPlus&list_uids=23407553%5Cnpapers://6ef7d602-1904-44f2-bd27-ffa0776e3fdb/Paper/p1921

221. Laufer C, Fischer B, Huber W, Boutros M. Measuring genetic interactions in human cells by RNAi and imaging. Nat Protoc [Internet]. Nature Publishing Group; 2014;9:2341–53. Available from: http://www.ncbi.nlm.nih.gov/pubmed/25211512

222. Blomen VA, Májek P, Jae LT, Bigenzahn JW, Nieuwenhuis J, Staring J, et al. Gene essentiality and synthetic lethality in haploid human cells. Science [Internet]. 2015;350:1092–6. Available from: http://www.sciencemag.org/cgi/doi/10.1126/science.aac7557%5Cnhttp://www.ncbi.nlm.nih.gov/pubmed/26472760

223. Liu SJ, Liu SJ, Horlbeck MA, Cho SW, Birk HS, Malatesta M, et al. CRISPRi-based genome-scale identification of functional long noncoding RNA loci in human cells. 2016;7111.

224. Ryan CJ, Roguev A, Patrick K, Xu J, Jahari H, Tong Z, et al. Hierarchical Modularity and the Evolution of Genetic Interactomes across Species. Mol. Cell. 2012;46:691–704.

225. Johnsson P, Lipovich L, Grandér D, Morris K V. Evolutionary conservation of long

non-coding RNAs; sequence, structure, function. Biochim. Biophys. Acta [Internet]. 2014;1840:1063–71. Available from: http://www.pubmedcentral.nih.gov/articlerender.fcgi?artid=3909678&tool=pmcentrez&rendertype=abstract

226. Lenstra TL, Larson DR. Single-Molecule mRNA Detection in Live Yeast. Curr. Protoc. Mol. Biol. [Internet]. 2016;113:14.24.1-14.24.15. Available from: http://eutils.ncbi.nlm.nih.gov/entrez/eutils/elink.fcgi?dbfrom=pubmed&id=27110320&retmode=ref&cmd=prlinks%5Cnpapers3://publication/doi/10.1002/0471142727.mb1424s113

227. Bajon E, Laterreur N, Wellinger RJ. A Single Templating RNA in Yeast Telomerase. Cell Rep. [Internet]. The Authors; 2015;12:441–8. Available from: http://dx.doi.org/10.1016/j.celrep.2015.06.045

228. Feng J, Funk WD, Wang SS, Weinrich SL, Avilion AA, Chiu CP, et al. The RNA component of human telomerase. Science. 1995;269:1236–41.

Chapter 6 - Appendices

Appendix 1 : *TLC1* negative genetic interactions (first SGA screen)

	Systematic Gene Name	Standard Gene name	Double Mutant average growth	Double Mutant growth StdDev	Single Mutant average growth	Single mutant growth StdDev	SGA score (log10)
1	*YMR284W*	*YKU70*	0.086594	0.016967	0.944648	0.018052	-2.38958
2	*YMR106C*	*YKU80*	0.170416	0.044363	1.022977	0.014941	-1.79223
3	*YBR106W*	*PHO88*	0.242119	0.312487	0.621283	0.398364	-0.94236
4	*YNR006W*	*VPS27*	0.276525	0.038408	0.650277	0.247032	-0.8551
5	*YCL037C*	*SRO9*	0.311294	0.268259	0.668148	0.250804	-0.76377
6	*YGL136C*	*MRM2*	0.328743	0.213871	0.684102	0.202842	-0.73283
7	*YGR097W*	*ASK10*	0.533527	0.2138	1.08389	0.210871	-0.7088
8	*YJL204C*	*RCY1*	0.39816	0.06539	0.771032	0.150339	-0.66088
9	*YJR077C*	*MIR1*	0.396478	0.345124	0.735967	0.434167	-0.61856
10	*YBL094C*	*ORF*	0.340063	0.33014	0.628384	0.338877	-0.61402
11	*YML013C-A*	*ORF*	0.345801	0.050019	0.628737	0.356629	-0.59785
12	*YGL045W*	*RIM8*	0.37795	0.056887	0.659967	0.027696	-0.55743
13	*YGL046W*	*ORF*	0.420352	0.057408	0.723114	0.008869	-0.54247
14	*YNL235C*	*ORF*	0.430421	0.048364	0.739042	0.027183	-0.54059
15	*YOL004W*	*SIN3*	0.36867	0.02199	0.61443	0.027316	-0.51079
16	*YGL167C*	*PMR1*	0.371145	0.027558	0.596613	0.047138	-0.47468
17	*YFL013W-A*	*ORF*	0.455658	0.045864	0.728602	0.057412	-0.46938
18	*YNL121C*	*TOM70*	0.389286	0.067199	0.618402	0.058746	-0.46282
19	*YCL010C*	*SGF29*	0.415835	0.059589	0.659907	0.020008	-0.46181
20	*YBL031W*	*SHE1*	0.614006	0.639105	0.927644	0.255199	-0.41264
21	*YPL055C*	*LGE1*	0.502154	0.079441	0.752647	0.046696	-0.40469
22	*YFL007W*	*BLM10*	0.668231	0.600832	0.995898	0.111486	-0.39901
23	*YOR275C*	*RIM20*	0.409593	0.050671	0.603187	0.04682	-0.38706
24	*YLR199C*	*PBA1*	0.445319	0.08687	0.639839	0.048092	-0.36243
25	*YPR172W*	*ORF*	0.457619	0.068654	0.657322	0.070224	-0.36214
26	*YGR229C*	*SMI1*	0.494224	0.034773	0.681433	0.060845	-0.32121
27	*YGR055W*	*MUP1*	0.625333	0.077427	0.848528	0.047836	-0.30522
28	*YHR030C*	*SLT2*	0.651619	0.056298	0.872298	0.02188	-0.29167
29	*YFL003C*	*MSH4*	0.543302	0.143536	0.698652	0.023115	-0.25149
30	*YNL215W*	*IES2*	0.481979	0.134276	0.619457	0.081783	-0.25094
31	*YBR294W*	*SUL1*	0.702556	0.298681	0.901649	0.044132	-0.2495
32	*YLR297W*	*ORF*	0.619324	0.254228	0.779975	0.122275	-0.23063
33	*YER092W*	*IES5*	0.548314	0.056395	0.687486	0.039936	-0.22619
34	*YOR026W*	*BUB3*	0.591074	0.070191	0.736214	0.026177	-0.21958
35	*YDR004W*	*RAD57*	0.621013	0.153638	0.770742	0.096034	-0.216
36	*YDR162C*	*NBP2*	0.506893	0.028856	0.628054	0.029382	-0.21433
37	*YOR030W*	*DGF16*	0.633645	0.084133	0.776196	0.034243	-0.20292
38	*YGL163C*	*RAD54*	0.75255	0.013982	0.919419	0.019016	-0.20027
39	*YLR056W*	*ERG3*	0.681159	0.122115	0.831636	0.042326	-0.1996
40	*YOR179C*	*SYC1*	0.697667	0.090159	0.849363	0.024789	-0.19674

41	*YML035C*	*AMD1*	0.783576	0.045215	0.951878	0.006218	-0.19457
42	*YPL105C*	*SYH1*	0.827649	0.013897	1.004998	0.00676	-0.19415
43	*YJR088C*	*EMC2*	0.855813	0.031472	1.037812	0.036076	-0.19282
44	*YMR019W*	*STB4*	0.856732	0.013251	1.03667	0.003724	-0.19064
45	*YGR027C*	*RPS25A*	0.607861	0.093213	0.733517	0.011214	-0.1879
46	*YER095W*	*RAD51*	0.757907	0.063097	0.913731	0.066897	-0.18698
47	*YBR213W*	*MET8*	0.743774	0.029145	0.894544	0.025557	-0.18458
48	*YLR070C*	*XYL2*	0.83618	0.011778	1.005181	0.016775	-0.18408
49	*YPL261C*	*ORF*	0.730867	0.081686	0.877334	0.020997	-0.18266
50	*YMR207C*	*HFA1*	0.699425	0.038704	0.838282	0.023567	-0.1811
51	*YFR010W*	*UBP6*	0.571986	0.068204	0.68485	0.065217	-0.18009
52	*YLR184W*	*ORF*	0.746682	0.028546	0.892784	0.037595	-0.1787
53	*YDR463W*	*STP1*	0.664845	0.038056	0.794177	0.042628	-0.17775
54	*YLR388W*	*RPS29A*	0.744296	0.040341	0.88505	0.030458	-0.17321
55	*YMR225C*	*MRPL44*	0.837703	0.032349	0.992854	0.033662	-0.16992
56	*YNL302C*	*RPS19B*	0.756286	0.147604	0.89578	0.142519	-0.16927
57	*YNL119W*	*ORF*	0.750077	0.045495	0.885964	0.011066	-0.1665
58	*YJL049W*	*ORF*	0.874943	0.042247	1.033365	0.061713	-0.16642
59	*YJL066C*	*MPM1*	0.827328	0.027661	0.977079	0.036774	-0.16637
60	*YNR010W*	*CSE2*	0.676234	0.077716	0.798043	0.037963	-0.16562
61	*YNR005C*	*ORF*	0.935462	0.016017	1.103603	0.028185	-0.16529
61	*YCR043C*	*ORF*	0.748948	0.01058	0.882725	0.031995	-0.16434
63	*YNL116W*	*DMA2*	0.890447	0.012309	1.048929	0.012335	-0.1638
64	*YGL162W*	*SUT1*	0.871484	0.021752	1.026154	0.038165	-0.16338
65	*YCL016C*	*DCC1*	0.714737	0.104908	0.839179	0.035306	-0.16051
66	*YNL097C*	*PHO23*	0.915172	0.030531	1.073627	0.029607	-0.15969
67	*YHR033W*	*ORF*	0.891797	0.05364	1.044688	0.065105	-0.15824
68	*YGL176C*	*ORF*	0.807829	0.008671	0.945426	0.011228	-0.15729
69	*YFL013C*	*IES1*	0.631608	0.048255	0.738835	0.027921	-0.15681
70	*YDR440W*	*DOT1*	0.908371	0.013759	1.062277	0.006506	-0.15652
71	*YNL120C*	*ORF*	0.769037	0.031646	0.899263	0.020385	-0.15644
72	*YFL052W*	*ORF*	0.81287	0.017281	0.948838	0.006782	-0.15467
73	*YBL001C*	*EMC15*	0.767749	0.040981	0.89611	0.021205	-0.1546
74	*YJL070C*	*ORF*	0.865063	0.035111	1.009517	0.018995	-0.15443
75	*YOR297C*	*TIM18*	0.839814	0.10685	0.979826	0.028178	-0.15419
76	*YNL003C*	*PET8*	0.908519	0.020627	1.058956	0.013803	-0.15322
77	*YGR260W*	*TNA1*	0.776116	0.025248	0.903018	0.038926	-0.15144
78	*YER178W*	*PDA1*	0.783814	0.036138	0.911833	0.007763	-0.15129
79	*YER177W*	*BMH1*	0.926048	0.040703	1.077142	0.049343	-0.15114
80	*YHL027W*	*RIM101*	0.759774	0.046936	0.883171	0.026363	-0.1505

Appendix 2: *TLC1* negative genetic interactions (second SGA screen)

	Systematic Gene Name	Standard Gene name	Double mutant average growth	Double mutant growth StdDev	Single Mutant average growth	Single mutant StdDev	SGA score (log10)
1	*YMR284W*	*YKU70*	0,474198	0,026484	1,181111	0,016802	-0,91259

2	*YDR530C*	*APA2*	0,460931	0,042603	0,805735	0,011459	-0,55851
3	*YEL066W*	*HPA3*	0,475069	0,044713	0,736778	0,020905	-0,43883
4	*YER151C*	*UBP3*	0,535073	0,026342	0,793706	0,048767	-0,39431
5	*YFR010W*	*UBP6*	0,511438	0,060944	0,73218	0,026263	-0,3588
6	*YER131W*	*RPS26B*	0,525468	0,044249	0,735322	0,020464	-0,33602
7	*YBL056W*	*PTC3*	0,756788	0,054663	1,043607	0,030468	-0,32135
8	*YAL068C*	*PAU8*	0,66391	0,093837	0,900594	0,021956	-0,30491
9	*YER033C*	*ZRG8*	0,579752	0,062961	0,783209	0,035638	-0,3008
10	*YBL003C*	*HTA2*	0,541899	0,058301	0,721332	0,04004	-0,28602
11	*YBL001C*	*ECM15*	0,593176	0,096882	0,783802	0,03205	-0,27867
12	*YEL071W*	*DLD3*	0,627993	0,029328	0,825887	0,027964	-0,27393
13	*YDR463W*	*STP1*	0,623245	0,052805	0,817688	0,011316	-0,27154
14	*YDR455C*	*ORF*	0,568637	0,020387	0,727123	0,014729	-0,24585
15	*YAL056W*	*GPB2*	0,759261	0,036329	0,967556	0,009322	-0,24243
16	*YER074W*	*RPS24A*	0,596696	0,030926	0,75961	0,022503	-0,2414
17	*YFL052W*	*ORF*	0,6785	0,049724	0,86366	0,032551	-0,24129
18	*YER128W*	*VFA1*	0,608567	0,036058	0,773478	0,018432	-0,23979
19	*YBR215W*	*HPC2*	0,63209	0,030034	0,787771	0,021988	-0,22018
20	*YPR141C*	*KAR3*	0,535704	0,160382	0,662222	0,183673	-0,21202
21	*YBL055C*	*ORF*	0,820857	0,06329	1,014252	0,011496	-0,21156
22	*YFL013W-A*	*ORF*	0,633389	0,015634	0,77164	0,004822	-0,19743
23	*YGL163C*	*RAD54*	0,58014	0,099029	0,704454	0,070018	-0,19415
24	*YEL059W*	*HHY1*	0,585256	0,028869	0,709348	0,057602	-0,1923
25	*YOR297C*	*TIM18*	0,868749	0,111819	1,047658	0,039234	-0,18726
26	*YER016W*	*BIM1*	0,515324	0,026939	0,620622	0,002684	-0,18593
27	*YFL003C*	*MSH4*	0,724832	0,037484	0,871127	0,017892	-0,18385
28	*YEL056W*	*HAT2*	0,559679	0,041731	0,669658	0,062943	-0,1794
29	*YNR019W*	*ARE2*	0,838007	0,047324	1,001457	0,020008	-0,17819
30	*YER095W*	*RAD51*	0,711848	0,047045	0,850405	0,042528	-0,17785
31	*YPR167C*	*MET16*	0,814639	0,03788	0,973015	0,047993	-0,17765
32	*YGL042C*	*ORF*	0,580137	0,05824	0,689346	0,050148	-0,17248
33	*YDR535C*	*ORF*	0,789551	0,01284	0,936679	0,024234	-0,17088
34	*YPL261C*	*ORF*	0,650707	0,057572	0,770324	0,01705	-0,16875
35	*YER117W*	*RPL23B*	0,796782	0,071945	0,942809	0,02878	-0,16828
36	*YBR118W*	*TEF2*	0,573655	0,049718	0,677116	0,023235	-0,16581
37	*YEL067C*	*ORF*	0,729007	0,194728	0,856764	0,052879	-0,16148
38	*YNL255C*	*GIS2*	0,649868	0,061961	0,762936	0,05157	-0,16041
39	*YEL068C*	*ORF*	0,742282	0,136894	0,868794	0,033095	-0,15738
40	*YER118C*	*SHO1*	0,798509	0,049772	0,933844	0,023441	-0,15656
41	*YDR513W*	*GRX2*	0,719834	0,066513	0,839755	0,025211	-0,15409
42	*YBR072W*	*HSP26*	0,758186	0,017629	0,883566	0,011905	-0,15304
43	*YFL036W*	*RPO41*	0,706128	0,079978	0,822285	0,035058	-0,15229
44	*YDR375C*	*BCS1*	0,524123	0,068618	0,609375	0,05411	-0,15071

45	*YDR536W*	*STL1*	0,809193	0,031246	0,940204	0,014343	-0,15006

Appendix 3: *TLC1* positive genetic interactions (first screen)

	Systematic Gene Name	Standard Gene name	Double mutant average growth	Double mutant growth StdDev	Single Mutant average growth	Single mutant StdDev	SGA score (log10)
1	YER001W	MNN1	0.973595	0.012238	0.620645	0.112143	0.450236
2	YER004W	FMP52	1.036991	0.016402	0.698977	0.045781	0.394461
3	YGL252C	RTG2	0.875358	0.033904	0.624389	0.073147	0.337859
4	YPR191W	QCR2	0.979928	0.029153	0.735078	0.064032	0.287503
5	YER005W	YND1	1.026933	0.02057	0.774462	0.050479	0.282163
6	YER007C-A	TMA20	1.010678	0.005371	0.764341	0.017211	0.279362
7	YER007W	PAC2	1.035467	0.018703	0.794388	0.044467	0.265036
8	YER020W	GPA2	0.792043	0.028235	0.618115	0.041527	0.247941
9	YMR255W	GFD1	1.139364	0.023875	0.894513	0.01796	0.241945
10	YGL066W	SGF73	0.813378	0.021743	0.641762	0.021559	0.236978
11	YGL255W	ZRT1	0.786053	0.068006	0.621892	0.067937	0.234257
12	YER010C	ORF	1.047354	0.01908	0.831709	0.045181	0.23054
13	YKL197C	PEX1	0.824776	0.017148	0.655488	0.05255	0.229731
14	YHR081W	LRP1	0.955873	0.085414	0.770426	0.140737	0.215681
15	YDL048C	STP4	0.98091	0.02392	0.792377	0.390238	0.213443
16	YNL190W	ORF	1.142468	0.059576	0.924383	0.011487	0.211819
17	YGR183C	QCR9	0.938564	0.046187	0.760819	0.048395	0.209955
18	YNL052W	COX5A	1.102774	0.011034	0.896413	0.018513	0.207183
19	YBL046W	PSY4	0.765062	0.150887	0.623372	0.016778	0.204813
20	YNL167C	SKO1	1.114195	0.011356	0.908235	0.024388	0.204384
21	YNL035C	ORF	1.101444	0.032091	0.899474	0.011864	0.202567
22	YPR134W	MSS18	0.998639	0.029565	0.817425	0.042365	0.200234
23	YAL014C	SYN8	1.317033	0.023404	1.078527	0.021914	0.199785
24	YNL289W	PCL1	1.109427	0.018481	0.909396	0.01259	0.198819
25	YMR254C	ORF	1.124506	0.038858	0.922167	0.015903	0.198373
26	YKL030W	ORF	1.047272	0.051109	0.86238	0.089917	0.194248
27	YNL274C	GOR1	1.020393	0.088883	0.842162	0.040023	0.191971
28	YMR271C	URA10	1.130383	0.009665	0.93441	0.021958	0.190396
29	YNL146W	ORF	1.108429	0.029004	0.916362	0.011743	0.190288
30	YAL045C	ORF	0.96353	0.195447	0.800672	0.098402	0.185152
31	YMR282C	AEP2	0.847427	0.019101	0.704528	0.047468	0.184676
32	YMR252C	ORF	1.038688	0.077972	0.866227	0.077458	0.181567
33	YLR098C	CHA4	1.099466	0.0068	0.918048	0.022773	0.180331
34	YKL062W	MSN4	1.014099	0.027352	0.84758	0.010498	0.179371
35	YAL002W	VPS8	1.008041	0.015087	0.842648	0.030844	0.179214
36	YPL120W	VPS30	0.967177	0.010245	0.809075	0.018037	0.17849
37	YLL043W	FPS1	0.953954	0.023135	0.798176	0.026457	0.178286
38	YJR032W	CPR7	0.934962	0.016504	0.784978	0.009695	0.17485
39	YPR069C	SPE3	0.835261	0.011955	0.702618	0.017135	0.17293

40	YNL301C	RPL18B	1.102109	0.01795	0.927655	0.026747	0.172321
41	YLR441C	RPS1A	0.949551	0.018118	0.80045	0.011957	0.170816
42	YNL201C	PSY2	1.145129	0.038436	0.965441	0.012978	0.170687
43	YBR098W	MMS4	0.938802	0.035049	0.791797	0.349398	0.1703
44	YBL052C	SAS3	1.170493	0.013428	0.987266	0.026487	0.17024
45	YJL211C	ORF	0.925396	0.024957	0.78235	0.020319	0.16792
46	YLR425W	TUS1	1.009176	0.044555	0.854915	0.024816	0.165887
47	YLL045C	RPL8B	1.002628	0.044947	0.849769	0.028716	0.165416
48	YLL056C	ORF	1.128322	0.013595	0.956923	0.010666	0.164765
49	YLR330W	CHS5	1.009318	0.026686	0.856281	0.011564	0.164431
50	YLL057C	JLP1	1.154033	0.029449	0.979299	0.031225	0.164181
51	YJR117W	STE24	1.124159	0.017656	0.954101	0.05438	0.164021
52	YBR151W	APD1	1.25489	0.034406	1.065579	0.024809	0.16353
53	YJL210W	PEX2	0.859702	0.023478	0.730106	0.038221	0.163396
54	YOR065W	CYT1	0.859802	0.028992	0.730379	0.063936	0.163139
55	YOL041C	NOP12	0.819053	0.014237	0.696124	0.022555	0.162622
56	YNL329C	PEX6	0.959301	0.030254	0.816303	0.036368	0.161419
57	YAL015C	NTG1	1.022017	0.15189	0.869901	0.078409	0.161154
58	YJL130C	URA2	1.114281	0.018302	0.949087	0.009639	0.160464
59	YDR158W	HOM2	0.853996	0.015853	0.727587	0.019651	0.160192
60	YLR038C	COX12	0.969505	0.005617	0.826171	0.030182	0.159984
61	YLR345W	ORF	1.122031	0.03255	0.95816	0.008215	0.15788
62	YHR198C	AIM18	1.134985	0.020236	0.96963	0.019849	0.157459
63	YOL027C	MDM38	0.927252	0.029453	0.792189	0.02426	0.157425
64	YPR060C	ARO7	1.011532	0.019634	0.864496	0.028157	0.157074
65	YHR066W	SSF1	1.084777	0.028913	0.927298	0.034807	0.156855
66	YNL068C	FKH2	1.096454	0.038327	0.937366	0.015866	0.156764
67	YMR179W	SPT21	0.978624	0.030261	0.837267	0.014985	0.156004
68	YNL183C	NPR1	0.901756	0.125138	0.772395	0.041247	0.154848
69	YKR048C	NAP1	1.049132	0.024942	0.898756	0.017113	0.154707
70	YLR360W	VPS38	1.034919	0.020835	0.887113	0.026189	0.154107
71	YDL083C	RPS16B	0.927209	0.087982	0.795124	0.057937	0.153681
72	YOR196C	LIP5	0.743453	0.046877	0.638095	0.051023	0.152818
73	YMR170C	ALD2	1.128002	0.021666	0.96841	0.01318	0.152547
74	YPL106C	SSE1	0.839708	0.02113	0.721497	0.03871	0.151727
75	YJR059W	PTK2	0.998028	0.007013	0.857635	0.034868	0.151603
76	YLR344W	RPL26A	1.074949	0.033343	0.923822	0.016397	0.151509
77	YBL051C	PIN4	1.083192	0.049426	0.931299	0.012212	0.151088
78	YJL101C	GSH1	0.922664	0.028276	0.793365	0.020984	0.150981
79	YPL260W	ORF	0.900534	0.052861	0.774358	0.03105	0.150953
80	YNL187W	SWT21	1.150784	0.037812	0.989717	0.025052	0.150779
81	YML102C-A	ORF	1.013405	0.03278	0.871752	0.018707	0.150566
82	YBR137W	ORF	1.309937	0.03144	1.126872	0.019128	0.150533
83	YBR131W	CCZ1	1.112113	0.031604	0.956776	0.026806	0.150448
84	YGR077C	PEX8	0.897553	0.011135	0.772944	0.021788	0.149466
85	YGL127C	SOH1	0.779038	0.008571	0.670891	0.049044	0.149454

86	YNL096C	RPS7B	0.967835	0.016666	0.833603	0.014508	0.149304
87	YLR427W	MAG2	1.080006	0.017487	0.930376	0.014383	0.149134
88	YFR021W	ATG18	1.111655	0.011307	0.957806	0.013059	0.14896
89	YHR116W	COX23	0.972967	0.008976	0.838622	0.034123	0.14859
90	YER119C	AVT6	0.982739	0.016107	0.847101	0.409554	0.148523
91	YMR158C-B	ORF	1.094701	0.021944	0.943764	0.013437	0.14836
92	YAL007C	ERP2	1.283059	0.007895	1.106929	0.016712	0.147658
93	YER028C	MIG3	0.971868	0.040544	0.838667	0.014899	0.147406
94	YKL205W	LOS1	1.154438	0.047809	0.996626	0.021798	0.146994
95	YKR099W	BAS1	0.990434	0.021258	0.855084	0.179824	0.146943
96	YBR223C	TDP1	0.924396	0.032862	0.798271	0.013833	0.146692
97	YNL034W	ORF	1.137479	0.024054	0.982434	0.008755	0.146536
98	YHR008C	SOD2	0.994988	0.013678	0.860008	0.024687	0.145789
99	YML001W	YPT7	0.810216	0.008673	0.700647	0.020288	0.145297
100	YLR428C	ORF	1.140477	0.027279	0.987073	0.030409	0.144458
101	YNL166C	BNI5	1.158767	0.025762	1.003227	0.025503	0.144134
102	YBR150C	TBS1	1.206187	0.015145	1.045531	0.016895	0.142939
103	YBR138C	ORF	1.237903	0.035741	1.073202	0.016332	0.142773
104	YPL090C	RPS6A	0.909631	0.029759	0.788622	0.111829	0.142752
105	YML081C-A	ATP18	1.115105	0.052309	0.966889	0.052779	0.14262
106	YBR128C	ATG14	1.179631	0.016099	1.023081	0.015119	0.142383
107	YNL299W	TRF5	1.075277	0.060993	0.932827	0.028552	0.142114
108	YML102W	CAC2	0.978095	0.019215	0.848627	0.017529	0.141987
109	YNL318C	HXT14	1.185045	0.032605	1.028664	0.041044	0.141519
110	YAL029C	MYO4	1.234678	0.013949	1.071844	0.010829	0.141429
111	YMR299C	DYN3	1.102996	0.01734	0.958686	0.018196	0.140222
112	YMR169c	ALD3	1.097027	0.019691	0.953704	0.018391	0.140006
113	YNL227C	JJJ1	0.849311	0.01767	0.738409	0.038375	0.139928
114	YBL032W	HEK2	1.238333	0.02207	1.077065	0.018636	0.139527
115	YMR058W	FET3	1.113624	0.009421	0.969526	0.005006	0.138568
116	YHR180W	ORF	0.879003	0.140621	0.765464	0.091783	0.138306
117	YNL144C	ORF	1.172516	0.025978	1.02117	0.00824	0.138202
118	YJL123C	MTC1	1.147916	0.045519	1.000018	0.053582	0.13793
119	YKL056C	TMA19	0.919851	0.020545	0.80172	0.095266	0.137453
120	YPL183C	RTT10	0.78121	0.045751	0.681116	0.069112	0.137111
121	YMR086C-A	ORF	1.220822	0.049871	1.064562	0.057664	0.136961
122	YMR157C	AIM36	1.099035	0.014689	0.958471	0.007586	0.136849
123	YAL030W	SNC1	1.215111	0.024964	1.060567	0.017976	0.136031
124	YCL049C	ORF	1.177282	0.009962	1.027709	0.024149	0.135877
125	YKL187C	ORF	0.94765	0.062166	0.827672	0.078994	0.135368
126	YBR149W	ARA1	1.302304	0.017438	1.137523	0.016192	0.135282
127	YMR253C	ORF	1.163313	0.009804	1.016209	0.013275	0.135192
128	YNL286W	CUS2	1.112532	0.060421	0.97188	0.018153	0.135161
129	YLR232W	ORF	1.14351	0.031783	0.998994	0.012171	0.135109
130	YLR096W	KIN2	1.169112	0.028205	1.021474	0.025369	0.134998
131	YLR097C	HRT3	1.106301	0.016149	0.967338	0.007843	0.134229

132	YOL028C	YAP7	1.011109	0.030701	0.884256	0.03231	0.134056
133	YBR212W	NGR1	1.032016	0.051992	0.903001	0.008688	0.133545
134	YAL031C	GIP4	1.16931	0.040034	1.023812	0.033583	0.132881
135	YGR196C	FYV8	1.174763	0.015775	1.02917	0.015478	0.132314
136	YER011W	TIR1	0.845889	0.014165	0.741569	0.042555	0.131619
137	YDR090C	ORF	1.167286	0.023514	1.023419	0.011583	0.131532
138	YBR145W	ADH5	1.226077	0.012704	1.075186	0.029529	0.131326
139	YCR089W	FIG2	1.215836	0.010864	1.06688	0.02284	0.130694
140	YBR134W	ORF	1.283059	0.0695	1.125933	0.029438	0.130635
141	YGR178C	PBP1	1.213897	0.023584	1.06559	0.030562	0.130307
142	YAL005C	SSA1	1.204897	0.0383	1.057748	0.025741	0.130252
143	YHL020C	OPI1	1.075316	0.015865	0.945561	0.020229	0.128592
144	YNL316C	PHA2	1.149675	0.038139	1.011249	0.014008	0.128293
145	YJR011C	ORF	1.106082	0.018564	0.972936	0.020957	0.128261
146	YAL028W	FRT2	1.241774	0.014615	1.092623	0.00967	0.127959
147	YLR233C	**EST1**	1.101527	0.009222	0.969503	0.023743	0.127669
148	YNL165W	ORF	0.781899	0.043359	0.688274	0.096568	0.127538
149	YPR151C	SUE1	0.93258	0.036415	0.821496	0.03794	0.126829
150	YDR502C	SAM2	0.982438	0.017841	0.865749	0.018521	0.126443
151	YNL300W	TOS6	1.15411	0.021004	1.017054	0.010068	0.126419
152	YNL051W	COG5	1.110314	0.044123	0.978529	0.022041	0.126348
153	YBR169C	SSE2	1.113726	0.010802	0.981628	0.007839	0.126254
154	YAR047C	ORF	0.975572	0.040575	0.86019	0.038764	0.12587
155	YMR302C	YME2	1.150229	0.035924	1.014204	0.031008	0.125857
156	YBL029W	ORF	1.350254	0.024429	1.192029	0.018365	0.124636
157	YAL017W	PSK1	1.257471	0.005519	1.110374	0.042306	0.124405
158	YMR283C	RIT1	1.142246	0.034594	1.009349	0.017873	0.123691
159	YML076C	WAR1	1.091318	0.016546	0.964353	0.01077	0.123684
160	YNL032W	SIW14	1.138587	0.047419	1.006394	0.022872	0.123415
161	YAL004W	ORF	1.173503	0.014069	1.037282	0.019784	0.123389
162	YPL226W	NEW1	0.709595	0.037298	0.627416	0.083706	0.123085
163	YML060W	OGG1	1.081804	0.019004	0.956747	0.006366	0.122846
164	YMR313C	TGL3	1.089026	0.021939	0.963436	0.014117	0.122533
165	YER061C	CEM1	0.882362	0.027045	0.780788	0.040298	0.122299
166	YJL154C	VPS35	0.921823	0.024903	0.816001	0.021359	0.121937
167	YLR216C	CPR6	1.110531	0.029599	0.983217	0.01467	0.121764
168	YKL218C	SRY1	1.13935	0.021885	1.008925	0.015273	0.121573
169	YIL074C	SER33	1.147075	0.010694	1.015883	0.01456	0.121457
170	YMR041C	ARA2	1.127473	0.005812	0.998534	0.024284	0.121446
171	YPR201W	ARR3	1.05751	0.01864	0.936616	0.03582	0.121399
172	YKL168C	KKQ8	1.001491	0.025181	0.887291	0.008285	0.121073
173	YDR493W	MZM1	0.967949	0.0268	0.857608	0.011163	0.121032
174	YHR082C	KSP1	1.154336	0.019304	1.023047	0.024662	0.12074
175	YDR215C	ORF	1.161925	0.016218	1.030082	0.013934	0.120439
176	YLR342W	FKS1	1.005195	0.019987	0.891444	0.014666	0.120095
177	YIL073C	SPO22	1.133516	0.00616	1.005475	0.006472	0.119865

178	YBL064C	PRX1	1.120822	0.013003	0.994367	0.009006	0.119711
179	YPL155C	KIP2	0.973101	0.033897	0.863405	0.013271	0.119605
180	YPR073C	LTP1	0.98221	0.031036	0.871593	0.015065	0.119482
181	YOR221C	MCT1	0.892177	0.020845	0.791769	0.036605	0.119395
182	YBL049W	MOH1	1.238226	0.035188	1.099411	0.007583	0.118905
183	YER024W	YAT2	0.955918	0.023671	0.848788	0.018582	0.118862
184	YBR235W	VHC1	1.258627	0.019071	1.11765	0.058949	0.118794
185	YBL028C	ORF	1.33703	0.04841	1.187434	0.043539	0.118656
186	YBL063W	KIP1	1.167482	0.013492	1.036864	0.007667	0.118648
187	YHR181W	SVP26	1.192933	0.04268	1.05989	0.019022	0.11825
188	YCL036W	GFD2	1.27907	0.052311	1.136472	0.044654	0.118204
189	YIR019C	FLO11	1.124792	0.014831	0.999513	0.01064	0.118085
190	YDR315C	IPK1	1.082649	0.012295	0.962121	0.009293	0.118026
191	YHR200W	RPN10	1.116815	0.026154	0.992961	0.028401	0.117546
192	YML075C	HMG1	1.108339	0.008964	0.98545	0.015973	0.117519
193	YDR515W	SLF1	0.96909	0.054764	0.861678	0.02641	0.117475
194	YJL110C	GZF3	1.111233	0.05425	0.9887	0.069327	0.116834
195	YBR148W	YSW1	1.293165	0.02587	1.150679	0.043922	0.11674
196	YMR244C-A	COA6	0.958643	0.034804	0.853495	0.038482	0.116179
197	YBR119W	MUD1	0.908161	0.013377	0.808817	0.017337	0.115849
198	YBR250W	SPO23	1.173151	0.022381	1.045005	0.032542	0.115672
199	YLR112W	ORF	1.135265	0.010111	1.011265	0.008509	0.115664
200	YBR130C	SHE3	1.337783	0.030098	1.191715	0.031837	0.11562
201	YDL110C	TMA17	1.151756	0.024413	1.026081	0.014634	0.115541
202	YDR102C	ORF	1.143678	0.023859	1.019217	0.015938	0.115215
203	YHR203C	RPS4B	0.765687	0.023984	0.682489	0.089363	0.115028
204	YLR011W	LOT6	1.10847	0.032504	0.98827	0.060704	0.11478
205	YIR018W	YAP5	1.158532	0.021163	1.032961	0.022647	0.114725
206	YLL054C	ORF	1.141774	0.015224	1.018071	0.012453	0.114674
207	YLL055W	YCT1	1.113243	0.013447	0.992807	0.019449	0.114496
208	YPR192W	AQY1	1.095388	0.022011	0.977007	0.013035	0.11437

Appendix 4: *TLC1* positive genetic interactions (second screen)

	Systematic Gene Name	Standard Gene name	Double mutant average growth	Double mutant growth StdDev	Single Mutant average growth	Single mutant StdDev	SGA score (log10)
1	YOL081W	IRA2	0.924148	0.009934	0.643794	0.043276	0.361493
2	YML102C-A	ORF	0.900778	0.056102	0.634683	0.407586	0.350134
3	YOL031C	SIL1	0.898131	0.018207	0.644986	0.094137	0.331087
4	YOL006C	TOP1	0.812942	0.008558	0.593288	0.020076	0.314981
5	YOL129W	VPS68	0.844352	0.029417	0.633389	0.10383	0.287485
6	YPL090C	RPS6A	0.784141	0.017525	0.600971	0.023328	0.266042
7	YER010C	ORF	1.136518	0.046472	0.880746	0.027369	0.254954
8	YER007W	PAC2	1.10889	0.027189	0.869253	0.013555	0.24348
9	YOL132W	GAS4	0.903842	0.019993	0.720746	0.079309	0.226368
10	YER004W	FMP52	1.018884	0.010434	0.827955	0.01158	0.207504

11	YLR384C	IKI3	0.752181	0.032595	0.612858	0.025492	0.204844
12	YOL032W	OPI10	0.91923	0.018676	0.757488	0.030695	0.193529
13	YER007C-A	TMA20	0.976255	0.026612	0.805199	0.017635	0.192634
14	YER005W	YND1	1.025791	0.014581	0.849715	0.028778	0.188318
15	YNR051C	BRE5	0.759005	0.018454	0.628945	0.059234	0.187964
16	YER001W	MNN1	0.917546	0.031452	0.763288	0.019885	0.184067
17	YOR184W	SER1	0.789702	0.029001	0.665145	0.028563	0.17165
18	YJR139C	HOM6	0.845696	0.024234	0.712823	0.0344	0.170927
19	YCL025C	AGP1	0.791546	0.024884	0.66887	0.055909	0.168399
20	YLR287C-A	RPS30A	0.79248	0.047006	0.670425	0.068606	0.167256
21	YOR183W	FYV12	0.790257	0.016139	0.668939	0.084686	0.166665
22	YPL161C	BEM4	0.738606	0.051046	0.62727	0.033356	0.163388
23	YKL197C	PEX1	0.838117	0.04798	0.711888	0.007372	0.163236
24	YLR188W	MDL1	0.757442	0.075618	0.64377	0.092087	0.162606
25	YOR196C	LIP5	0.716014	0.020835	0.609653	0.093723	0.160809
26	YBR201W	DER1	0.875789	0.066676	0.746926	0.298573	0.15916
27	YJL136C	RPS21B	0.781445	0.02982	0.667894	0.029802	0.157015
28	YNL315C	ATP11	0.908925	0.049589	0.778195	0.098015	0.155286
29	YKL110C	KTI12	0.745692	0.034278	0.64127	0.032222	0.150862
30	YLR191W	PEX13	0.73898	0.00691	0.636878	0.040128	0.148693
31	YDL136W	RPL35B	0.724206	0.0259	0.624929	0.069749	0.147438
32	YOL131W	ORF	0.865531	0.031629	0.747191	0.077634	0.147022
33	YKL184W	SPE1	0.721873	0.02132	0.624862	0.028303	0.144318
34	YLR089C	ALT1	0.82196	0.037595	0.711572	0.055585	0.144215
35	YPL102C	ORF	0.756656	0.012557	0.655476	0.028847	0.143546
36	YJR059W	PTK2	0.800572	0.016447	0.695455	0.044145	0.14076
37	YAR047C	ORF	1.026609	0.058095	0.892237	0.042718	0.140285
38	YOL036W	ORF	0.956192	0.02743	0.831405	0.050591	0.139843
39	YBR161W	CSH1	0.67939	0.026474	0.591377	0.028493	0.138741
40	YDL192W	ARF1	0.803608	0.012462	0.701199	0.038807	0.136321
41	YIL159W	BNR1	1.01225	0.034871	0.883448	0.262696	0.136099
42	YIL125W	KGD1	1.070782	0.038371	0.934943	0.302998	0.135659
43	YOL136C	PFK27	0.933824	0.020917	0.816665	0.031544	0.13406
44	YOL035C	ORF	0.834834	0.072735	0.730717	0.08945	0.133207
45	YFR032C-A	RPL29	0.947263	0.042172	0.829391	0.035976	0.132886
46	YER031C	YPT31	1.035827	0.015906	0.907257	0.010478	0.13253
47	YOL116W	MSN1	0.85165	0.026965	0.746107	0.01262	0.132306
48	YOR069W	VPS5	0.688252	0.056814	0.603692	0.05755	0.131091
49	YER066W	RRT13	1.344158	0.010877	1.18148	0.017227	0.129
50	YOL041C	NOP12	0.875525	0.095394	0.769952	0.230876	0.128496
51	YBL107C	MIC23	0.926421	0.027859	0.816186	0.069115	0.126686
52	YAL022C	FUN26	1.224299	0.019662	1.080796	0.025435	0.12467
53	YJR074W	MOG1	0.668162	0.013223	0.590038	0.028819	0.124344
54	YKR007W	MEH1	0.85859	0.031366	0.758309	0.038596	0.1242
55	YOL007C	CSI2	0.971263	0.021181	0.859042	0.035838	0.122779
56	YLR346C	ORF	0.960823	0.10803	0.852245	0.163592	0.119916

57	YBR223C	TDP1	0.936633	0.024851	0.831751	0.025569	0.118758
58	YBR156C	SLI15	1.297505	0.017521	1.152459	0.021929	0.118545
59	YGR092W	DBF2	0.849252	0.057055	0.754708	0.037307	0.118026
60	YOL019W	ORF	0.990379	0.021107	0.88061	0.03456	0.117472
61	YER065C	ICL1	1.346316	0.020212	1.19711	0.015083	0.117462
61	YLR318W	**EST2**	0.630292	0.052221	0.561677	0.050712	0.115256

Appendix 5: *EST1* negative genetic interactions

	Systematic Gene Name	Standard Gene name	Double mutant average growth	Double mutant growth StdDev	Single Mutant average growth	Single mutant StdDev	SGA score (log10)
1	*YMR106C*	*YKU80*	0,306301	0,010055	0,951543	0,029866	-1,13351
2	*YDL080C*	*THI3*	0,55734	0,069125	1,102456	0,019318	-0,68212
3	*YMR284W*	*YKU70*	0,676315	0,020237	1,181111	0,016802	-0,55755
4	*YDR530C*	*APA2*	0,477037	0,020583	0,805735	0,011459	-0,52416
5	*YER151C*	*UBP3*	0,522563	0,037026	0,793706	0,048767	-0,41797
6	*YER095W*	*RAD51*	0,583738	0,112049	0,850405	0,042528	-0,37626
7	*YFL013W-A*	*ORF*	0,547077	0,018813	0,77164	0,004822	-0,34393
8	*YER131W*	*RPS26B*	0,533178	0,019554	0,735322	0,020464	-0,32145
9	*YFR010W*	*UBP6*	0,537337	0,084943	0,73218	0,026263	-0,3094
10	*YGL105W*	*ARC1*	0,805239	0,491644	1,074778	0,058117	-0,28873
11	*YEL066W*	*HPA3*	0,561741	0,051493	0,736778	0,020905	-0,27124
12	*YPL055C*	*LGE1*	0,545493	0,057311	0,708677	0,044015	-0,26171
13	*YOR297C*	*TIM18*	0,828564	0,169121	1,047658	0,039234	-0,23462
14	*YML032C*	*RAD52*	0,55785	0,059042	0,70485	0,023483	-0,23389
15	*YEL071W*	*DLD3*	0,658703	0,042525	0,825887	0,027964	-0,22619
16	*YGL115W*	*SNF4*	0,67122	0,023955	0,836271	0,072155	-0,21986
17	*YER033C*	*ZRG8*	0,634955	0,059034	0,783209	0,035638	-0,20985
18	*YGR118W*	*RPS23A*	0,54332	0,017149	0,670054	0,09198	-0,20966
19	*YFL003C*	*MSH4*	0,709919	0,054	0,871127	0,017892	-0,20464
20	*YER061C*	*CEM1*	0,677635	0,044789	0,824431	0,020089	-0,19608
21	*YNL165W*	*ORF*	0,896334	0,046338	1,083476	0,08182	-0,18962
22	*YDR535C*	*ORF*	0,777333	0,034916	0,936679	0,024234	-0,18647
23	*YDR463W*	*STP1*	0,686062	0,076998	0,817688	0,011316	-0,17551
24	*YDR455C*	*ORF*	0,613396	0,017068	0,727123	0,014729	-0,17009
25	*YDR536W*	*STL1*	0,796812	0,039695	0,940204	0,014343	-0,16548
26	*YER074W*	*RPS24A*	0,643929	0,06524	0,75961	0,022503	-0,16522
27	*YMR244W*	*ORF*	0,974177	0,018631	1,148139	0,007293	-0,1643
28	*YFL052W*	*ORF*	0,733011	0,070904	0,86366	0,032551	-0,16402
29	*YEL059W*	*HHY1*	0,603765	0,054185	0,709348	0,057602	-0,16116
30	*YGL153W*	*PEX14*	0,568818	0,038551	0,667062	0,042318	-0,15932
31	*YER128W*	*VFA1*	0,66111	0,047465	0,773478	0,018432	-0,15698
32	*YDR533C*	*HSP31*	0,697662	0,041309	0,812785	0,010725	-0,15273
33	*YPL250C*	*ICY2*	0,676336	0,096399	0,786572	0,059177	-0,15099
34	*YMR279C*	*ORF*	1,2161	0,032511	1,413406	0,074069	-0,15035

Appendix 6: EST1 positive genetic interactions

	Systematic Gene Name	Standard Gene name	Double mutant average growth	Double mutant growth StdDev	Single Mutant average growth	Single mutant StdDev	SGA score (log10)
1	YLR384C	IKI3	0.823388	0.015723	0.612858	0.025492	0.295294
2	YER010C	ORF	1.159706	0.038767	0.880746	0.027369	0.275152
3	YLR188W	MDL1	0.839915	0.01623	0.64377	0.092087	0.26596
4	YER007W	PAC2	1.118996	0.016062	0.869253	0.013555	0.252552
5	YER007C-A	TMA20	1.028929	0.033999	0.805199	0.017635	0.245184
6	YOL138C	RTC1	0.830466	0.060706	0.657884	0.070082	0.232959
7	YOL031C	SIL1	0.803876	0.038021	0.644986	0.094137	0.220216
8	YNL224C	SQS1	0.830168	0.024833	0.667329	0.055249	0.218345
9	YNL199C	GCR2	0.772778	0.005062	0.622086	0.030174	0.216913
10	YLR056W	ERG3	0.783407	0.085419	0.63556	0.217719	0.209145
11	YNL223W	ATG4	0.791323	0.015765	0.642147	0.073568	0.20889
12	YER004W	FMP52	1.018751	0.020867	0.827955	0.01158	0.207374
13	YDR393W	SHE9	0.744795	0.013183	0.608307	0.065078	0.202429
14	YLR089C	ALT1	0.867697	0.03596	0.711572	0.055585	0.198366
15	YNL274C	GOR1	0.841234	0.083799	0.691231	0.058325	0.196396
16	YCL025C	AGP1	0.813481	0.023247	0.66887	0.055909	0.195734
17	YER005W	YND1	1.019189	0.024012	0.849715	0.028778	0.181861
18	YLR191W	PEX13	0.763416	0.01163	0.636878	0.040128	0.181226
19	YNL294C	RIM21	0.728591	0.015906	0.607895	0.031754	0.181111
20	YOL129W	VPS68	0.758251	0.0343	0.633389	0.10383	0.17993
21	YJR059W	PTK2	0.830677	0.039327	0.695455	0.044145	0.177675
22	YMR165C	PAH1	0.73255	0.080826	0.614681	0.08379	0.175428
23	YER002W	NOP16	0.842776	0.045108	0.707355	0.030905	0.175168
24	YER001W	MNN1	0.905155	0.037506	0.763288	0.019885	0.170471
25	YLR346C	ORF	1.008182	0.055328	0.852245	0.163592	0.16803
26	YJR139C	HOM6	0.842955	0.006631	0.712823	0.0344	0.16768
27	YGL219C	MDM34	0.829412	0.11023	0.701662	0.034504	0.167265
28	YLR077W	FMP25	0.912007	0.025959	0.772483	0.064737	0.166038
29	YLR073C	RFU1	0.909882	0.019516	0.771571	0.059068	0.164886
30	YNR051C	BRE5	0.74167	0.018815	0.628945	0.059234	0.164859
31	YOR183W	FYV12	0.78857	0.023666	0.668939	0.084686	0.164528
32	YNL242W	ATG2	0.757744	0.033148	0.643214	0.046282	0.163868
33	YLR406C	RPL31B	0.89729	0.025622	0.762348	0.034441	0.162975
34	YBL015W	ACH1	0.931553	0.033623	0.793517	0.014285	0.160378
35	YKL157W	APE2	0.729928	0.013892	0.621954	0.087064	0.160079
36	YKR001C	VPS1	0.74265	0.074918	0.633482	0.083663	0.158993
37	YNR005C	ORF	0.864053	0.023884	0.737114	0.03891	0.158892
38	YNL237W	YTP1	0.853139	0.017983	0.731352	0.082097	0.154029
39	YML102C-A	ORF	0.73882	0.093522	0.634683	0.407586	0.151929
40	YLR287C-A	RPS30A	0.779787	0.030267	0.670425	0.068606	0.151109

Appendix 7: *SUT457* negative genetic interactions (first SGA screen)

	Systematic Gene Name	Standard Gene name	Double Mutant average growth	Double Mutant growth StdDev	Single Mutant average growth	Single mutant growth StdDev	SGA score (log10)
1	*YBL031W*	*SHE1*	0.182855	0.2628	0.893442	0.35811	-1.58639
2	*YFL010C*	*WWM1*	0.295525	0.453512	1.125582	0.079596	-1.3373
3	*YDR004W*	*RAD57*	0.182318	0.166327	0.67957	0.138532	-1.31571
4	*YNL136W*	*EAF7*	0.270512	0.471279	0.855921	0.077821	-1.15186
5	*YMR256C*	*COX7*	0.320133	0.19261	0.82195	0.065036	-0.94294
6	*YBR023C*	*CHS3*	0.476659	0.45418	1.105004	0.087505	-0.8408
7	*YNL292W*	*PUS4*	0.361776	0.389662	0.789503	0.210526	-0.78038
8	*YCL014W*	*BUD3*	0.426642	0.146702	0.927643	0.018135	-0.7767
9	*YPL261C*	*ORF*	0.447519	0.105867	0.926434	0.021053	-0.72762
10	*YJL123C*	*MTC1*	0.536211	0.544128	1.090585	0.060311	-0.70994
11	*YNL277W*	*MET2*	0.360792	0.410327	0.727223	0.085471	-0.70093
12	*YIL159W*	*BNR1*	0.474891	0.355872	0.951412	0.044146	-0.69486
13	*YLR056W*	*ERG3*	0.397232	0.212558	0.778652	0.038339	-0.67304
14	*YNL275W*	*BOR1*	0.438065	0.465508	0.851892	0.048788	-0.66509
15	*YBR032W*	*ORF*	0.509855	0.595659	0.983527	0.046589	-0.65702
16	*YBR294W*	*SUL1*	0.473181	0.501981	0.899512	0.043914	-0.64238
17	*YCL024W*	*KCC4*	0.482954	0.110662	0.895243	0.012125	-0.61718
18	*YNL012W*	*SPO1*	0.498944	0.518657	0.908293	0.151457	-0.59907
19	*YLR218C*	*COA4*	0.435483	0.086852	0.768641	0.018517	-0.56817
20	*YGL036W*	*ORF*	0.588423	0.197813	0.985484	0.054804	-0.51569
21	*YOR297C*	*TIM18*	0.591277	0.426	0.987472	0.033828	-0.51286
22	*YER119C-A*	*ORF*	0.577965	0.135326	0.965	0.038655	-0.51261
23	*YMR224C*	*MRE11*	0.405373	0.103438	0.66559	0.055848	-0.49587
24	*YML066C*	*SMA2*	0.555116	0.60017	0.900421	0.058216	-0.48368
25	*YIL067C*	*ORF*	0.650058	0.54719	1.053107	0.03696	-0.48244
26	*YMR120C*	*ADE17*	0.438891	0.311119	0.705797	0.067617	-0.47508
27	*YCL016C*	*DCC1*	0.501104	0.257785	0.79115	0.016938	-0.45668
28	*YKL204W*	*EAP1*	0.618541	0.652486	0.948479	0.036614	-0.4275
29	*YOR083W*	*WHI5*	0.640745	0.28954	0.980792	0.049171	-0.42573
30	*YDR274C*	*ORF*	0.48279	0.092522	0.728815	0.035907	-0.41184
31	*YCL009C*	*ILV6*	0.558811	0.141293	0.840077	0.025799	-0.40768
32	*YCL012W*	*BUD3*	0.584873	0.125341	0.874447	0.03237	-0.4022
33	*YNR010W*	*CSE2*	0.569988	0.141633	0.830007	0.116173	-0.37582
34	*YGL147C*	*RPL9A*	0.687402	0.443036	0.995446	0.034319	-0.37027
35	*YLR239C*	*LIP2*	0.477675	0.050756	0.6891	0.046366	-0.36646
36	*YPL033C*	*SRL4*	0.640381	0.076106	0.920575	0.027986	-0.36294
37	*YPL041C*	*ORF*	0.677799	0.062549	0.965903	0.022347	-0.35421
38	*YNL299W*	*TRF5*	0.717977	0.762171	1.022184	0.035545	-0.35326
39	*YPL147W*	*PXA1*	0.737804	0.237157	1.048129	0.028034	-0.35108
40	*YOL152W*	*FRE7*	0.711038	0.289917	1.009812	0.032705	-0.35079
41	*YLR261C*	*VPS63*	0.51952	0.06198	0.734366	0.024038	-0.3461
42	*YDR463W*	*STP1*	0.511821	0.174089	0.723306	0.038861	-0.34586

43	*YMR216C*	*SKY1*	0.660459	0.174045	0.930413	0.018433	-0.34269
44	*YOR082C*	*ORF*	0.633737	0.099048	0.890992	0.047904	-0.3407
45	*YMR031W-A*	*ORF*	0.449883	0.495226	0.630708	0.35003	-0.33786
46	*YOR275C*	*RIM20*	0.466099	0.366958	0.647731	0.037301	-0.32908
47	*YCL025C*	*AGP1*	0.456543	0.172244	0.633314	0.058791	-0.32728
48	*YCL022C*	*ORF*	0.669922	0.137602	0.927752	0.03702	-0.3256
49	*YDR123C*	*INO2*	0.478512	0.043413	0.661754	0.03704	-0.32421
50	*YCL011C*	*GBP2*	0.679114	0.111464	0.932568	0.019155	-0.31715
51	*YLR084C*	*RAX2*	0.699648	0.143443	0.950247	0.043525	-0.30615
52	*YCL027W*	*FUS1*	0.806862	0.317692	1.086901	0.014319	-0.29793
53	*YNL021W*	*HDA1*	0.456099	0.157998	0.610175	0.082608	-0.29103
54	*YDR440W*	*DOT1*	0.766135	0.168751	1.01935	0.046014	-0.28556
55	*YOR101W*	*RAS1*	0.68257	0.758731	0.907638	0.141237	-0.28498
56	*YBR201W*	*DER1*	0.701974	0.496422	0.931174	0.01849	-0.28255
57	*YNL237W*	*YTP1*	0.736448	0.369752	0.976889	0.015691	-0.28253
58	*YCL044C*	*MGR1*	0.752179	0.148563	0.993973	0.008933	-0.27874
59	*YPL174C*	*NIP100*	0.507563	0.090599	0.670614	0.013097	-0.27857
60	*YER061C*	*CEM1*	0.596782	0.115949	0.785865	0.010306	-0.27523
61	*YCL026C*	*HBN1*	0.863522	0.174347	1.132107	0.04065	-0.27082
62	*YOR221C*	*MCT1*	0.630268	0.109414	0.825211	0.03429	-0.26949
63	*YER153C*	*PET122*	0.765108	0.199881	0.998276	0.018239	-0.26601
64	*YPR122W*	*AXL1*	0.795996	0.284457	1.035282	0.034223	-0.26284
65	*YDR072C*	*IPT1*	0.728925	0.212654	0.946817	0.058578	-0.26154
66	*YPL172C*	*COX10*	0.625773	0.148441	0.81043	0.082945	-0.25858
67	*YDR375C*	*BCS1*	0.580134	0.531324	0.751279	0.052622	-0.25852
68	*YNL224C*	*SQS1*	0.696117	0.273066	0.901216	0.019355	-0.25823
69	*YML028W*	*TSA1*	0.651753	0.158233	0.84337	0.03421	-0.25774
70	*YNL135C*	*FPR1*	0.680925	0.362344	0.880528	0.05579	-0.25707
71	*YMR020W*	*FMS1*	0.668947	0.203923	0.864561	0.013203	-0.25652
72	*YNR018W*	*RCF2*	0.636878	0.172583	0.822168	0.051056	-0.25537
73	*YML032C*	*RAD52*	0.604305	0.038776	0.775127	0.031412	-0.24895
74	*YJL145W*	*SFH5*	0.712393	0.319125	0.910537	0.044603	-0.24541
75	*YNR001C*	*CIT1*	0.772626	0.253903	0.98462	0.048859	-0.24246
76	*YJL160C*	*PIR5*	0.867947	0.282394	1.105159	0.071462	-0.24161
77	*YML036W*	*CGI121*	0.71596	0.055941	0.91107	0.011506	-0.241
78	*YOR061W*	*CKA2*	0.801588	0.266418	1.019669	0.022633	-0.24064
79	*YOL029C*	*ORF*	0.837939	0.541372	1.064678	0.062556	-0.23948
80	*YGL127C*	*SOH1*	0.623466	0.081103	0.791947	0.025427	-0.2392
81	*YNL257C*	*SIP3*	0.599279	0.429608	0.761085	0.127232	-0.23902
82	*YDR372C*	*VPS74*	0.843957	0.194167	1.071532	0.031781	-0.23874
83	*YOR277C*	*ORF*	0.734882	0.17617	0.929115	0.021108	-0.23452
84	*YCL029C*	*BIK1*	0.843045	0.106351	1.064244	0.005791	-0.233
85	*YNL254C*	*RTC4*	0.732623	0.106897	0.922121	0.06327	-0.23005
86	*YML048W-A*	*ORF*	0.797252	0.204715	1.002243	0.007859	-0.22882
87	*YBR223C*	*TDP1*	0.678483	0.346141	0.852806	0.04455	-0.22867
88	*YPL262W*	*FUM1*	0.629706	0.098967	0.789966	0.022547	-0.22674

89	*YMR225C*	*MRPL44*	0.710954	0.164931	0.889228	0.038495	-0.22375
90	*YFL036W*	*RPO41*	0.629512	0.157383	0.786752	0.06304	-0.22297
91	*YOL090W*	*MSH2*	0.730528	0.231459	0.90939	0.056003	-0.21901
92	*YOR191W*	*ULS1*	0.825785	0.078724	1.027115	0.047508	-0.21817
93	*YOR065W*	*CYT1*	0.7106	0.14149	0.882121	0.014451	-0.21622
94	*YOR043W*	*WHI2*	0.702936	0.107266	0.870184	0.056333	-0.21344
95	*YHR108W*	*GGA2*	0.705728	0.086831	0.873457	0.019326	-0.21323
96	*YLL049W*	*LDB18*	0.650385	0.168395	0.804005	0.030957	-0.21204
97	*YDR514C*	*ORF*	0.714702	0.446209	0.882697	0.076637	-0.21112
98	*YBL011W*	*SCT1*	0.692049	0.054703	0.852914	0.042985	-0.209
99	*YPR064W*	*ORF*	0.707705	0.440041	0.871398	0.011212	-0.20807
100	*YOL132W*	*GAS4*	0.696366	0.031446	0.857152	0.020426	-0.20774
101	*YOL137W*	*BSC6*	0.784178	0.186076	0.965022	0.02849	-0.20751
102	*YLR346C*	*ORF*	0.781945	0.510399	0.960258	0.038852	-0.20542
103	*YML035C-A*	*ORF*	0.71596	0.070557	0.878361	0.030921	-0.20443
104	*YCL028W*	*RNQ1*	0.914017	0.118653	1.120724	0.024506	-0.20388
105	*YPL248C*	*GAL4*	0.779042	0.071861	0.953859	0.031618	-0.20245
106	*YCL001W*	*RER1*	0.749038	0.1277	0.916916	0.021129	-0.20223
107	*YPR196W*	*ORF*	0.678084	0.079131	0.829816	0.023039	-0.20193
108	*YMR304W*	*UBP15*	0.657863	0.13976	0.801916	0.013331	-0.19801
109	*YNL020C*	*ARK1*	0.805524	0.223673	0.981789	0.012675	-0.19788
110	*YNL032W*	*SIW14*	0.876786	0.362361	1.06737	0.061343	-0.19669
111	*YOR325W*	*ORF*	0.734695	0.048294	0.894126	0.024142	-0.19639
112	*YBL072C*	*RPS8A*	0.677381	0.182474	0.823673	0.076842	-0.19554
113	*YMR181C*	*ORF*	0.764169	0.091809	0.927914	0.018313	-0.19415
114	*YOL106W*	*ORF*	0.8248	0.251988	1.000394	0.028004	-0.19301
115	*YGR223C*	*HSV2*	0.884419	0.0994	1.070652	0.013384	-0.19109
116	*YPL109C*	*ORF*	0.750052	0.164493	0.907874	0.012668	-0.19096
117	*YLR262C*	*YPT6*	0.626391	0.062484	0.757325	0.02288	-0.18982
118	*YEL066W*	*HPA3*	0.748116	0.218332	0.903107	0.041612	-0.18828
119	*YDR063W*	*AIM7*	0.737364	0.100078	0.889827	0.01375	-0.18794
120	*YFL003C*	*MSH4*	0.867018	0.198989	1.046086	0.054924	-0.18775
121	*YOL086C*	*ADH1*	0.64892	0.238715	0.782934	0.034972	-0.18774
122	*YBR215W*	*HPC2*	0.750611	0.21288	0.902042	0.048243	-0.18377
123	*YLR394W*	*CST9*	0.893569	0.233205	1.071789	0.025415	-0.18186
124	*YNL219C*	*ALG9*	0.707594	0.220958	0.848517	0.026954	-0.18162
125	*YDR461W*	*MFA1*	0.79714	0.545336	0.955481	0.081495	-0.18118
126	*YGR080W*	*TWF1*	0.838134	0.193011	1.00373	0.013454	-0.1803
127	*YDR392W*	*SPT3*	0.718288	0.17748	0.85862	0.029688	-0.17846
128	*YCL035C*	*GRX1*	0.916344	0.20181	1.094892	0.015755	-0.17802
129	*YNL236W*	*SIN4*	0.507907	0.083829	0.606473	0.059311	-0.17736
130	*YDR207C*	*UME6*	0.597938	0.053164	0.713765	0.00998	-0.17707
131	*YOR132W*	*VPS17*	0.568371	0.230647	0.678428	0.025864	-0.17701
132	*YJR034W*	*PET191*	0.765574	0.227554	0.913185	0.017113	-0.17631
133	*YDR251W*	*PAM1*	0.874363	0.121486	1.04265	0.026038	-0.17603
134	*YNL320W*	*ORF*	0.754373	0.085747	0.899474	0.031223	-0.17592

135	*YOR035C*	*SHE4*	0.761404	0.129532	0.907638	0.009644	-0.17568
136	*YOR350C*	*MNE1*	0.791403	0.155914	0.942582	0.030865	-0.17482
137	*YOR188W*	*MSB1*	0.811551	0.20896	0.965679	0.025295	-0.17388
138	*YPL110C*	*GDE1*	0.79174	0.212791	0.939954	0.023847	-0.1716
139	*YGL180W*	*ATG1*	0.720589	0.188457	0.853847	0.036218	-0.16968
140	*YNL241C*	*ZWF1*	0.735137	0.062754	0.870185	0.066516	-0.16865
141	*YML042W*	*CAT2*	0.82522	0.053925	0.975836	0.033337	-0.16764
142	*YPR145W*	*ASN1*	0.890235	0.133272	1.052303	0.013866	-0.16725
143	*YDR272W*	*GLO2*	0.789504	0.27322	0.932653	0.026359	-0.16663
144	*YOL039W*	*RPP2A*	0.832355	0.1104	0.982434	0.036483	-0.16577
145	*YHR116W*	*COX23*	0.84518	0.147273	0.997366	0.020338	-0.16557
146	*YOR185C*	*GSP2*	0.770602	0.129801	0.90928	0.036171	-0.16548
147	*YGL212W*	*VAM7*	0.659089	0.081259	0.777283	0.018522	-0.16495
148	*YGR028W*	*MSP1*	0.799842	0.179033	0.94306	0.029663	-0.16472
149	*YPR046W*	*MCM16*	0.857983	0.293888	1.010822	0.051428	-0.16393
150	*YGR254W*	*ENO1*	0.910478	0.152933	1.071565	0.020852	-0.16291
151	*YMR209C*	*ORF*	0.728257	0.181658	0.856845	0.058233	-0.1626
152	*YER124C*	*DSE1*	0.926364	0.110707	1.089673	0.039465	-0.16237
153	*YDR426C*	*ORF*	0.888616	0.085448	1.044196	0.013528	-0.16134
154	*YDR158W*	*HOM2*	0.744185	0.098138	0.874445	0.019023	-0.1613
155	*YDR089W*	*ORF*	0.89656	0.092419	1.051835	0.02297	-0.15973
156	*YOL009C*	*MDM12*	0.647424	0.172725	0.759029	0.042137	-0.15904
157	*YOR286W*	*RDL2*	0.906017	0.267186	1.062033	0.054476	-0.15888
158	*YPL227C*	*ALG5*	0.718139	0.192135	0.841634	0.11187	-0.15868
159	*YKL167C*	*MRP49*	0.820887	0.07076	0.961948	0.037178	-0.15858
160	*YNL120C*	*ORF*	0.711965	0.072993	0.833383	0.015458	-0.15746
161	*YHL023C*	*NPR3*	0.701952	0.134265	0.821593	0.015848	-0.15738
162	*YDR025W*	*RPS11A*	0.675281	0.373619	0.790232	0.025493	-0.1572
163	*YMR186W*	*HSC82*	0.888774	0.1415	1.039624	0.030564	-0.15677
164	*YEL067C*	*ORF*	0.848359	0.207923	0.992064	0.038863	-0.15648
165	*YPL264C*	*ORF*	1.019127	0.078573	1.191625	0.06409	-0.15637
166	*YOR069W*	*VPS5*	0.671512	0.183235	0.785093	0.072787	-0.15627
167	*YMR003W*	*AIM34*	0.888883	0.058493	1.039081	0.02928	-0.15613
168	*YKL103C*	*APE1*	0.881747	0.12793	1.029619	0.049957	-0.15504
169	*YJL106W*	*IME2*	0.688377	0.212923	0.803725	0.054907	-0.15492
170	*YOL013W-A*	*ORF*	0.919401	0.08871	1.073439	0.021107	-0.1549
171	*YPL155C*	*KIP2*	0.818259	0.145156	0.954954	0.061725	-0.15449
172	*YDR257C*	*RKM4*	0.857137	0.171976	1.000156	0.018782	-0.15431
173	*YER092W*	*IES5*	0.706034	0.162406	0.823688	0.023712	-0.15413
174	*YLR072W*	*ORF*	0.738826	0.103536	0.861675	0.022801	-0.15382
175	*YPL232W*	*SSO1*	0.851294	0.252218	0.992728	0.023471	-0.1537
176	*YER142C*	*MAG1*	0.884738	0.19279	1.030331	0.0317	-0.15234
177	*YGL054C*	*ERV14*	0.711306	0.124643	0.828214	0.051607	-0.15217
178	*YOL042W*	*NGL1*	0.819982	0.192188	0.954399	0.026152	-0.1518
179	*YDR399W*	*HPT1*	0.842454	0.231621	0.980016	0.002478	-0.15125
180	*YML030W*	*RCF1*	0.80487	0.065761	0.936064	0.028775	-0.151

182	*YPR070W*	*MED1*	0.616325	0.180713	0.716279	0.008975	-0.1503
183	*YHR031C*	*RRM3*	0.71957	0.201668	0.83625	0.030679	-0.15027

Appendix 8: *SUT457* negative genetic interactions (second SGA screen)

	Systematic Gene Name	Standard Gene name	Double mutant average growth	Double mutant growth StdDev	Single Mutant average growth	Single mutant StdDev	SGA score (log10)
1	YCL009C	ILV6	0,292181	0,048569	0,746674	0,028273	-0,93826
2	YCL012W	BUD3	0,40155	0,076578	0,84889	0,023542	-0,7486
3	YBR201W	DER1	0,379898	0,240051	0,746926	0,298573	-0,67606
4	YIL159W	BNR1	0,473792	0,347511	0,883448	0,262696	-0,62306
5	YAL014C	SYN8	0,775266	0,348124	1,269878	0,0242	-0,49347
6	YCL013W	ORF	0,520327	0,070192	0,825725	0,016667	-0,46181
7	YGL105W	ARC1	0,680786	0,403681	1,074778	0,058117	-0,45662
8	YOR297C	TIM18	0,666788	0,353753	1,047658	0,039234	-0,45184
9	YIL125W	KGD1	0,600275	0,51783	0,934943	0,302998	-0,4431
10	YNL299W	TRF5	0,723971	0,322471	1,108125	0,093383	-0,42567
11	YCL011C	GBP2	0,559768	0,084105	0,847643	0,038364	-0,41494
12	YBR294W	SUL1	0,472272	0,417831	0,704084	0,211754	-0,39934
13	YNL255C	GIS2	0,515197	0,131401	0,762936	0,05157	-0,39263
14	YDR058C	TGL2	0,511413	0,089074	0,751478	0,020156	-0,38487
15	YNL275W	BOR1	0,553344	0,096001	0,810313	0,076615	-0,38144
16	YCL026C	ORF	0,850022	0,071683	1,2215	0,02578	-0,36257
17	YJL123C	MTC1	0,740573	0,436368	1,055462	0,081559	-0,35431
18	YDR281C	PHM6	0,487707	0,094463	0,691298	0,015754	-0,34886
19	YPR069C	SPE3	0,572046	0,077784	0,806029	0,034837	-0,3429
20	YNL254C	RTC4	0,534374	0,091554	0,737327	0,116826	-0,32194
21	YML102C-A	ORF	0,461434	0,320773	0,634683	0,407586	-0,31879
22	YCL006C	ORF	0,695318	0,082704	0,955676	0,03601	-0,31805
23	YBL003C	HTA2	0,538967	0,077447	0,721332	0,04004	-0,29145
24	YML032C	RAD52	0,528133	0,046971	0,70485	0,023483	-0,28864
25	YBL072C	RPS8A	0,490195	0,070579	0,654056	0,074933	-0,28839
26	YDR265W	PEX10	0,505432	0,050341	0,670235	0,033979	-0,28222
27	YBR008C	FLR1	0,604625	0,167726	0,789965	0,019449	-0,26738
28	YCL022C	ORF	0,715038	0,156671	0,927629	0,031848	-0,2603
29	YBL032W	HEK2	0,928194	0,132107	1,203125	0,008148	-0,25944
30	YCL026C-A	FRM2	0,909863	0,139809	1,174755	0,013648	-0,25552
31	YBR006W	UGA2	0,57215	0,170719	0,735957	0,033362	-0,25177
32	YLR055C	SPT8	0,546528	0,095961	0,702552	0,029168	-0,25113
33	YDR169C	STB3	0,620698	0,086186	0,79739	0,03772	-0,2505
34	YGR028W	MSP1	0,699767	0,080345	0,896197	0,017636	-0,24741
35	YGL260W	ORF	0,749509	0,132462	0,958715	0,032398	-0,24618
36	YLR418C	CDC73	0,664625	0,277873	0,849516	0,139125	-0,24544
37	YOR275C	RIM20	0,599905	0,131095	0,765091	0,147617	-0,24322
38	YNL253W	TEX1	0,557698	0,060323	0,709904	0,089004	-0,24131

39	YPL261C	ORF	0,605567	0,046996	0,770324	0,01705	-0,24065
40	YGR023W	MTL1	0,663442	0,154277	0,843051	0,051944	-0,23959
41	YOR030W	DFG16	0,53596	0,104098	0,680969	0,077747	-0,23946
42	YJL160C	ORF	0,904052	0,156703	1,147581	0,093564	-0,23853
43	YCL016C	DCC1	0,65429	0,23186	0,828322	0,032338	-0,23585
44	YGR081C	SLX9	0,668351	0,094466	0,84355	0,022621	-0,23281
45	YCL024W	KCC4	0,676731	0,165877	0,851798	0,017428	-0,23008
46	YDR408C	ADE8	0,635487	0,0978	0,795449	0,006977	-0,22452
47	YDR018C	ORF	0,654082	0,073321	0,817968	0,040832	-0,22359
48	YDR282C	ORF	0,667783	0,127609	0,833304	0,015506	-0,22144
49	YPL036W	PMA2	0,658535	0,106511	0,819496	0,028146	-0,21867
50	YGL028C	SCW11	0,773071	0,047343	0,958416	0,02651	-0,21491
51	YCL014W	BUD3	0,714925	0,148103	0,88078	0,025776	-0,20863
52	YCL028W	RNQ1	1,043373	0,106739	1,281853	0,040037	-0,20585
53	YCL023C	ORF	0,722972	0,031982	0,88587	0,037144	-0,2032
54	YNL249C	MPA43	0,595016	0,289987	0,728151	0,041934	-0,20192
55	YBL078C	ATG8	0,712088	0,174004	0,871344	0,049308	-0,20184
56	YLR346C	ORF	0,697216	0,306798	0,852245	0,163592	-0,20078
57	YBL096C	ORF	0,583369	0,192904	0,712034	0,057767	-0,19931
58	YLR334C	ORF	0,811738	0,056687	0,989066	0,011839	-0,19758
59	YMR031W-A	ORF	0,795138	0,334579	0,96675	0,031124	-0,19542
60	YDR094W	ORF	0,826002	0,098522	0,99715	0,02226	-0,1883
61	YOL091W	SPO21	0,843919	0,117814	1,01869	0,021767	-0,18822
62	YOR140W	SFL1	0,816135	0,085609	0,984875	0,017771	-0,18793
63	YGR148C	RPL24B	0,54116	0,075469	0,651707	0,059274	-0,18588
64	YDR375C	BCS1	0,507063	0,028967	0,609375	0,05411	-0,1838
65	YCL029C	BIK1	0,974805	0,073208	1,171327	0,040389	-0,18366
66	YDR514C	ORF	0,685695	0,076676	0,822668	0,02054	-0,18212
67	YGR014W	MSB2	0,803068	0,119219	0,961108	0,056154	-0,17965
68	YJR137C	MET5	1,016509	0,072272	1,215662	0,022242	-0,17891
69	YKL068W	NUP100	0,997335	0,024542	1,191049	0,018171	-0,1775
70	YDR059C	UBC5	0,688009	0,047455	0,820589	0,047032	-0,17622
71	YJL067W	ORF	0,685269	0,156488	0,816315	0,06721	-0,17499
72	YDR393W	SHE9	0,511195	0,072293	0,608307	0,065078	-0,17393
73	YLR394W	CST9	0,915141	0,163953	1,088794	0,020823	-0,17375
74	YEL067C	ORF	0,720965	0,157552	0,856764	0,052879	-0,17257
75	YGL259W	YPS5	0,841902	0,156758	0,999696	0,039891	-0,17179
76	YJL115W	ASF1	0,583793	0,027507	0,692774	0,13306	-0,17116
77	YDR253C	MET32	0,705517	0,12911	0,836799	0,002842	-0,17065
78	YJL051W	IRC8	0,862954	0,055142	1,021681	0,039035	-0,16884
79	YOL155C	HPF1	0,864916	0,114994	1,020858	0,02946	-0,16577
80	YCL001W-A	ORF	0,834495	0,151666	0,983619	0,057496	-0,16441
81	YCL001W	RER1	0,795734	0,080686	0,93542	0,017046	-0,16173
82	YGL162W	SUT1	0,709475	0,122099	0,832581	0,029297	-0,16001
83	YNR025C	ORF	0,939149	0,10372	1,101386	0,048911	-0,15935
84	YGR015C	ORF	0,891207	0,127601	1,044665	0,025639	-0,15887

85	YGL177W	ORF	0,703148	0,148323	0,823707	0,02891	-0,15825
86	YIL132C	CSM2	0,773046	0,112898	0,90436	0,032803	-0,15689
87	YKR065C	PAM17	0,863739	0,017767	1,007963	0,019367	-0,15442
88	YDR440W	DOT1	0,879422	0,048189	1,025635	0,014115	-0,1538
89	YOR058C	ASE1	0,643703	0,22637	0,750551	0,110362	-0,15357
90	YNL190W	ORF	0,931812	0,106265	1,086037	0,020774	-0,15316
91	YNR019W	ARE2	0,859614	0,064753	1,001457	0,020008	-0,15273
92	YDR360W	OPI7	0,772936	0,137806	0,899794	0,030953	-0,15197
93	YOR115C	TRS33	0,929923	0,130402	1,082311	0,109735	-0,15175
94	YLR032W	RAD5	0,771624	0,071188	0,898055	0,025651	-0,15173
95	YCL002C	ORF	0,797434	0,07592	0,927318	0,019109	-0,1509
96	YDR148C	KGD2	0,634617	0,147794	0,737889	0,063867	-0,15077
97	YKL199C	PTK1	1,03893	0,021304	1,20725	0,018895	-0,15015

Appendix 9: *SUT457* positive genetic interactions (first screen)

	Systematic Gene Name	Standard Gene name	Double mutant average growth	Double mutant growth StdDev	Single Mutant average growth	Single mutant StdDev	SGA score (log10)
1	YER002W	NOP16	0.958295	0.072662	0.615936	0.051305	0.442013
2	YER001W	MNN1	1.059337	0.053344	0.762017	0.027045	0.329429
3	YER004W	FMP52	1.066293	0.080739	0.767452	0.075353	0.328868
4	YGL252C	RTG2	0.871553	0.086635	0.641841	0.06107	0.305936
5	YJL053W	PEP8	0.940877	0.013967	0.707149	0.013215	0.285572
6	YER007C-A	TMA20	0.98042	0.050398	0.737837	0.040423	0.284258
7	YOL089C	HAL9	0.89805	0.067967	0.694417	0.462972	0.257152
8	YER005W	YND1	1.02501	0.120876	0.792853	0.038648	0.25682
9	YER011W	TIR1	0.929785	0.037026	0.719535	0.066951	0.256348
10	YMR269W	TMA23	0.901597	0.053727	0.698587	0.023131	0.255108
11	YBR283C	SSH1	1.059333	0.095435	0.823112	0.017741	0.252303
12	YLR191W	PEX13	0.843495	0.019401	0.659395	0.036012	0.246231
13	YER007W	PAC2	1.086251	0.069609	0.851862	0.027939	0.243063
14	YER019C-A	SBH2	0.978595	0.041865	0.77688	0.045778	0.230832
15	YER010C	ORF	1.092409	0.083283	0.871051	0.060164	0.22644
16	YBL046W	PSY4	0.890344	0.118291	0.716602	0.090378	0.217087
17	YBR290W	BSD2	1.242579	0.016624	1.002401	0.017221	0.214791
18	YPR151C	SUE1	1.021414	0.113729	0.825026	0.043688	0.213529
19	YAL002W	VPS8	1.097904	0.12306	0.886884	0.022223	0.213444
20	YBR292C	ORF	1.170677	0.060648	0.952051	0.022841	0.206718
21	YNL140C	ORF	1.20304	0.091627	0.98364	0.009472	0.201348
22	YHR012W	VPS29	0.925031	0.060061	0.760032	0.029775	0.196466
23	YNR032C-A	HUB1	1.102251	0.047254	0.908076	0.013875	0.193782
24	YOR379C	ORF	1.126518	0.046922	0.928982	0.005692	0.192797
25	YDL167C	NRP1	1.092143	0.101008	0.901373	0.048175	0.191978
26	YER016W	BIM1	0.729527	0.103237	0.602626	0.056032	0.1911
27	YDL062W	ORF	1.073528	0.10327	0.889552	0.02002	0.187988

28	YDL181W	INH1	1.038507	0.054842	0.863282	0.020462	0.184798
29	YNL023C	FAP1	1.124564	0.177931	0.936058	0.019753	0.183473
30	YJL148W	RPA34	1.04751	0.031811	0.87306	0.038561	0.182168
31	YMR035W	IMP2	0.829138	0.111783	0.691562	0.024586	0.181434
32	YDL066W	IDP1	1.081555	0.046291	0.903015	0.020537	0.180417
33	YOL048C	RRT8	1.167399	0.033547	0.975097	0.023771	0.179996
34	YDL037C	BSC1	1.172887	0.091212	0.981057	0.024582	0.178593
35	YPL051W	ARL3	1.131651	0.091902	0.94729	0.019293	0.177827
36	YPR073C	LTP1	1.050921	0.038849	0.879756	0.039578	0.177778
37	YKR080W	MTD1	0.857738	0.047399	0.719072	0.029953	0.176338
38	YMR145C	NDE1	1.167475	0.025593	0.980509	0.015	0.174527
39	YPR095C	SYT1	1.067275	0.09336	0.896572	0.059463	0.174286
40	YDL056W	MBP1	0.99511	0.072046	0.836028	0.019497	0.174192
41	YOL047C	ORF	1.138712	0.0903	0.956809	0.024018	0.17405
42	YDL173W	PAR32	1.050142	0.056785	0.882437	0.014131	0.173993
43	YDL065C	PEX19	0.759858	0.091998	0.639663	0.023925	0.17219
44	YBR297W	MAL33	1.023382	0.029794	0.861969	0.041288	0.171649
45	YJL107C	ORF	0.95977	0.02987	0.808413	0.019497	0.171621
46	YPR084W	ORF	1.087861	0.07248	0.918179	0.062426	0.169577
47	YBR298C	MAL31	1.022335	0.035417	0.863063	0.02272	0.169357
48	YGR200C	ELP2	0.89746	0.048948	0.75789	0.042573	0.16903
49	YMR272C	SCS7	1.011988	0.0945	0.854723	0.031799	0.168894
50	YBR291C	CTP1	1.124953	0.033608	0.951285	0.0326	0.167682
51	YDL071C	ORF	1.058752	0.06954	0.895462	0.009096	0.167506
52	YDL039C	PRM7	1.214074	0.082778	1.028233	0.012246	0.16614
53	YMR254C	ORF	1.335946	0.057995	1.132808	0.033262	0.16494
54	YLL045C	RPL8B	1.046684	0.059748	0.887652	0.04764	0.164803
55	YDR133C	ORF	1.110671	0.083805	0.942612	0.033731	0.164064
56	YOR106W	VAM3	0.802902	0.099634	0.681495	0.101589	0.163944
57	YDL177C	ORF	1.078763	0.112549	0.915712	0.022883	0.163869
58	YPL061W	ALD6	1.044454	0.075365	0.887072	0.024162	0.163324
59	YBL103C	RTG3	1.099756	0.123579	0.93418	0.040868	0.163174
60	YBR295W	PCA1	1.000578	0.048337	0.850038	0.029098	0.163052
61	YNL298W	CLA4	1.255066	0.045249	1.066934	0.030628	0.162399
62	YBR286W	APE3	1.05689	0.082935	0.900716	0.018106	0.159896
63	YOL081W	IRA2	1.091959	0.03085	0.930635	0.041165	0.159862
64	YDL178W	DLD2	1.052818	0.030747	0.898418	0.022025	0.15859
65	YMR244W	ORF	1.136369	0.040009	0.969921	0.008968	0.158379
66	YDR493W	MZM1	0.952108	0.044045	0.812694	0.027989	0.158324
67	YGL152C	ORF	0.843704	0.119672	0.720196	0.019985	0.158278
68	YPR074C	TKL1	1.032851	0.102628	0.881998	0.031375	0.157888
69	YDL157C	ORF	1.133795	0.04707	0.968251	0.02725	0.157834
70	YIL153W	RRD1	0.956658	0.124251	0.817281	0.030154	0.157463
71	YDL170W	UGA3	1.133097	0.074395	0.969345	0.034107	0.156089
72	YML001W	YPT7	0.885945	0.05091	0.758284	0.043983	0.155597
73	YGL124C	MON1	1.01892	0.031742	0.873212	0.00886	0.154319

74	YKL069W	ORF	1.018431	0.074017	0.873857	0.038004	0.153102
75	YFL041W	FET5	1.023071	0.106596	0.877928	0.095499	0.153
76	YOR008C	SLG1	0.784397	0.117343	0.673172	0.01553	0.152915
77	YNR024W	MPP6	1.19083	0.087487	1.022078	0.029	0.152813
78	YJL211C	ORF	0.954967	0.053535	0.820897	0.023666	0.151279
79	YPL048W	CAM1	1.100188	0.076362	0.945757	0.041648	0.15125
80	YBR288C	APM3	1.153341	0.060143	0.991565	0.038189	0.151134
81	YAL066W	ORF	1.03107	0.07037	0.886669	0.168176	0.150881
82	YHL033C	RPL8A	0.995729	0.066425	0.856319	0.023774	0.150832
83	YBR131W	CCZ1	0.880639	0.587885	0.75756	0.505649	0.150545

Appendix 10: *SUT457* positive genetic interaction (second screen)

	Systematic Gene Name	Standard Gene name	Double mutant average growth	Double mutant growth StdDev	Single Mutant average growth	Single mutant StdDev	SGA score (log10)
1	YKL157W	APE2	0.850673	0.053921	0.621954	0.087064	0.313161
2	YGL124C	MON1	0.882808	0.036704	0.647918	0.009173	0.309344
3	YNL199C	GCR2	0.818199	0.052039	0.622086	0.030174	0.274026
4	YOL031C	SIL1	0.844343	0.063053	0.644986	0.094137	0.26933
5	YCR061W	ORF	1.105481	0.079462	0.844839	0.024127	0.268891
6	YER002W	NOP16	0.911494	0.023319	0.707355	0.030905	0.253552
7	YER001W	MNN1	0.964745	0.025788	0.763288	0.019885	0.234228
8	YLR384C	IKI3	0.774222	0.065879	0.612858	0.025492	0.233725
9	YKL184W	SPE1	0.787508	0.027952	0.624862	0.028303	0.231343
10	YKL110C	KTI12	0.807919	0.005957	0.64127	0.032222	0.23101
11	YFR032C-A	RPL29	1.032906	0.058363	0.829391	0.035976	0.21944
12	YBR293W	VBA2	1.242732	0.067158	1.000448	0.035741	0.216864
13	YOR069W	VPS5	0.749326	0.120462	0.603692	0.05755	0.216109
14	YJR139C	HOM6	0.88098	0.022567	0.712823	0.0344	0.211802
15	YBR292C	ORF	1.182097	0.062617	0.958689	0.030038	0.209479
16	YER007W	PAC2	1.070642	0.040294	0.869253	0.013555	0.208379
17	YIL008W	URM1	0.767995	0.052771	0.624266	0.025116	0.207206
18	YER005W	YND1	1.044449	0.023028	0.849715	0.028778	0.206343
19	YKL137W	CMC1	0.853302	0.021445	0.695168	0.06797	0.204959
20	YHR030C	SLT2	0.786011	0.064075	0.640794	0.058737	0.204262
21	YDL054C	MCH1	1.161923	0.032424	0.947678	0.037472	0.203817
22	YER004W	FMP52	1.01402	0.040291	0.827955	0.01158	0.202718
23	YLL002W	RTT109	0.737564	0.03612	0.606065	0.024704	0.196365
24	YLR191W	PEX13	0.770689	0.044561	0.636878	0.040128	0.190706
25	YHL023C	NPR3	0.809151	0.031785	0.66928	0.064577	0.189783
26	YJL070C	ORF	0.843267	0.064043	0.6976	0.080831	0.189638
27	YLR287C-A	RPS30A	0.809556	0.071229	0.670425	0.068606	0.188574
28	YDL038C	PRM7	1.283419	0.023042	1.065995	0.029548	0.18562
29	YER010C	ORF	1.059318	0.03168	0.880746	0.027369	0.184611
30	YDL180W	ORF	0.855688	0.158245	0.712914	0.026485	0.182546
31	YLR188W	MDL1	0.770793	0.099932	0.64377	0.092087	0.180078

32	YDL170W	UGA3	1.070687	0.054823	0.895116	0.034246	0.179103
33	YDL037C	BSC1	1.239558	0.050456	1.037324	0.028509	0.17811
34	YJR059W	PTK2	0.827741	0.049486	0.695455	0.044145	0.174135
35	YJL211C	ORF	0.99883	0.057411	0.839801	0.035372	0.17342
36	YDL053C	PBP4	1.075447	0.07711	0.909555	0.007268	0.167537
37	YCL069W	VBA3	1.353574	0.017719	1.145981	0.009909	0.166488
38	YGL059W	PKP2	1.095738	0.068152	0.9295	0.01974	0.164537
39	YDL071C	ORF	1.041447	0.025174	0.883897	0.01574	0.164026
40	YMR275C	BUL1	0.960526	0.052617	0.815541	0.09574	0.163629
41	YDL036C	PUS9	1.261885	0.025215	1.071812	0.030012	0.163257
42	YGL176C	ORF	0.807759	0.067335	0.686107	0.012398	0.16323
43	YNL069C	RPL16B	0.841315	0.13271	0.715453	0.116318	0.162051
44	YBR290W	BSD2	1.180057	0.062062	1.003772	0.010563	0.161798
45	YGR282C	BGL2	1.069757	0.077447	0.911267	0.026998	0.16035
46	YOL129W	VPS68	0.742857	0.16377	0.633389	0.10383	0.159418
47	YDL173W	PAR32	0.991692	0.053845	0.846708	0.021166	0.158056
48	YBR281C	DUG2	1.244432	0.123791	1.062671	0.050865	0.157894
49	YDL157C	ORF	1.17643	0.0164	1.004914	0.035573	0.157582
50	YDL076C	RXT3	0.813754	0.052975	0.695878	0.044845	0.156484
51	YDL171C	GLT1	1.115795	0.021419	0.957962	0.047119	0.152515
52	YBR287W	ORF	1.02966	0.08306	0.884624	0.031192	0.151821
53	YOR014W	RTS1	0.798531	0.065558	0.687255	0.025573	0.150068
54	YLR089C	ALT1	0.826183	0.060129	0.711572	0.055585	0.14934
55	YDL183C	ORF	0.946244	0.059331	0.815026	0.03101	0.149281
56	YBR118W	TEF2	0.78511	0.063796	0.677116	0.023235	0.147982
57	YBR301W	PAU24	1.064907	0.028256	0.918592	0.006889	0.147801
58	YCR089W	FIG2	1.438237	0.027403	1.241964	0.020558	0.146724
59	YDR072C	IPT1	1.106665	0.042408	0.955995	0.038947	0.146354
60	YBR214W	SDS24	0.89997	0.207022	0.777534	0.077594	0.146235
61	YJL136C	RPS21B	0.771016	0.087958	0.667894	0.029802	0.14358
62	YNL322C	KRE1	0.924348	0.03708	0.801457	0.07807	0.142658
63	YDL155W	CLB3	1.269026	0.095189	1.100586	0.053677	0.142407
64	YNR005C	ORF	0.849505	0.015553	0.737114	0.03891	0.141911
65	YCR105W	ADH7	1.358335	0.040716	1.17891	0.002525	0.141669
66	YCR075C	ERS1	1.529586	0.06682	1.327767	0.051769	0.141498
67	YGR118W	RPS23A	0.771871	0.124017	0.670054	0.09198	0.141459
68	YDL191W	RPL35A	1.13994	0.085128	0.992103	0.032369	0.138904
69	YHR129C	ARP1	0.864363	0.010827	0.753475	0.025244	0.137297
70	YCR076C	FUB1	1.477451	0.090574	1.288813	0.082367	0.136597
71	YBR131W	CCZ1	1.123634	0.112534	0.981345	0.014533	0.135399
72	YBR280C	SAF1	1.219951	0.04729	1.06641	0.013475	0.134513
73	YOL006C	TOP1	0.678168	0.109312	0.593288	0.020076	0.133716
74	YBR128C	ATG14	1.270539	0.064785	1.112554	0.010618	0.132784
75	YGL211W	NCS6	0.992982	0.038833	0.869674	0.035633	0.132594
76	YDL199C	ORF	1.399289	0.064194	1.226903	0.005956	0.131471
77	YDL184C	RPL41A	0.951118	0.037845	0.834555	0.046628	0.130739

78	YDL134C-A	RPL41B	1.280926	0.040137	1.124374	0.024919	0.130357
79	YLR073C	RFU1	0.877625	0.041153	0.771571	0.059068	0.128791
80	YDL144C	ORF	1.104575	0.038089	0.971154	0.020206	0.128731
81	YDR316W	OMS1	1.218995	0.047182	1.071987	0.023542	0.128513
82	YER007C-A	TMA20	0.914606	0.026771	0.805199	0.017635	0.127404
83	YDR199W	ORF	1.160275	0.097037	1.022872	0.034144	0.126042
84	YBR269C	FMP21	1.266532	0.079764	1.116791	0.034856	0.125823
85	YER011W	TIR1	0.805337	0.044873	0.71042	0.033775	0.125405
86	YDL182W	LYS20	0.916777	0.046099	0.809001	0.015532	0.125064
87	YAL045C	ORF	0.861945	0.120044	0.761551	0.05229	0.123835
88	YDL019C	OSH2	1.271746	0.049912	1.123647	0.021164	0.123811
89	YDL052C	SLC1	1.076354	0.083028	0.95121	0.011022	0.1236
90	YKL062W	MSN4	1.019756	0.036829	0.901413	0.03265	0.123355
91	YKL162C	ORF	0.9477	0.03023	0.837961	0.05364	0.123067
92	YBR005W	RCR1	0.714804	0.158628	0.632954	0.04008	0.12161
93	YDL216C	RRI1	1.244984	0.037159	1.102854	0.025481	0.121222
94	YBR250W	SPO23	1.344168	0.051136	1.191271	0.013976	0.120754
95	YHR031C	RRM3	0.766364	0.03497	0.679683	0.01469	0.120031
96	YER016W	BIM1	0.6997	0.011045	0.620622	0.002684	0.119929
97	YDL181W	INH1	0.935931	0.029853	0.8304	0.027358	0.119634
98	YKL213C	DOA1	0.917471	0.052105	0.814284	0.038633	0.119312
99	YGL060W	YBP2	1.144716	0.030644	1.016348	0.033939	0.118941
100	YKR027W	BCH2	0.812944	0.025307	0.722065	0.020506	0.118547
101	YPL090C	RPS6A	0.67622	0.19568	0.600971	0.023328	0.117972
102	YGL041C	ORF	1.147116	0.098601	1.019738	0.034873	0.117705
103	YPL102C	ORF	0.736886	0.050152	0.655476	0.028847	0.11707
104	YLL040C	VPS13	0.85825	0.010249	0.764436	0.017349	0.115757
105	YCR073W-A	SOL2	1.373408	0.088702	1.223473	0.026219	0.115602
106	YHR159W	TDA11	1.062613	0.028163	0.947045	0.018346	0.115139
107	YJL077C	ICS3	0.940583	0.052958	0.838836	0.014965	0.114485
108	YDL169C	UGX2	1.067401	0.085693	0.952041	0.026324	0.114374
109	YDR198C	RKM2	1.314144	0.101042	1.172256	0.020563	0.114256

Appendix 11: SUT014 negative genetic interactions

	Systematic Gene Name	Standard Gene name	Double mutant average growth	Double mutant growth StdDev	Single Mutant average growth	Single mutant StdDev	SGA score (log10)
1	YLR114C	AVL9	0,206515	0,41303	1,071302	0,059962	-1,64626
2	YOR125C	CAT5	0,211784	0,423568	0,916726	0,052444	-1,46524
3	YBR200W	BEM1	0,282693	0,565385	0,859413	0,057545	-1,11189
4	YFL010C	WWM1	0,354266	0,493094	0,935728	0,063564	-0,97128
5	YLR038C	COX12	0,347562	0,44532	0,888017	0,004743	-0,93805
6	YOR297C	TIM18	0,414195	0,230604	0,984552	0,148265	-0,86585
7	YMR031W-A	ORF	0,348124	0,408168	0,759338	0,146512	-0,77989
8	YDR440W	DOT1	0,574789	0,199029	1,052311	0,019796	-0,60474
9	YNL315C	ATP11	0,356945	0,513898	0,649419	0,221101	-0,5985

10	YDR004W	RAD57	0,478594	0,369149	0,798917	0,051002	-0,5124
11	YBR132C	AGP2	0,658766	0,433024	1,056584	0,019094	-0,47243
12	YML090W	ORF	0,512523	0,120052	0,821455	0,018009	-0,47173
13	YOR083W	WHI5	0,615096	0,228748	0,974293	0,013464	-0,45993
14	YMR282C	AEP2	0,543334	0,387801	0,835979	0,032853	-0,43088
15	YMR224C	MRE11	0,462473	0,119432	0,707074	0,02803	-0,42455
16	YML035C	AMD1	0,572113	0,197523	0,861705	0,027283	-0,40958
17	YDR375C	BCS1	0,455407	0,423584	0,636006	0,425225	-0,33402
18	YHR162W	MPC2	0,663537	0,443968	0,926398	0,016394	-0,33372
19	YLR200W	YKE2	0,504494	0,098777	0,704265	0,095477	-0,3336
20	YDL074C	BRE1	0,498947	0,077973	0,691868	0,215757	-0,3269
21	YBL031W	SHE1	0,514627	0,373789	0,713275	0,283956	-0,32643
22	YNR010W	CSE2	0,56485	0,076017	0,782203	0,038136	-0,32555
23	YNL249C	MPA43	0,623353	0,185085	0,857558	0,082813	-0,31897
24	YNL120C	ORF	0,55663	0,048401	0,759254	0,014309	-0,31044
25	YGL045W	RIM8	0,557692	0,066988	0,760369	0,024956	-0,31
26	YML041C	VPS71	0,695134	0,023406	0,940763	0,029744	-0,30259
27	YML026C	RPS18B	0,61089	0,119807	0,814126	0,02753	-0,2872
28	YNL224C	SQS1	0,727548	0,149873	0,954262	0,038978	-0,27126
29	YOR311C	DGK1	0,686896	0,075445	0,899488	0,02175	-0,26964
30	YLR084C	RAX2	0,718832	0,139311	0,938982	0,014013	-0,26717
31	YOL044W	PEX15	0,594925	0,114696	0,775091	0,015	-0,26455
32	YOL012C	HTZ1	0,718095	0,086506	0,932788	0,015456	-0,26158
33	YKL137W	CMC1	0,734215	0,227449	0,950782	0,023949	-0,25848
34	YOL042W	NGL1	0,760707	0,099031	0,983222	0,020337	-0,25659
35	YER153C	PET122	0,714375	0,089038	0,922511	0,012759	-0,25569
36	YER177W	BMH1	0,784427	0,220657	1,012123	0,02942	-0,25485
37	YLR192C	HCR1	0,488969	0,052033	0,630741	0,061608	-0,2546
38	YJR074W	MOG1	0,659261	0,288674	0,847779	0,035453	-0,2515
39	YOL035C	ORF	0,523821	0,053268	0,671207	0,04474	-0,24793
40	YMR133W	REC114	0,706532	0,049869	0,902796	0,016493	-0,24513
41	YER151C	UBP3	0,633446	0,07203	0,809147	0,045527	-0,2448
42	YMR019W	STB4	0,73738	0,075106	0,941123	0,029883	-0,24397
43	YLR261C	VPS63	0,604623	0,043198	0,770425	0,017736	-0,24234
44	YDR463W	STP1	0,616743	0,083516	0,785634	0,036981	-0,24204
45	YKR098C	UBP11	0,831305	0,554674	1,057686	0,03302	-0,24084
46	YPL055C	LGE1	0,602721	0,137521	0,76522	0,075723	-0,23871
47	YKL157W	APE2	0,734029	0,116451	0,930184	0,023945	-0,23683
48	YLR218C	COA4	0,557326	0,140585	0,703097	0,019632	-0,23234
49	YMR026C	PEX12	0,654499	0,029268	0,82566	0,021971	-0,23231
50	YIL060W	ORF	0,713444	0,475803	0,899881	0,013943	-0,23216
51	YNL234W	ORF	0,719208	0,074601	0,904825	0,015475	-0,22959
52	YOL150C	ORF	0,815169	0,069837	1,024004	0,009378	-0,22808
53	YNL235C	ORF	0,635562	0,05402	0,798187	0,038657	-0,22783
54	YBR095C	RXT2	0,775583	0,012123	0,973609	0,014415	-0,22739
55	YBR023C	CHS3	0,685845	0,322249	0,859413	0,314487	-0,2256

56	YNL098C	RAS2	0,723438	0,046979	0,89592	0,019796	-0,21384
57	YGL149W	ORF	0,647368	0,138495	0,799348	0,014404	-0,21088
58	YML030W	RCF1	0,77021	0,086904	0,950735	0,016219	-0,21057
59	YNL054W	VAC7	0,858214	0,573339	1,055649	0,039199	-0,20706
60	YDR317W	HIM1	0,740036	0,252862	0,907643	0,034928	-0,20415
61	YNL169C	PSD1	0,579234	0,021387	0,710388	0,064454	-0,2041
62	YMR104C	YPK2	0,775165	0,130702	0,949654	0,016882	-0,20302
63	YMR225C	MRPL44	0,75237	0,083386	0,920818	0,027437	-0,20203
64	YOR068C	VAM10	0,706497	0,093534	0,864618	0,009721	-0,20197
65	YNL116W	DMA2	0,773239	0,032655	0,945014	0,005548	-0,20061
66	YKL204W	EAP1	0,749901	0,389997	0,915879	0,06579	-0,19994
67	YGL127C	SOH1	0,601091	0,033789	0,733249	0,020647	-0,19874
68	YFL013W-A	ORF	0,771997	0,011477	0,938107	0,017279	-0,19488
69	YNL012W	SPO1	0,817479	0,094445	0,993081	0,028556	-0,19459
70	YLR191W	PEX13	0,683209	0,044729	0,828988	0,033688	-0,1934
71	YNL299W	TRF5	0,663847	0,373316	0,804923	0,135887	-0,1927
72	YDR207C	UME6	0,526271	0,083884	0,637439	0,047049	-0,19164
73	YOL036W	ORF	0,805588	0,079372	0,97369	0,048433	-0,18952
74	YMR007W	ORF	0,758317	0,142551	0,915652	0,017546	-0,18853
75	YNL241C	ZWF1	0,727911	0,074126	0,878337	0,034573	-0,18785
76	YER178W	PDA1	0,798023	0,089903	0,9597	0,047524	-0,18448
77	YLR414C	PUN1	0,831356	0,156005	0,998011	0,051111	-0,18271
78	YNL003C	PET8	0,766107	0,02017	0,91864	0,008515	-0,18157
79	YOL015W	IRC10	0,827272	0,061096	0,990823	0,033971	-0,1804
80	YML128C	MSC1	0,824721	0,085582	0,98702	0,021278	-0,17965
81	YLR055C	SPT8	0,747234	0,014086	0,893628	0,01815	-0,17891
82	YGL202W	ARO8	0,760057	0,129606	0,908839	0,011685	-0,17877
83	YER164W	CHD1	0,839847	0,074466	1,002286	0,034226	-0,17682
84	YOL126C	MDH2	0,830045	0,14917	0,990582	0,039645	-0,17681
85	YLR184W	ORF	0,671054	0,116993	0,800583	0,01982	-0,17649
86	YER161C	SPT2	0,801261	0,088054	0,954781	0,028938	-0,1753
87	YNL004W	HRB1	0,767195	0,039322	0,912703	0,019194	-0,17367
88	YML009c	MRPL39	0,760423	0,131111	0,903997	0,035992	-0,17295
89	YML032C	RAD52	0,67717	0,040562	0,804394	0,016252	-0,17217
90	YBR092C	PHO3	0,790155	0,039943	0,938545	0,008475	-0,1721
91	YMR135C	GID8	0,747167	0,047553	0,886696	0,007373	-0,17121
92	YOL137W	BSC6	0,786425	0,034842	0,93315	0,028245	-0,17107
93	YOL132W	GAS4	0,760076	0,026217	0,901056	0,012342	-0,17015
94	YOR195W	SLK19	0,897115	0,110242	1,062734	0,035712	-0,16942
95	YML066C	SMA2	0,757449	0,520555	0,897149	0,04454	-0,16926
96	YML010C-B	ORF	0,715204	0,081639	0,847047	0,014431	-0,16919
97	YOL141W	PPM2	0,863958	0,025879	1,023038	0,037268	-0,16901
98	YOR026W	BUB3	0,688343	0,083529	0,814907	0,032362	-0,16879
99	YIL067C	ORF	0,795778	0,191513	0,941085	0,036346	-0,16771
100	YPR078C	ORF	0,7896	0,178297	0,932439	0,015775	-0,16628
101	YMR006C	PLB2	0,817163	0,019312	0,964792	0,033312	-0,16607

102	YDR485C	VPS72	0,952242	0,01831	1,124048	0,011426	-0,16587
103	YDR469W	SDC1	0,853314	0,008463	1,006845	0,005334	-0,16545
104	YML129C	COX14	0,999574	0,04458	1,179221	0,012948	-0,16528
105	YNR005C	ORF	0,840204	0,026534	0,989656	0,023086	-0,16371
106	YMR022W	UBC7	0,797837	0,062121	0,939441	0,017524	-0,16338
107	YNL009W	IDP3	0,851082	0,109918	1,002101	0,036038	-0,16335
108	YLR188W	MDL1	0,759028	0,041001	0,893161	0,014743	-0,16273
109	YMR237W	BCH1	0,893354	0,116756	1,050699	0,066723	-0,16223
110	YOL030W	GAS5	0,757555	0,03987	0,89092	0,030096	-0,16216
111	YBR103W	SIF2	0,904179	0,034083	1,062228	0,011924	-0,1611
112	YNL123W	NMA111	0,877796	0,030935	1,030645	0,016358	-0,16053
113	YFL013C	IES1	0,661728	0,077644	0,776647	0,022103	-0,16013
114	YLR024C	UBR2	0,774312	0,175536	0,908473	0,014879	-0,15979
115	YNL119W	NCS2	0,635441	0,059964	0,74464	0,037922	-0,15858
116	YDR423C	CAD1	0,887239	0,056531	1,038875	0,024414	-0,15778
117	YOR082C	ORF	0,735241	0,027856	0,860636	0,0347	-0,15747
118	YOL039W	RPP2A	0,850217	0,044133	0,994202	0,044452	-0,15645
119	YOR309C	ORF	0,762707	0,0796	0,891024	0,057281	-0,1555
120	YGL049C	TIF4632	0,957424	0,046335	1,117952	0,081553	-0,15501
121	YOL147C	PEX11	0,896863	0,03669	1,046928	0,024152	-0,15471
122	YHR041C	SRB2	0,550856	0,061378	0,64156	0,052951	-0,15243
123	YOL131W	ORF	0,741544	0,040457	0,863532	0,023204	-0,1523
124	YOR221C	MCT1	0,698387	0,115707	0,813113	0,034164	-0,1521
125	YDR336W	ORF	0,808425	0,131995	0,939986	0,013973	-0,15078
126	YNL015W	PBI2	0,827753	0,02724	0,962255	0,019282	-0,15056
127	YDR426C	ORF	0,871183	0,046251	1,012723	0,011064	-0,15055
128	YPR013C	CMR3	0,973586	0,035037	1,131595	0,016024	-0,1504

Appendix 12: *SUT451* negative genetic interactions

	Systematic Gene Name	Standard Gene name	Double Mutant average growth	Double Mutant growth StdDev	Single Mutant average growth	Single mutant growth StdDev	SGA score (log10)
1	*YBR292C*	*ORF*	0.230059	0.205953	1.044282	0.032393	-1.51275
2	*YKL204W*	*EAP1*	0.657124	0.516419	1.03455	0.114859	-0.45385
3	*YLR437C*	*DIF1*	0.855381	0.570684	1.223978	0.017719	-0.35831
4	*YOL035C*	*ORF*	0.5425	0.056374	0.762881	0.016291	-0.34091
5	*YLR438W*	*CAR2*	0.830353	0.554287	1.151251	0.015072	-0.32675
6	*YLR192C*	*HCR1*	0.487391	0.053765	0.665873	0.031781	-0.31203
7	*YPL250C*	*ICY2*	0.658424	0.086555	0.878453	0.017458	-0.28831
8	*YER061C*	*CEM1*	0.613064	0.066494	0.817575	0.031511	-0.28787
9	*YLR418C*	*CDC73*	0.797496	0.115284	1.053241	0.026098	-0.27815
10	*YOR297C*	*TIM18*	0.7966	0.160757	1.014318	0.081915	-0.24162
11	*YNL299W*	*TRF5*	0.884818	0.185653	1.106381	0.060569	-0.22347
12	*YKR066C*	*CCP1*	0.886053	0.591933	1.101406	0.015386	-0.21757
13	*YLR320W*	*MMS22*	0.63521	0.043102	0.787374	0.039872	-0.21475
14	*YOL004W*	*SIN3*	0.559514	0.040902	0.689459	0.020474	-0.20884

15	*YFL013W-A*	*ORF*	0.643757	0.098031	0.781471	0.067713	-0.19386
16	*YOR312C*	*RPL20B*	0.487439	0.113698	0.588491	0.069118	-0.1884
17	*YDR440W*	*DOT1*	0.8111	0.081537	0.97807	0.035822	-0.18719
18	*YDR463W*	*STP1*	0.63078	0.118505	0.757512	0.010269	-0.18308
19	*YIL071C*	*PCI8*	0.722197	0.081447	0.866548	0.03338	-0.18222
20	*YOR275C*	*RIM20*	0.551882	0.062385	0.658455	0.038634	-0.17656
21	*YBR023C*	*CHS3*	0.849733	0.21987	1.013233	0.094604	-0.17598
22	*YHL023C*	*NPR3*	0.676772	0.132196	0.806567	0.026591	-0.17545
23	*YNL111C*	*CYB5*	0.912167	0.049529	1.086335	0.030931	-0.17474
24	*YLR125W*	*ORF*	0.837893	0.077396	0.995187	0.048859	-0.17204
25	*YPL261C*	*ORF*	0.808198	0.089877	0.958392	0.026259	-0.17045
26	*YPR179C*	*HDA3*	0.62359	0.033054	0.738557	0.055435	-0.16921
27	*YMR294W-A*	*ORF*	0.761606	0.067443	0.901688	0.027136	-0.16884
28	*YPR075C*	*OPY2*	0.790983	0.057525	0.936244	0.044195	-0.1686
29	*YOL086C*	*ADH1*	0.824054	0.032382	0.973354	0.020957	-0.16651
30	*YLR415C*	*ORF*	0.956598	0.04287	1.126384	0.035311	-0.16338
31	*YDR459C*	*PFA5*	0.920668	0.036202	1.083535	0.054395	-0.16288
32	*YOR196C*	*LIP5*	0.596379	0.092649	0.701176	0.046148	-0.16188
33	*YPR076W*	*ORF*	0.791209	0.021411	0.927997	0.037598	-0.15947
34	*YMR158W-A*	*ORF*	0.91062	0.053836	1.067807	0.058256	-0.15924
35	*YNL056W*	*OCA2*	0.668835	0.044114	0.781312	0.072506	-0.15544
36	*YFL033C*	*RIM15*	0.776486	0.058266	0.905966	0.033626	-0.15422
37	*YOL116W*	*MSN1*	0.653312	0.066946	0.762206	0.020106	-0.15416
38	*YLR209C*	*PNP1*	0.964935	0.058996	1.125278	0.053	-0.15372
39	*YNR018W*	*RCF2*	0.718165	0.176416	0.834644	0.025854	-0.15031

Appendix 13: *SUT469* negative genetic interactions

	Systematic Gene Name	Standard Gene name	Double Mutant average growth	Double Mutant growth StdDev	Single Mutant average growth	Single mutant growth StdDev	SGA score (log10)
1	*YFL010C*	*WWM1*	0.524972	0.6503	1.125582	0.079596	-0.76271
2	*YBR032W*	*ORF*	0.486149	0.550819	0.983527	0.046589	-0.70463
3	*YGR229C*	*SMI1*	0.371785	0.05595	0.701291	0.046285	-0.63461
4	*YOR101W*	*RAS1*	0.483895	0.559138	0.907638	0.141237	-0.62898
5	*YIL159W*	*BNR1*	0.53634	0.551181	0.951412	0.044146	-0.57318
6	*YPL262W*	*FUM1*	0.447443	0.301929	0.789966	0.022547	-0.56844
7	*YBL031W*	*SHE1*	0.515055	0.40901	0.893442	0.35811	-0.55081
8	*YFL003C*	*MSH4*	0.618432	0.091281	1.046086	0.054924	-0.52562
9	*YGL042C*	*ORF*	0.488059	0.087908	0.810553	0.076391	-0.50728
10	*YMR224C*	*MRE11*	0.418806	0.023882	0.66559	0.055848	-0.46327
11	*YFL013W-A*	*ORF*	0.472055	0.030977	0.743604	0.108229	-0.45441
12	*YDR123C*	*INO2*	0.427261	0.022082	0.661754	0.03704	-0.4375
13	*YDR076W*	*RAD55*	0.598122	0.106671	0.916717	0.031786	-0.427
14	*YER119C-A*	*ORF*	0.633167	0.144259	0.965	0.038655	-0.42139
15	*YOL029C*	*ORF*	0.705947	0.477437	1.064678	0.062556	-0.41089
16	*YOL009C*	*MDM12*	0.505037	0.181106	0.759029	0.042137	-0.40741

17	*YDR080W*	*VPS41*	0.515098	0.069432	0.771309	0.046539	-0.40373
18	*YPR008W*	*HAA1*	0.80008	0.563415	1.17542	0.023408	-0.38467
19	*YDR004W*	*RAD57*	0.46489	0.347697	0.67957	0.138532	-0.37966
20	*YGR055W*	*MUP1*	0.727825	0.170309	1.052609	0.040205	-0.36897
21	*YNL235C*	*ORF*	0.527107	0.078192	0.757056	0.031014	-0.36203
22	*YDR440W*	*DOT1*	0.713723	0.093271	1.01935	0.046014	-0.35643
23	*YBR171W*	*SEC66*	0.604234	0.153309	0.860439	0.022446	-0.35348
24	*YER061C*	*CEM1*	0.55808	0.037325	0.785865	0.010306	-0.34228
25	*YBR023C*	*CHS3*	0.797687	0.37215	1.105004	0.087505	-0.32589
26	*YNL236W*	*SIN4*	0.439019	0.069957	0.606473	0.059311	-0.32312
27	*YOL116W*	*MSN1*	0.593077	0.073033	0.814662	0.020532	-0.31745
28	*YDR274C*	*ORF*	0.531506	0.033118	0.728815	0.035907	-0.3157
29	*YCR028C-A*	*RIM1*	0.55429	0.040463	0.754592	0.035577	-0.30849
30	*YKL204W*	*EAP1*	0.706062	0.428286	0.948479	0.036614	-0.29516
31	*YNL215W*	*IES2*	0.567207	0.141545	0.760323	0.06952	-0.29302
32	*YPL261C*	*ORF*	0.699214	0.18513	0.926434	0.021053	-0.28139
33	*YOR035C*	*SHE4*	0.68643	0.073072	0.907638	0.009644	-0.27934
34	*YLR038C*	*COX12*	0.706707	0.059773	0.926417	0.017126	-0.27071
35	*YJL123C*	*MTC1*	0.832956	0.568048	1.090585	0.060311	-0.26949
36	*YDR469W*	*SDC1*	0.705519	0.088195	0.923627	0.026683	-0.26937
37	*YHR030C*	*SLT2*	0.64882	0.079262	0.846397	0.042787	-0.26583
38	*YLL029W*	*FRA1*	0.604337	0.036897	0.780225	0.020393	-0.25545
39	*YDR463W*	*STP1*	0.560473	0.081016	0.723306	0.038861	-0.25505
40	*YLR192C*	*HCR1*	0.603489	0.049101	0.778434	0.008795	-0.25456
41	*YOR179C*	*SYC1*	0.751723	0.120019	0.962717	0.049476	-0.24739
42	*YDR455C*	*ORF*	0.577792	0.054973	0.739611	0.035704	-0.24691
43	*YOR297C*	*TIM18*	0.771594	0.122776	0.987472	0.033828	-0.24669
44	*YLL002W*	*RTT109*	0.593195	0.00662	0.756763	0.00998	-0.24353
45	*YNR010W*	*CSE2*	0.655625	0.304971	0.830007	0.116173	-0.23585
46	*YLR239C*	*LIP2*	0.545483	0.096196	0.6891	0.046366	-0.23371
47	*YGL214W*	*ORF*	0.79723	0.536301	1.001603	0.118731	-0.22821
48	*YOR221C*	*MCT1*	0.659236	0.048762	0.825211	0.03429	-0.22456
49	*YDL078C*	*MDH3*	0.882606	0.043237	1.097081	0.030241	-0.21753
50	*YGL243W*	*TAD1*	0.78795	0.057856	0.977649	0.029769	-0.21572
51	*YGL081W*	*ORF*	0.893871	0.027389	1.10436	0.016224	-0.21146
52	*YBR170C*	*NPL4*	0.599737	0.195948	0.740145	0.170523	-0.21035
53	*YFR056C*	*ORF*	0.78795	0.076873	0.969142	0.028068	-0.20698
54	*YDR207C*	*UME6*	0.580949	0.098197	0.713765	0.00998	-0.20589
55	*YKL069W*	*ORF*	0.716536	0.075012	0.873857	0.038004	-0.19849
56	*YNL292W*	*PUS4*	0.647846	0.482651	0.789503	0.210526	-0.19775
57	*YDR375C*	*BCS1*	0.616718	0.414804	0.751279	0.052622	-0.19737
58	*YLR190W*	*MMR1*	0.665498	0.026867	0.810534	0.022695	-0.19716
59	*YGL046W*	*RIM8*	0.529709	0.070531	0.64408	0.031296	-0.19549
60	*YMR207C*	*HFA1*	0.568388	0.076569	0.691018	0.04943	-0.19536
61	*YOL018C*	*TLG2*	0.544178	0.067715	0.661454	0.07534	-0.19516
61	*YOR083W*	*WHI5*	0.810575	0.313484	0.980792	0.049171	-0.19062

63	*YPR141C*	*KAR3*	0.648501	0.083974	0.782832	0.02205	-0.18825
64	*YLR055C*	*SPT8*	0.696356	0.054675	0.838172	0.021539	-0.18536
65	*YDR459C*	*PFA5*	0.826068	0.110465	0.994172	0.027711	-0.18523
66	*YMR143W*	*RPS16A*	0.531444	0.067484	0.638966	0.110377	-0.18425
67	*YGL115W*	*SNF4*	0.697923	0.025461	0.83896	0.019353	-0.18405
68	*YOR106W*	*VAM3*	0.567923	0.090459	0.681495	0.101589	-0.1823
69	*YLR056W*	*ERG3*	0.649483	0.084192	0.778652	0.038339	-0.18139
70	*YLR188W*	*MDL1*	0.741178	0.085721	0.886266	0.01651	-0.17878
71	*YAL055W*	*PEX22*	0.610978	0.058069	0.729395	0.02308	-0.17715
72	*YER092W*	*IES5*	0.690137	0.058472	0.823688	0.023712	-0.1769
73	*YMR256C*	*COX7*	0.691342	0.21696	0.82195	0.065036	-0.17304
74	*YDR075W*	*PPH3*	0.868852	0.07662	1.029702	0.026332	-0.16985
75	*YNL249C*	*MPA43*	0.716542	0.296026	0.848082	0.089138	-0.16854
76	*YLR393W*	*ATP10*	0.744986	0.055816	0.880064	0.031748	-0.16663
77	*YER178W*	*PDA1*	0.723294	0.082939	0.853747	0.039457	-0.16582
78	*YOR026W*	*BUB3*	0.638073	0.091614	0.752459	0.027158	-0.16489
79	*YJL066C*	*MPM1*	0.754585	0.065118	0.889826	0.032368	-0.16486
80	*YPR096C*	*ORF*	0.996762	0.04508	1.174604	0.029011	-0.16417
81	*YLR185W*	*RPL37A*	0.519215	0.060565	0.608907	0.042486	-0.15935
82	*YLR218C*	*COA4*	0.657295	0.067314	0.768641	0.018517	-0.15649
83	*YNL120C*	*ORF*	0.713364	0.109561	0.833383	0.015458	-0.1555
84	*YLL042C*	*ATG10*	0.797649	0.046173	0.931752	0.012028	-0.1554
85	*YML035C*	*AMD1*	0.734636	0.042706	0.857497	0.014772	-0.15464
86	*YPR089W*	*ORF*	0.535855	0.152166	0.623024	0.039758	-0.15072
87	*YMR116C*	*ASC1*	0.524012	0.083324	0.609191	0.042723	-0.15062
88	*YPR172W*	*ORF*	0.808831	0.298417	0.939785	0.077824	-0.15006

Appendix 14: *SUT042* negative genetic interactions

	Systematic Gene Name	Standard Gene name	Double Mutant average growth	Double Mutant growth StdDev	Single Mutant average growth	Single mutant growth StdDev	SGA score
1	*YOL004W*	*SIN3*	0.403277	0.020794	0.689459	0.020474	-0.53628
2	*YDR455C*	*ORF*	0.535356	0.039564	0.767796	0.031699	-0.36059
3	*YDL179W*	*PCL9*	0.73967	0.054837	0.972003	0.020042	-0.27315
4	*YOL018C*	*TLG2*	0.538053	0.051356	0.704969	0.015426	-0.2702
5	*YDR459C*	*PFA5*	0.82753	0.054772	1.083535	0.054395	-0.26954
6	*YOR184W*	*SER1*	0.474807	0.042252	0.617554	0.019804	-0.26286
7	*YDR463W*	*STP1*	0.591177	0.032283	0.757512	0.010269	-0.24792
8	*YDL173W*	*PAR32*	0.771825	0.03491	0.988192	0.017845	-0.24712
9	*YOL081W*	*IRA2*	0.804687	0.152008	1.021923	0.012905	-0.23899
10	*YPR076W*	*ORF*	0.738768	0.114897	0.927997	0.037598	-0.22804
11	*YNL165W*	*ORF*	0.789578	0.038455	0.977584	0.022944	-0.21359
12	*YOL035C*	*ORF*	0.618568	0.025527	0.762881	0.016291	-0.20969
13	*YFL033C*	*RIM15*	0.734596	0.080102	0.905966	0.033626	-0.20968
14	*YFR010W*	*UBP6*	0.581167	0.089099	0.707186	0.08265	-0.19626
15	*YDL172C*	*ORF*	0.887983	0.085751	1.078028	0.054637	-0.19394

16	*YDL177C*	*ORF*	0.785399	0.099252	0.946238	0.044368	-0.1863
17	*YFL036W*	*RPO41*	0.720482	0.154786	0.867682	0.035864	-0.1859
18	*YPR062W*	*FCY1*	0.899894	0.054685	1.068545	0.058907	-0.17178
19	*YOL086C*	*ADH1*	0.821192	0.090371	0.973354	0.020957	-0.16999
20	*YBL107C*	*MIC23*	0.826672	0.073658	0.979134	0.045586	-0.16926
21	*YFL013W-A*	*ORF*	0.660304	0.056624	0.781471	0.067713	-0.16848
22	*YAL066W*	*ORF*	0.908585	0.074151	1.075168	0.066814	-0.16834
23	*YDL156W*	*CMR1*	0.919915	0.073173	1.086806	0.01706	-0.16672
24	*YER151C*	*UBP3*	0.634396	0.057633	0.749416	0.09473	-0.16662
25	*YDL077C*	*VAM6*	0.542736	0.0798	0.639338	0.05494	-0.16381
26	*YDL062W*	*ORF*	0.80576	0.058571	0.940196	0.031818	-0.1543
27	*YDR503C*	*LPP1*	0.85438	0.183676	0.995903	0.046327	-0.15327
28	*YJR117W*	*STE24*	1.076959	0.110565	1.253461	0.032358	-0.15177
29	*YKL132C*	*RMA1*	0.799887	0.069795	0.92968	0.063508	-0.15037
30	*YOR297C*	*TIM18*	0.873	0.076066	1.014318	0.081915	-0.15004

Appendix 15: *SUT123* negative genetic interactions

	Systematic Gene Name	Standard Gene name	Double Mutant average growth	Double Mutant growth StdDev	Single Mutant average growth	Single mutant growth StdDev	SGA score (log10)
1	*YBR106W*	*PHO88*	0.268278	0.422223	0.621283	0.398364	-0.83976
2	*YFL010C*	*WWM1*	0.490027	0.567787	1.060816	0.11005	-0.77233
3	*YOR101W*	*RAS1*	0.485746	0.57404	0.840276	0.560396	-0.54804
4	*YJR077C*	*MIR1*	0.438588	0.398707	0.735967	0.434167	-0.51762
5	*YLR192C*	*HCR1*	0.416474	0.041322	0.677477	0.042978	-0.48655
6	*YNR006W*	*VPS27*	0.424647	0.145194	0.650277	0.247032	-0.42614
7	*YCL037C*	*SRO9*	0.444771	0.478537	0.668148	0.250804	-0.40695
8	*YNL292W*	*PUS4*	0.678314	0.48897	1.010299	0.050861	-0.39839
9	*YDR455C*	*ORF*	0.472676	0.033483	0.678735	0.047517	-0.36182
10	*YER061C*	*CEM1*	0.555582	0.072391	0.780788	0.040298	-0.34029
11	*YPL174C*	*NIP100*	0.44614	0.090091	0.600565	0.023365	-0.29724
12	*YML013C-A*	*ORF*	0.470682	0.043198	0.628737	0.356629	-0.28953
13	*YGL136C*	*MRM2*	0.515465	0.108716	0.684102	0.202842	-0.28304
14	*YPL262W*	*FUM1*	0.577682	0.393721	0.761274	0.114537	-0.27597
15	*YBR023C*	*CHS3*	0.874211	0.221458	1.13982	0.045186	-0.2653
16	*YML102C-A*	*ORF*	0.677271	0.454999	0.871752	0.018707	-0.25243
17	*YMR031W-A*	*ORF*	0.765551	0.510563	0.984943	0.100613	-0.25199
18	*YJL123C*	*MTC1*	0.779233	0.588502	1.000018	0.053582	-0.24946
19	*YLR199C*	*PBA1*	0.504226	0.086526	0.639839	0.048092	-0.23819
20	*YER153C*	*PET122*	0.741467	0.050123	0.937873	0.029735	-0.23498
21	*YER151C*	*UBP3*	0.516965	0.037599	0.653011	0.066021	-0.23362
22	*YER173W*	*RAD24*	0.997496	0.016447	1.234122	0.011239	-0.21287
23	*YER174C*	*GRX4*	0.98506	0.016367	1.213353	0.026051	-0.20844
24	*YOR297C*	*TIM18*	0.796199	0.044187	0.979826	0.028178	-0.20753
25	*YER170W*	*ADK2*	1.015386	0.015829	1.246246	0.015319	-0.20487

26	*YBL094C*	*ORF*	0.513214	0.52925	0.628384	0.338877	-0.20246
27	*YLR337C*	*VRP1*	0.212289	0.016066	0.259545	0.303833	-0.20098
28	*YER175C*	*TMT1*	0.950042	0.013947	1.159374	0.025965	-0.19913
29	*YLR297W*	*ORF*	0.641238	0.192312	0.779975	0.122275	-0.19586
30	*YDR438W*	*THI74*	0.960951	0.016113	1.168336	0.017989	-0.19541
31	*YDR431W*	*ORF*	0.953315	0.017532	1.155157	0.023433	-0.19205
32	*YDR453C*	*TSA2*	1.007532	0.010659	1.220732	0.027025	-0.19195
33	*YGR080W*	*TWF1*	0.864175	0.069514	1.045815	0.022046	-0.19078
34	*YDR451C*	*YHP1*	1.054985	0.033033	1.274289	0.019485	-0.18886
35	*YER176W*	*ECM32*	0.931061	0.015184	1.124162	0.010825	-0.18847
36	*YJL218W*	*ORF*	0.869086	0.580093	1.049028	0.010386	-0.18818
37	*YHR033W*	*ORF*	0.866277	0.124278	1.044688	0.065105	-0.18727
38	*YDR439W*	*LRS4*	0.971751	0.019328	1.171393	0.039372	-0.18685
39	*YFL013C*	*IES1*	0.614805	0.068367	0.738835	0.027921	-0.18377
40	*YDR428C*	*BNA7*	1.024876	0.023741	1.230221	0.042518	-0.18262
41	*YER158C*	*ORF*	0.936843	0.011473	1.123213	0.024651	-0.18143
42	*YIR002C*	*MPH1*	0.839315	0.041947	1.005273	0.036898	-0.18043
43	*YDR436W*	*PPZ2*	1.040476	0.040537	1.24614	0.044417	-0.18037
44	*YIL054W*	*ORF*	0.855151	0.107884	1.021991	0.043321	-0.17823
45	*YDR452W*	*PPN1*	1.009277	0.024109	1.206078	0.0346	-0.17814
46	*YDR435C*	*PPM1*	0.939679	0.009052	1.12237	0.019652	-0.17766
47	*YNL277W*	*MET2*	0.823313	0.133138	0.982751	0.033799	-0.17702
48	*YER155C*	*BEM2*	0.87499	0.026262	1.043932	0.027209	-0.17654
49	*YGR059W*	*SPR3*	0.943262	0.077238	1.125086	0.029898	-0.17627
50	*YDR458C*	*HEH2*	0.974587	0.008405	1.160534	0.01879	-0.17462
51	*YGL046W*	*RIM8*	0.609854	0.039688	0.723114	0.008869	-0.17035
52	*YGR028W*	*MSP1*	0.828611	0.026653	0.982149	0.038863	-0.16999

Appendix 16: Features of the six SGA-tested SUTs

	Long non-coding RNA	SUT locus size (nt)	Expression level	Genomic sequence (5'-3')
1	SUT457	345	High	TTAGGGTTGAGTGGGGAGTAAAGAATAAAGCGAATCCTATTCGTG TAAGCCGGTCTACTTATTGATAACAATATTTTACAGGCGGCTATCA TGTTTCAGCTTACGCATTCACAGTCAGGTTGGTGCTCTACATGAAT ACCAGCGTTTACTTTCATTTACAGAGTACTAGCACCTCCACTGTCG CTAATACTGAATTTAGTTTTGAAGAGTGAAAACAACTAAATCAGGC GGTAGAAGAAAATCAATAGCTCATATATTCTTATATATTACAGGTG ATATTTGTATATGATTATGAATGGCTTTTCGTAGCCCGTGATCTTT CATTTCTATATTATGTGTAGCTAA
2	SUT014	1729	Medium	TTCATATTACATATAAAGGTGCCACAGCAAGTTAATGTCACGGCAG CTAGTGACGCTATTGCTAGTTTACACCTAGATGAGGCCACTGGAG AAATGGTCTCTAAGACAGAGTTGAAGAAGCGTATTAAGGGAATAC AAATTGAGGCCAAAAAGCTGTCAAAAAGACTCTTGCGAAACCAAA ACCAGCTTCGAAAAGACTAATTTCCTGGCCGGTTTATAGTCATCTC AATACTAGATCACAGCAAATCCAATTAAGAAACAGACTCTTGATAT AAATTTTTATCCATACAAGTTCCGATTATATATATTCAATCCTGAAT TTTTGGCCAAGTATGCCCATTCAAAAAGGCGAAAATTTCCCTTAAG AGAAGTTTCACATTGCTAGGAGAGTTCATGCAGAAAGAGAATCAG CTTAAAAATTGAAATTCTACGTTCTCAATGGTGGTGTTGAGCTCTA AATTATTTTACAATTTCAGGATTATTACGACGAGAACCCATAAAAA GGAGCATGACCTTTAAGGAGGAGTAATATATATCCACCAAAGAAG ACCGGCGGAGATGAGATATATTTTTTTCGTTAACAGAGTGCAATTG

				ACAACTTGTTTGCACTTGCCTGCTAACTGTTTTGGTTTCAAAGATC AAGAAAATAGATAGAACCCGTTTTATTATTCAATTGACATCGCCCG TTATATCAGACGATTTTTGGATCAAAAAAAGTTTATTGGAGCAGAA GCAATTCTGAAATGAAGGTCCTAATATGACCCCAATATGACACATA ATTCGGAATCTGCCACTTGTGAGTTTTATCAAGCCTATGCGGATGT TTGTGACTAGTTGGATATGACTGAATTAATACTTTCAGAAATGGAC AAGGAGATATGTGATTCTCTATTATCAAATACCATTTGAACCTTACT GGTCCAGCTAAAAAAGAGCTAGAATTCATCTGTTCTAGCCCATGG AAGAGAACCGATATGATTGGCAGATAGAAACCATACTGATTCGCG TCGTATCTAGCACAACCCACGTAAGAACCTTAATTGACGAACAGT CAAACCTTCTTGGCTTTTACAACCGAGAGGAAATACTAAGTCAACA TCAAGGTGGCAAACACAATTCACAGTATCTAATTTTTCGTTATATC ACATTGGAAAAAGTATTAACGTATAATTTCCATCTGCTGAGCACTT GCTGCCGTTGAGACCGGCGAATTTTTGAAAGAAGTGTATGCCAAT AATAAATTGGAAAGCCCATTAAATAATGCTCTTATGTTGGATAAGC TTTCTTCGGTGGAATAAAAGGCACATGTATCAACCTGACTTTCACT TTTACTTAACCCCAAGCTATGTCTCCATTGGCCAGGTACTCAAAAG AACAACCGGGTTTATGTGAGCGTTTCGAGGTTTTTGTATCTAAAAA GGAGATATGTAATGCGTAAACCCGAACTGAACAATTCGTTTGACC AAAAGGGGCTTTCCTACAAACAAGCAGGGCAATAGGAGCAAGGC AAATGGATCAAGGTGATGCTTATGCATAATTTATACGATGGAATCC TTTGTAATGCTCCGTACTACGGTTTACCACCAACCGGCTTTTGGG TTGTAATATTGACAGATTCACCATGTTCTCAATGGTTCTGTCACAA TTCGAAAGTTCTATTACTCGCAAATTCGAAAGCAGATGTTTTAAGA GACGAGGTGAAGTAAAAAAGAAGAAAAATGATTGCCAT
3	SUT451	392	Medium	TTCGCCTTTGTCCAAGTCCTCATCTAAGTCTTCACTGTAGTCGACA GAAGGAATTTCAGTCTCTTCAATACTGCCATAGTTTCCATCCTTGC TTTTCGGTAGTACTTGTGTTTACTAGATTTAAGCATTGCAGAAAAA AATCTGATTTGGAATTAATGTTTCATTTACTACATTTTAAAGCATTT TGTACCATTCAGAGGCAAGAATTGGCCAATACTGTGTGTTCTTATA ACGATAACTAGTATATATATTCTCGAAATTGTATATTTCTGTGGATT TGCACACAATCATCTAATAGCAAATTAGGAAGAAAGCCACACATG CACATATATCGCATCACTTACCGAGCCTTAGAATGTGGTTGCCAC ACATTAGGACATGTTACCCCCCGCA
4	SUT469	985	Medium	GCAACAATTACGGTGGGGAGAAATATCAACAAAAGGGCAAGGCTA TGCCTTCTGGAAAGTGGCAGACTTGCACTTTCCTCGAAAAGAAAA ATGACCGCAAGATCCGGTTGTTCTCAACCTTCTACATTAAGACATA CTTCTACGATTTTCGAATGCCGAAGCAACTATCGCTGAAATTTGTC ATGTCAAAATTGCTACTGGGGGAGAAGAATATATATGGAAGTAATT ATTATTTACGTTGCTGAAATGGCAGGTTAGACGCATGTTTTGCAAA ATAAGTGGTTTTGAAAAGAATTGATACTAGGAATCGGTGCAATACC TTCTACCTTTCTTAATAGGTATTCTTGAATAATCTACCTCACTTTCT GTCCCAGATACGAGATGTCGAGCGCCTCGAAAATAGATATCGTTT ATTACGTTAGATACGGAAAGGTCTACGTGTCATAATAAATTGCATC TGGATTGCGATTTTGGGTCATGCCTAACTGGGAAAATATTTACATC TCCATGTTCTCATTCTGCCTTTGCTTTCCTTCAAAACATGGTTTTCA ATTCAACCTAGGGTCTACCGCGGAACCATATGTACGCCGTAAATG CGAGTGTTCTTGAAAGGTAGTAATGTGTTCCCTCTCAATATGTAAG TCCTTCAAGAGTATGCACTTGCAGTTGCACTGTTTCGGGTAATTAT CCGTCATTAAGAAAAAGATGCTTCCACTTTCTCGTGTTTTTACGCA CAATCGTGCCATTTAACCGGAAATAGACTCCATTGCATTGATTGCT CTCATAAAAATTATAGCCCGCGTTTGATACTTGTTTAAAATAGGTG TCGACAAAGTTAGTTTCTGTCTTCCATTTAGTTTTTACAATATGACA CGTCAAATAAATCTTTTCGATTTAGTTAAAAGAGTTACCTGGCGAT AGCCTTCTGGTAAAACACCTATTCATAAAACAATCTTAAAAAACCA AAAAATTACCAAACAACTAT
5	SUT042	1873	Low	TTCTTCCATCGTCCAGTGATATCGGTAAACCGGTAGCTTTTTCTTA ACTTTGAACAAAGAAGAGATAACTACGGACCCTTCTCCACGTTTC GATCTTTGGCTTCACTTCCTCATAGCCTGTATTTGAATCTAGCAGG TGTAATATTGTGGAAGAATGAAAACAGTATTTTTAATGGATTACTAA GGCATATTTAATGCGTTGTCAAGGAGGATGCTTGCACTGCAAAAA CGATACATAAGTTAGCATGGGAATTTCATTAATGAAAGAATAAATG CACCGAAACAAAATCATGAATTAATTGTGGTTTCAGAATAATGAAA AATCCATTGGCTGTTCCTGTTCCTATGTGAATGGTTCATCTCTGCC ATAATAATTACTATTTTGTTTAAAGAGTCTTTACTAGATATTGCCGT TCACCTTTTGCCTACGAGCTAGCGATAGAGATTTCTGTATGGTATC TGACTTGACATAATGTCCGACATCCCGTTGAAGATATCAAACAATA CATGACAAAGGTCGGGCATTAATCTGCTCAAACATTAATTCTTTAA ACCTATCTCGATCATATCTAAGAAAGAAAAAAAACTGGCTTTTCGG

				TTCCTAGTGTTAACTCCAGTACCTGGTGTTGAGAAAAATTTACTAT GTGGCCCGGCTAAGTAGTGCAATATTCTGGTACCATACTTCTAGA AATTTTTGCGCGATAACCTAGTGTTTTCTGACGAAGATTTTGGTGT CATTTGTATCTTCGTCGGTACAAAATGGTAATCATAGTATGTTTCC ATGTTTTTGGACAAAAAAAAGAAGAAGGTAGCCAAAGAGCTGAAT TTGCTATTCTTTTGTGATTATTGTGCGCAAAATAGTGACATTTTCTT TCTCAAATTAGTTACACCCCGGATCCTAACCTTTACTGGCCTGTTG ACGTTATTTGTTACGGGCTCAGCCCATCTGAGTAAATTTGGCAATT GTGTTCAAGTCAACGCCTGGAATCATTCCCAGCGTTTTATTATGGA CTGGGACTCTTGCAACTGTTCTACTGGCACAGTGGATTTATAGTG AACTGGATTTTTCAAAAATGGCTTCACTTTGAGAAACACTATTTACT ATGTTTGTTAACTTCTTAACAGTGTGTATTACTTTTTTGCCATATTG ATATTAAAAAAGTCATTTCGACTGCTGACAGAGAATACAACTAGTA ACTGGAGAGATAGCTGGTGCAGTGAGTGATTCCACATAATGCCAG ACTTCTACTCGTCAGCCAGTTCGATTGTTGAGGAAACATAGCAAA GCAGTTAAGCTGTTTTATTTGTTGGCGAAATCGAACTTGTGAAAGT TGTGGGCTATCCTCGCTTTGATTACATGAGTAGAACCCAAGGATT TATGGAAAATTTGACTGGCTTCAAGATTTTTAAGGCAGTTCTATGA GATCACACACTTAATCCGCTTCCAGAATTTATTTTCTTTTTTTGATG ATTTATGCTCAAGGAATTTACCTGTTCTCAAGAATATGTTTTTAATT CGAAGCTTTGCGTATATGATGTTTATCAATAACGTGTGCATCGTCG ATATCTCTTCGCTAACAAAAAGCAATTTAAGTACCAAACAAACAGT AGTAATAGAGTGGGTCTACTTTGTCGATTGCCGTAGCAGGACATT TAACGCAAACGCTTCGGTAATCTGGTGAAATGATTGGATTAGGTG TTTTGTAAATTTTTTTTTTTTTTAGAAGATATTAATGCTGCATAGGG GAGAGATAAACGTCGCGGGAATTTGTGGCGGTGGAGCCCAGGTA CGTATTAATTTTGAATGGCGCAAATCTACTAAGTACGGTATCATTT TGATGTCGGAATACGGATAGTCAGTCCATAACTGCAC
6	SUT123	233	Medium	AAGAGGGGTGAAAAGACATTCTAAATTTTGTTATCGAATGTGAACA GAACACTTAAGAAAACGCCAAGGTTAAGAAGGCCTTGAGAGTATT GATTAAGGCGCATGGAGCACAGGTAAACGCGAAAGACGTTTTGTA CTTCCTTTTACTGAGCACCTCTTACATGTAGTAGTAACCATCGCAG CGGAATAAGCACACAAAAAATGGTATTTACTTTTAGGCAAACTTGT GGGAA